EFFECT OF FETAL ALCOHOL EXPOSURE ON MAMMARY GLAND DEVELOPMENT AND TUMORIGENESIS IN OFFSPRING

By

CATINA CRISMALE-GANN

A dissertation submitted to the

Graduate School – New Brunswick

Rutgers, The State University of New Jersey

and

The Graduate School of Biomedical Sciences

University of Medicine and Dentistry of New Jersey

in partial fulfillment of the requirements

for the degree of

Doctor of Philosophy

Graduate Program in Cell and Developmental Biology

written under the direction of

Dr. Wendie S. Cohick

and approved by

_____

_____

_____

_____

New Brunswick, New Jersey

May 2014

ABSTRACT OF THE DISSERTATION

Effect of Fetal Alcohol Exposure on Mammary Gland Development and Tumorigenesis in Offspring

By CATINA CRISMALE-GANN

Dissertation Director:

Dr. Wendie S. Cohick

Alcohol exposure *in utero* increases susceptibility to carcinogen-induced mammary tumorigenesis in adult rats. However, the mechanisms underlying the enhanced susceptibility are not well understood. Pregnant Sprague Dawley rats were fed either a liquid diet containing 6.7% ethanol, an isocaloric liquid control diet, or rat chow *ad libitum* from gestation day 7 until parturition. At birth, female pups were cross-fostered to control dams. To determine if fetal alcohol alters the insulin-like growth factor (IGF)/estradiol (E2) axis in mammary gland development, we analyzed time points in pre-pubertal, pubertal, and mature F1 offspring. Mammary glands from alcohol-exposed animals displayed increased epithelial cell proliferation and aromatase expression at PND 20 and 40. Animals exposed to alcohol *in utero* exhibited increased hepatic IGF-I expression at all time points, increased mammary IGF-I expression at PND 20, and decreased mammary IGFBP-5 expression at PND 40. To investigate tumorigenesis, N-

nitroso-N-methylurea (NMU) was administered on PND 50 to induce tumors and offspring were euthanized at 16 weeks post-NMU injection. The alcohol group developed more tumors overall as well as more hyperplasias and adenocarcinomas as compared to control groups. Alcohol-exposed animals developed more progesterone receptor positive tumors and exhibited increased Snail, IGF-II, and IGFBP-5, as well as decreased ERα tumor mRNA expression. To determine if fetal alcohol induces alterations in DNA methylation in the mammary gland, we assessed an IGFBP-5 promoter CpG island, the first CpG island in IGFBP-5 exon I, and an estrogen receptor (ER) α promoter/exon I CpG island in tumors and contralateral mammary glands as well as PND 40 mammary glands. While the IGFBP-5 promoter CpG island did not exhibit methylation, low levels of methylation were observed in the IGFBP-5 exon I CpG island in all tissues examined. Tumors from alcohol-exposed animals exhibited partial ERα methylation. These data indicate that alcohol exposure *in utero* may promote mammary tumorigenesis by inducing changes in the IGF and E2 systems during early development. Furthermore, alterations in PR, Snail, IGF-II, and IGFBP-5 may be involved in the underlying mechanisms of enhanced carcinogen-induced tumorigenesis observed in alcohol-exposed offspring.

Dedication

In loving memory of my ninth grade biology teacher, John Bennett – without him I would have never discovered my love of science.

To my husband David and my daughter Seraphina – Thank you for your unconditional love and support. I am eternally grateful for all of the sacrifices you have made so I could accomplish this goal. I would have never made it through graduate school without you. I love you.

Acknowledgements

To my advisor, Wendie Cohick – Thank you for welcoming me into your lab. I am so grateful to have had such a wonderful mentor. Thank you for believing in me even when I didn't believe in myself. I truly appreciate all of the support and encouragement you have provided me in both the professional and personal aspects of my life.

To my dissertation committee members: Nanjoo Suh, Terri Wood, and Helmut Zarbl - Thank you for taking the time to critically think about my data and for all of your valuable input.

To Michael Reiss, Dipak Sarkar, and Mehmet Uzumcu – Thank you for all of your guidance early on in my graduate school career.

To the current members of the lab: Allyson Agostini-Dreyer, Kristie Butler, Amanda Jetzt, and Hillary Stires – Thank you for your constant support throughout graduate school. I truly appreciate the many hours you helped me with troubleshooting. It has been a pleasure work with all of you.

Hillary – Thank you for all of the technical assistance you have provided and for all of the discussions we have had about this data. I officially pass the torch onto you.

Amanda – Thank you for being a wonderful officemate and for all of the guidance and support you have given me both inside and outside the lab.

To Tiffany Polanco – Thank you for taking me under your wing and teaching me everything in the lab when I first joined. It was a pleasure to work with you on the animal studies.

To Christine Duncan – Thank you for all of your qRT-PCR help when I was first starting out in the lab.

To Kenneth Reuhl – Thank you for taking the time to read our tumor slides and discuss my data with me.

To Kathy Roberts – Thank you for helping me process my tissues, for teaching me how to embed and section them, and for answering all of my histology questions.

To Aparna Zama – Thank you for all of your immunohistochemistry and epigenetics help. I couldn't have gotten started with these techniques without you.

To my family, especially my parents – Thank you for all of the love and support you have provided me throughout my entire life. Thank you for always encouraging me to strive to do my best.

Acknowledgements of Previously Published Work

Chapter 2 Alcohol Exposure In Utero Leads to Enhanced Prepubertal Mammary Development and Alterations in Mammary IGF and Estradiol Systems

> Springer and Hormones and Cancer, volume 2, 2011, pgs. 239-248, Alcohol exposure in utero leads to enhanced prepubertal mammary development and alterations in mammary IGF and estradiol systems, Tiffany A. Polanco, Catina Crismale-Gann, and Wendie S. Cohick, figure numbers 1-6, original copyright notice is given to the publication in which the material was originally published with kind permission from Springer Science and Business Media.

Contributions to this work: Conducted all aspects of the animal study along with T.A. Polanco; Figures 1, 2, 3, 6; contributed to original manuscript; manuscript revisions

Table of Contents

List of Tables

Chapter 3

Chapter 4

animals exposed and not exposed to alcohol *in utero* (study 2).

List of Figures

Chapter 2

Chapter 3

Chapter 4

List of Abbreviations

ABI	Applied Biosystems
ANOVA	Analysis of Variance
BAC	Blood alcohol concentration
BPA	Bisphenol A
BrdU	Bromodeoxyuridine
DAB	3,3'-diaminobenzidine
DMBA	7,12-dimethylbenz[α]anthracene
DNA	Deoxyribonucleic acid
EIA	Enzyme-linked immunoassay
ELISA	Enzyme-linked immunosorbent assay
E2	17β-estradiol
ER	Estrogen receptor
FAS	Fetal alcohol syndrome
FASD	Fetal alcohol spectrum disorder
HER2	Human epidermal growth factor receptor 2
IGF	Insulin-like growth factor
IGFBP	Insulin-like growth factor binding protein
IHC	Immunohistochemistry
IP	Intraperitoneal
LOI	Loss of imprinting
MMTV	Mouse mammary tumor virus

NBF	Neutral buffered formalin
NMU	N-nitroso-N-methylurea
qRT-PCR	Quantitative reverse transcription polymerase chain reaction
PND	Postnatal day
PR	Progesterone receptor
RIA	Radioimmunoassay
RNA	Ribonucleic acid
SDS-PAGE	Sodium dodecyl sulfate-polyacrylamide gel electrophoresis
TEB	Terminal end bud
TBS	Tris buffered saline
TUNEL	Terminal deoxynucleotidyl transferase-mediated dUTP nick-end labeling

Chapter 1

Review of the Literature

Introduction

It has long been recognized that prenatal alcohol exposure can lead to fetal alcohol spectrum disorder (FASD), the most severe case being fetal alcohol syndrome (FAS) (1). Children with FAS exhibit growth deficiencies, facial abnormalities (small eye openings, short upturned nose, low nasal bridge, thin upper lip, flat philtrum), central nervous dysfunction, intellectual impairment (learning and memory), and behavioral problems (1-4). Thus, prenatal alcohol exposure has long-term effects on the child (2). It is estimated that among younger school children FASD affects 20 to 50 per 1000 live births in the U.S. and some Western European countries, while FAS affects 2 to 7 per 1000 live births in the U.S. (5). In 2005 the U.S. Surgeon General issued an advisory stating that women who are pregnant or who are planning on becoming pregnant should abstain from drinking alcohol (6). Despite reports indicating the negative effects of prenatal alcohol exposure on offspring and an advisory from the U.S. Surgeon General, many women continue to consume alcohol during pregnancy. The Centers for Disease Control report that 51.5% of women who are of child-bearing age and 7.6% of pregnant women consume alcohol. Of pregnant women surveyed in the U.S., 1.4% self-reported binge drinking (7). Of further concern is that worldwide, 41% of pregnancies are unplanned (8). Therefore, prenatal alcohol exposure is likely to occur during the early critical stages of fetal development before a woman may even know that she is pregnant. This is particularly concerning as alcohol is able to cross the placenta and as such,

consumption of alcohol by a pregnant woman exposes the fetus to similar blood alcohol levels as the mother (2, 9).

Breast cancer is the most common form of cancer among women and the National Cancer Institute estimates that there were 232,340 new cases among women in the U.S. in 2013 (10). Many factors influence a woman's risk of breast cancer. These include age, family and personal history, reproductive and menstrual history (age at menarche and menopause, age at first full-term pregnancy, parity), genetics, and obesity (11). Epidemiological analyses and animal studies have shown that alcohol consumption is associated with a higher risk of breast cancer with the relative risk ranging from 1.09 to 4.0 (12-24). A newly emerging concept is that environmental exposures and lifestyle choices during pregnancy may affect the offspring's risk of disease in adulthood (25-28). This has led to the idea that a woman's breast cancer risk may be pre-programmed prior to birth (29-31). In support of this hypothesis, our lab and the Hilakivi-Clarke lab have shown that moderate and high levels of alcohol exposure *in utero* increase susceptibility to carcinogen-induced mammary tumorigenesis in adulthood (32, 33). These studies suggest that an additional adverse outcome of alcohol consumption during pregnancy could be that women born to these mothers have increased risk of developing breast cancer as adults. Fetal exposure to alcohol has been shown to increase risk of childhood leukemia, suggesting that findings in rodent models may be relevant to human disease (34). If the findings of alcohol exposure *in utero* leading to enhanced risk of breast cancer extend to humans, then health professionals should be further encouraged to inform women of the numerous risks of alcohol consumption during pregnancy. Perhaps more importantly, women of alcoholic mothers should be informed that they may be at

increased risk of breast cancer and encouraged to get regular mammograms at an early age. Early detection of breast cancer is the best defense against the disease. For this reason, it is important to be able to identify subsets of women who are at higher risk for breast cancer (35). Thus, the identification of additional breast cancer risk factors, such as fetal alcohol exposure, is an essential component in the fight against this disease.

Mammary Gland Development Overview

Mammary gland development begins during embryogenesis, but unlike most other organs, the mammary gland is only a rudimentary ductal structure at birth (36-38). Its development mainly occurs postnatally during puberty with the gland becoming fully differentiated and functional during pregnancy and lactation (36-39). Mammary gland growth is isometric from birth until approximately 23 days of age in the rat. After this time, mammary gland growth becomes allometric, growing three times faster than the rest of the body (38, 40-43).

The mammary gland is composed of the epithelial or parenchymal compartment, which forms the ductal structure, and the stromal or mesenchymal compartment, which consists of adipocytes, fibroblasts, blood vessels, nerves, immune cells, and fibrous connective tissue, the latter which surrounds the ducts and separates them from the adipose tissue (38, 41, 43, 44). The mammary gland consists of two types of epithelium: basal and luminal. The basal epithelium includes myoepithelial cells, which form the outer layer of ducts. The contractile function of these cells during lactation results in the release of milk from alveoli and movement of the milk through the ducts to the nipples. The luminal epithelial cells line the ducts, ductules, and alveoli of the gland (37-39, 43).

The parenchyma (epithelial cells) invade the surrounding stroma extending from the nipple into the fat pad (38, 45).

Embryonic mammary gland development is orchestrated by epithelial and mesenchymal interactions (36, 46, 47). Mammary gland development begins when the mammary or milk line forms between embryonic days 10 and 11 (38, 42, 46, 48). The mammary line marks the future location of the mammary glands (49). It consists of a single layer of ectoderm that extends from the anterior to posterior limb buds along the ventral side of the body (36, 38, 50). Approximately one day later, epidermal cells migrate to form several layers that appear as lens shaped structures called placodes (50, 51). These placodes develop at the sites where the mammary glands will eventually form (36, 43). There are six pairs of mammary glands in the rat: one cervical, two thoracic, one abdominal, and two inguinal (52). Each placode increases in size to form a ball of cells that invaginates into the mesenchyme resulting in a bulb shaped structure with a narrow neck, called the mammary bud (38, 48, 51). Mesenchymal cells near the mammary bud arrange themselves in concentric layers surrounding the bud to form the mammary fat pad precursor (36).

After remaining quiescent for a few days, the mammary bud elongates, forming the mammary sprout (46). This mammary sprout protrudes through the mesenchyme and into the mammary fat pad precursor where it undergoes initial branching that results in the small ductal tree present at birth (36, 47, 48, 51). At this time, the mammary gland consists of one or two primary ducts arising from the nipple, with a total of 10-20 branching ducts (38, 46, 48, 52). This rudimentary ductal structure remains in an arrested developmental state until puberty, when branching morphogenesis takes place (43, 53).

During this time the mammary gland undergoes extensive branching, which ultimately results in a complex ductal network (37, 38). The ends of the ducts proliferate forming multiple layers of epithelial cells that appear as club-shaped structures called terminal end buds (TEBs) (45). TEBs are sites of rapid proliferation within the mammary gland (38, 43). During each estrous cycle TEBs undergo elongation, bifurcation, and lateral branching until they fill the mammary fat pad (44). The division of TEBs results in the formation of alveolar buds, which later give rise to alveolar lobules (38, 43). TEBs that do not differentiate become smaller finger shaped structures called terminal ducts (52).

Full differentiation of the mammary gland is achieved during pregnancy and lactation (37, 45). During pregnancy mammary gland development continues as it prepares for lactation by undergoing extensive secondary and tertiary branching, formation of alveolar buds at the ends of the tertiary branches, and proliferation of the luminal epithelium (38, 39). At this time alveolar buds cleave and differentiate into alveoli (38). The mammary gland becomes fully functional during lactation. Proliferating epithelial cells replace the adipose tissue in the space surrounding the ducts with lobular alveolar structures. It is during lactation that the alveoli synthesize milk products (protein, fat, lactose), which are secreted into the lumen as a result of the contraction of myoepithelial cells surrounding the alveoli (49). The luminal epithelium of the ducts serves as a conduit for milk as the milk is transported through the ductal lumen to the nipple (43).

At weaning the mammary gland undergoes involution, a two-step process that returns the gland to its pre-pregnancy state (38, 41). The first phase of involution involves apoptosis of milk producing epithelial cells. If nursing resumes within 48 hours, this

stage is reversible. During the second phase of involution, which is irreversible, apoptosis continues, alveoli collapse, the stroma undergoes extensive remodeling, and adipocytes differentiate to replace the epithelial cells (38, 54). The mammary gland undergoes this remarkable remodeling process with each cycle of pregnancy, lactation, and involution.

Estrogen and Insulin-like Growth Factor (IGF) in Mammary Gland Development and Breast Cancer

Postnatal development of the mammary gland is regulated by hormones and growth factors, such as estrogen, growth hormone (GH), IGF-I, progesterone, and prolactin (38). During puberty, estrogen, GH, and IGF-I regulate growth of the ductal tree (38, 41, 55). Progesterone promotes tertiary branching of the ducts as well as lobuloalveolar development (38, 39, 41, 55). The formation of alveoli occurs during pregnancy under the regulation of prolactin and progesterone (38). Although many hormones and growth factors play a role in mammary gland development, this section will focus on estrogen and IGF since both of these systems have been shown to play a crucial role in both mammary gland development as well as breast cancer etiology.

Estrogens exist in several forms: 17β-estradiol (E2), estrone, and estriol, with E2 being the major form found in circulation. The classical E2 signaling cascade is initiated when E2, a steroid hormone, diffuses across the plasma membrane and binds to estrogen receptor (ER) in the cytoplasm. There are two types of intracellular ERs, ERα and ERβ, which are both present in the rodent mammary gland (56-58). Binding of E2 to ER results in removal of heat shock proteins and receptor conformational change that leads to activation of the receptor. Dimerization of the receptor then occurs and the E2/ER

complex translocates to the nucleus where it binds to estrogen response elements in the promoter of target genes, thereby initiating transcription (56, 59). E2 can also act via a non-genomic or membrane-initiated mechanism (60). This pathway involves the binding of E2 to ERs localized to the plasma membrane (61-63). These include not only ERα and ERβ, but also ERα transcript variants (including ERα 36) and the G-protein-coupled ER 1 (GPER, formally known as GPR30), a G-protein coupled receptor that is structurally different from the classical ERs (64, 65). Binding of E2 to membrane-bound ERs leads to the formation of a complex that may include ERα, IGF-IR (62), IRS-1 (66, 67), or PI3K (68, 69), which can then activate the MAPK or Akt signaling pathways, leading to gene transcription (56).

Estrogens are involved in the growth and differentiation of the mammary gland particularly during pubertal development of the tissue (38, 70). Implanting E2 into mammary glands of ovariectomized animals results in TEB proliferation (37, 71). This E2-stimulated ductal growth is inhibited by antiestrogens such as keoxifene and the selective ER modulator (SERM) tamoxifen (71, 72). E2 is also important for mammary gland development during pregnancy. Addition of hormones to hypophysectomized-ovariectomized-adrenalectomized mice revealed a role for E2 in lobuloalveolar development (73). Together, these studies indicate that E2 directly affects mammary gland development.

ERα knockout mice develop a rudimentary ductal structure that lacks TEBs (74, 75). ERβ knockout mice exhibit histologically normal mammary glands pre-pubertally (76, 77). However, post-pubertally they have decreased ductal side branching and impaired lobuloalveolar development (77). These data indicate that ERα is the primary

receptor for early mammary gland development, while ERβ plays a role in terminal differentiation of the mammary gland during pregnancy and lactation (77). To further understand the role of ERα, a Cre-lox based conditional knockout of ERα in mammary epithelial cells at specific stages of mammary gland development was generated (Feng et al. 2007). In virgin mice, this conditional ERα knockout results in aberrations in ductal elongation and side branching as well as limited TEB development (78). These researchers also employed the use of the whey acidic protein (WAP)-Cre-mediated deletion of ERα to specifically remove ERα in the mammary epithelial cells during late pregnancy and lactation (78). They found that mammary glands from these mice lacked ductal side branching and exhibited defective lobuloalveolar development as well as decreased milk production (78). These data indicate that during puberty ERα is required for ductal elongation and during pregnancy it is necessary for tertiary branching as well as alveolar proliferation and maintenance (78). When mammary epithelial cells isolated from wildtype and ERα negative mice were transplanted together into a cleared fat pad of C57BL6 mice, the ERα negative cells were stimulated to proliferate by paracrine signals from ERα wildtype cells. These data reveal the importance of ERα in ductal morphogenesis (75).

Estrogen plays an integral role in mammary gland development as well as breast cancer progression (79, 80). Many epidemiological studies have shown that a higher circulating E2 level is associated with an increased risk of breast cancer in postmenopausal women and this association is independent of ER tumor status (70, 81-86). Lifetime exposure to estrogen is a primary risk factor for breast cancer (79, 80). Women who experience menarche at an early age and/or menopause at a later age have

an increased risk of breast cancer. The increased risk has been proposed to result from more menstrual cycles throughout their lifetime, thus an increased overall exposure to E2 (79, 80, 87, 88). Recent meta-analyses have concluded that certain breast cancer risk factors such as age at menarche or first full-term pregnancy, parity, and family history are not associated with postmenopausal circulating hormone concentrations (89). These data suggest that the breast cancer risk induced by these factors does not work through postmenopausal hormone concentrations, rather they may act in the premenopausal woman by lengthening exposure time to premenopausal sex hormones or by inducing structural alterations in the breast (89). Animal studies also provide evidence for a relationship between estrogen and breast cancer by showing that diethylstilbestrol (DES), a synthetic estrogen, enhances carcinogen-induced mammary tumorigenesis (90). The ACI rat is particularly sensitive to E2-induced mammary carcinogenesis. When female ACI rats are treated with E2 alone, all animals develop mammary tumors. However, tamoxifen-treated or tamoxifen + E2-treated animals do not exhibit tumors (91). These data provide additional evidence for the role of E2 in breast cancer.

Further evidence that circulating E2 may contribute to breast cancer is provided by the findings that if the E2 system is blocked in ERα positive tumors, either through SERMs or aromatase inhibitors, breast cancer progression is inhibited (56, 92). For this reason, SERMs and aromatase inhibitors are currently used as treatment methods for women with ERα positive tumors (92). Although controversial, there is also some evidence that the widespread use of hormone replacement therapy has led to increased breast cancer incidence (93), again indicating an association between E2 and breast

cancer. Increased expression of ERα has been found in many breast tumors (56). For this reason, ERα has become a prognostic and predictive marker of this disease.

The IGF family consists of two ligands (IGF-I and IGF-II), two IGF receptors (IGF-IR and IGF-IIR), and six IGF-binding proteins (IGFBP-1 through IGFBP-6) that modulate the actions of IGFs (94, 95). IGF-I and IGF-II primarily act via the IGF-IR, but both IGFs can also bind the insulin receptor (IR), while IGF-II has the ability to bind the mannose-6-phosphate receptor/IGF-IIR as well (96). These ligands can also bind hybrid IGF-IR/IR receptors (97). IGF signaling begins when IGF binds to the receptor leading to recruitment of adaptor proteins, insulin receptor substrate (IRS) 1 and 2, which leads to autophosphorylation of the receptor (97). This initiates a downstream signaling cascade that activates the MAPK and PI3K/Akt pathways (97).

The IGF family plays an integral role in normal mammary gland development as knock-out models for components of this family result in aberrant mammary gland development (98). IGF-I null mice exhibit fewer TEBs and ducts, as well as a smaller area of the mammary fat pad that is occupied by the ductal tree. Administering IGF-I to these animals increases TEB formation and ductal branching (99). Genetic mouse models have shown that both circulating and local IGF-I play a role in the development of the mammary gland (100, 101). Transgenic mice with increased hepatic/circulating IGF-I and normal local IGF-I (HIT mice) exhibit enhanced mammary gland growth (more and larger TEBs as well as increased ductal branching) and increased proliferation in the mammary gland compared to IGF-I KO/HIT mice, which have increased circulating IGF-I, but no local IGF-I, or control mice (100). IGF-I midi mice have a mutation in the IGF-I gene that diminishes its transcription, resulting in reduced levels of both circulating and

local IGF-I levels (101, 102). In these mice, mammary gland ductal elongation is unaffected, but ductal branching is significantly reduced (101). Furthermore, liver specific deletion of IGF-I (LID mice), which decreases IGF-I levels by approximately 75%, does not affect ductal branching (101). Using the mouse mammary tumor virus-long terminal repeat (MMTV-LTR) promoter to drive IGF-I expression in the mammary gland, it was shown that local IGF-I enhances alveolar bud development in peripubertal virgin mice (103). Transfer of embryonic mammary buds from IGF-IR -/- embryos into the cleared fat pad of 3-week old wild-type mice caused limited ductal growth and reduced proliferation in the TEBs compared to glands from IGFR +/+ littermates (98, 104). Together these data indicate that IGF-I (both circulating and local) and IGF-IR play pivotal roles in mammary gland development.

The IGF system is also a critical factor in breast cancer etiology as the IGF ligands, receptors, and IGFBPs are expressed in breast cancer (95). Transgenic mice expressing IGF-I under the control of the bovine keratin 5 promoter overexpress IGF-I specifically in mammary gland myoepithelial cells, recapitulating the paracrine effects of stromal IGF-I on mammary epithelial cells (105). These transgenic mice display ductal hyperplasia, wider ducts, and increased alveolar bud formation. Pre-pubertally these mice exhibit increased mammary epithelial cell proliferation. In addition, the transgenic mice exhibit increased susceptibility to carcinogen-induced mammary tumors, indicating that increased local IGF-I expression stimulates mammary tumorigenesis (105). LID mice injected with the chemical carcinogen DMBA exhibit decreased mammary tumor incidence and delayed latency compared to mice with normal circulating IGF-I levels (106). In an epidemiological study where blood was drawn following a breast cancer

diagnosis, breast cancer patients were found to have higher serum IGF-I levels compared to controls (107). Using women from the Nurses' Health Study, a prospective epidemiological analysis on blood collected prior to a breast cancer diagnosis revealed an association between high circulating IGF-I levels and breast cancer risk in premenopausal women, with the highest risk observed in women less than 50 years old (85). However, a recent meta-analysis revealed that circulating IGF-I levels were not associated with breast cancer risk among all women or among postmenopausal women only. This meta-analysis found that increased circulating IGF-I was associated with a higher breast cancer risk in premenopausal women (108). Epidemiological studies have also shown that many breast tumors exhibit increased IGF-IR expression (109, 110). The expansive amount of data implicating a role for IGF-I in breast cancer has lead to development of breast cancer treatments targeting the IGF system. Although initially promising, phase III clinical trials have provided disappointing results, suggesting that the complexity of the IGF system needs further evaluation (111, 112).

There is substantial evidence that cross-talk between the IGF and E2 signaling pathways occurs during both normal mammary gland development as well as breast cancer (97, 113-116). E2 can alter the expression and activation of IGF-II, IGF-IR, IGF-IIR, IGFBPs and IRS; reciprocally, IGF-I can activate the ER and also enhance sensitivity of ER to E2 (59, 95, 97, 117-120). Treatment of MCF-7 breast cancer cells with IGF-I induces the association of IGF-IR with ERα, but this interaction is lost when IGF-IR expression is reduced through the use of IGF-IR anti-sense cDNA (121). Cooperation between IGF-I and E2 has been shown to promote complete ductal development in the mammary gland (98, 122). This is supported by the finding that

treatment of IGF-I knock-out mice with IGF-I and E2 restores mammary gland development (TEB formation, filling of the mammary fat pad with glandular elements, and ductal elongation), while E2 alone had no effect (99). Using a transgenic mouse model where IGF-I overexpression in the mammary gland is under the control of the bovine keratin 5 promoter, IGF/E2 crosstalk has been shown to be affected by developmental stage (67). In pre-pubertal animals, ERα/IRS-1 complexes are present which activate IRS-1, thereby promoting IGF-I signaling in the mammary gland through the PI3K/Akt pathway. However, in post-pubertal animals, when there is decreased ERα expression, ERα/IRS-1 complexes do not form, thus promoting IGF-I signaling in the mammary gland via the Ras/Raf/MAPK pathway. Crossing these IGF-I overexpressing transgenic mice with ERα knockout mice revealed the essential role of ERα expression in IGF-I induced mammary epithelial cell proliferation as well as IGF-I induced ductal and alveolar morphogenesis (67).

The expression of IGF-IR as well as IRS-1 and IRS-2 is increased by E2 in breast cancer cells, resulting in enhanced IRS-1 phosphorylation and activation of the MAPK pathway (59, 66, 95, 123). ER-α expression prevents degradation of IRS-1 and IRS-2 in breast cancer cells (66). Further evidence of E2/IGF crosstalk is the finding that the SERM tamoxifen inhibits IGF-I induced proliferation (118). IGF-IR expression is also correlated with ER tumor status (110). Involvement of IGF with the E2 pathway has led to current clinical trials for breast cancer therapies that block the IGF signaling pathway as well as trials that target both the E2 and IGF pathways, the success of which would be highly significant since IGF/E2 crosstalk may be involved in resistance to breast cancer treatments (59, 97, 109, 124). Current combination therapies targeting these two

pathways have not proven successful yet (109, 111, 124). Thus, a further understanding of the interaction between the IGF and E2 systems is necessary in order to utilize these pathways in potential future breast cancer treatments.

Effect of Fetal Environment on Mammary Gland Development and Tumorigenesis

Fetal exposure to a wide variety of environmental chemicals such as diethylstilbestrol (DES), genistein, nonylphenols, zearalenone, atrazine, and bisphenol A, have been shown to affect postnatal mammary gland development (125-130). Bisphenol A (BPA) is a xenoestrogen that is used during the manufacturing of plastics and epoxy resins and is found in many consumer products such as food and beverage containers/cans, baby bottles, dental materials, and sales receipts, among other items. Offspring exposed to environmentally relevant doses of BPA (250 ng/kg) prenatally have increased ductal area and ductal extension, enhanced epithelial cell penetration into the fat pad, decreased epithelial cell size, and delayed lumen formation at gestation day (GD) 18 (125). *In utero* BPA exposure also affects mammary gland development in older animals (127). At 6 months of age, animals exposed to 25 and 250 μg/kg BPA exhibit increased development of mammary gland structures (ducts, terminal ducts, terminal end buds (TEBs), and alveolar buds) (127). The increase in TEBs and terminal ducts in offspring exposed prenatally to BPA has been confirmed by others (129). In BPA-exposed animals (25 and 250 μg/kg), mammary epithelial cell proliferation is decreased at PND 10, while stromal proliferation is increased at 6 months of age, indicating that BPA alters the timing of DNA synthesis in the epithelial and stromal compartments of the mammary gland (127). In addition, *in utero* exposure to BPA (25 and 250 μg/kg) induces

alterations in mammary gene expression (129). Expanding the length of BPA exposure further alters mammary gland development (130). Perinatal BPA exposure increases TEB number and area, number of ductal epithelial cells expressing progesterone receptor (PR), and lateral branching as well as decreased apoptosis in the TEBs (130).

Zearalenone is a mycotoxin that is commonly found in cereal, fruits, and vegetables. Offspring exposed to zearalenone (0.2 μg/kg, 20 μg/kg, and 1 mg/kg) from GD 9 until PND 5 exhibit increased terminal end bud length at PND 30 and increased mammary gland differentiation at PND 180 (126). Some zearalenone-exposed animals (5 mg/kg) also develop mammary hyperplasias by 6 months of age (126). Nonylphenol is a metabolite of surfactants and detergents. Gestational exposure to nonylphenol (100 mg/kg) causes advanced mammary gland development and increased ERα expression in both epithelial cells and stroma (128). Atrazine is an herbicide that is applied to a variety of crops to control broadleaf and grassy weeds. In rats, prenatal exposure to atrazine (100 mg/kg) delays mammary gland development (128, 131) and increases PR expression in mammary epithelial cells (128). *In utero* exposure of rats to butyl benzyl phthalate (BBP; 500 mg/kg), a widely used plasticizer, increases the number of terminal ducts and alveolar buds as well as proliferation in TEBs and lobules (132). BBP exposure (120 mg/kg and 500 mg/kg) also alters mammary gland gene expression (132).

Overall, these data show that fetal exposure to many environmental chemicals alters mammary gland development, particularly, TEBs, ductal area, and density. TEBs are the sites of proliferation within the mammary gland and as such are considered highly susceptible to carcinogenic insults. Mammary gland density is also a well-established risk factor for breast cancer. Thus, these data together reveal that *in utero* exposures can alter

mammary gland development, therefore potentially affecting the offspring's susceptibility to mammary tumorigenesis.

The significant effects of the fetal environment on mammary gland development along with the emerging concept that environmental exposures and lifestyle choices during pregnancy may affect the offspring's risk of disease in adulthood (25-28), has lead to the idea that a woman's risk of breast cancer may be pre-programmed prior to birth (29-31). Rodent studies have shown that maternal exposures to dietary factors such as high fat lead to alterations in mammary morphology during development and/or an increased risk of mammary cancer in the offspring (133, 134). In one study, pregnant Sprague Dawley rats were exposed to a high fat diet (43% or 46% fat) *in utero*, given the carcinogen 7,12-dimethylbenz(a)anthracene (DMBA) on PND 55, followed by study termination at 18 weeks post-DMBA administration or earlier if tumor burden was too great (133). Animals exposed to the high fat diet had increased mammary tumor incidence and shorter latency. These offspring also exhibited increased density of TEBs and epithelial cells (133). In another study by the same group, pregnant Sprague Dawley rats were exposed to a high fat diet (43% fat) *in utero*, given the DMBA on PND 50, followed by study termination at 20 weeks post-DMBA administration (134). Offspring exposed to the high fat diet had an increased mammary tumor incidence as well as tumor multiplicity. Furthermore, the number of TEBs was increased at PND 21 and PND 50 in animals exposed to the high fat diet (134).

DES is a synthetic estrogen that was prescribed to pregnant women in the 1950s and 1960s in order to prevent spontaneous abortions and other pregnancy related complications (135). Epidemiological studies have provided evidence that women who

were exposed to DES in the fetal environment have an increased risk of breast cancer in adulthood (135). In addition, an association between dizygotic twin women and a higher risk of breast cancer has been documented and it is thought that increased circulating estradiol levels *in utero* is an influential factor (136). Thus, in situations in which estradiol is elevated in the fetal environment, offspring have an increased risk of mammary tumors.

To date only one other group besides our lab has studied mammary tumor susceptibility in an alcohol exposure model (33). Hilakivi-Clarke and colleagues fed pregnant Sprague Dawley rats a liquid diet containing either low or moderate levels of alcohol from gestation days 7 to 19 or a pair-fed isocaloric liquid diet. DMBA was administered by oral gavage to 47-day old offspring and the study was terminated at 17 weeks post-DMBA administration (33). These authors found that offspring exposed to moderate, but not low, levels of alcohol developed more tumors as a group relative to the isocaloric pair-fed controls, indicating that alcohol exposure *in utero* increases mammary tumor susceptibility to the carcinogen DMBA in adult offspring (33). Furthermore, this group found that alcohol-exposed animals had increased mammary gland density at 8 and 22 weeks of age as well as increased terminal end bud number at 3 weeks and 6 weeks of age. Animals from the alcohol group also had increased mammary gland ERα expression at 22 weeks of age (33). Thus, these changes in mammary gland morphology and gene expression induced by fetal alcohol may be involved in the underlying mechanism for the increased susceptibility to DMBA-induced mammary tumors observed in animals exposed to alcohol *in utero.*

In our previous work we fed pregnant Sprague Dawley rats a liquid diet containing 6.7% ethanol, representing 35.5% of total calories from days 11 through parturition (32). This level of alcohol is higher than the levels used in the Hilakivi-Clarke study (33). Control dams were fed an isocaloric liquid diet with the alcohol calories replaced by dextrin-maltose (pair-fed) or rat chow *ad libitum* (ad lib). At birth, female offspring were cross-fostered to ad lib dams so that female offspring were only exposed to alcohol in the fetal environment. Offspring were exposed to 50 mg/kg N-nitroso-N-methylurea (NMU) at 50 days of age by intraperitoneal injection and the study was terminated at 23 weeks post-injection (32). Similar to the Hilakivi-Clarke et al. (33), we found an increased number of tumors in the alcohol-exposed offspring at 16 weeks post-NMU injection compared to either control group (32). The increased number of tumors per group was a function of both increased tumor incidence (i.e. number of animals with tumors) as well as increased multiplicity (more tumors per animal). Furthermore, in this study the tumors from the alcohol-exposed offspring developed earlier and had a more malignant phenotype (i.e. more adenocarcinomas and more ERα negative tumors (32). In a separate study (Chapter 2), we used the same alcohol *in utero* model, however we did not inject the animals with NMU, rather we sacrificed subsets of animals at postnatal (PND) 20, 40, and 80, which correspond to pre-pubertal, pubertal, and mature developmental timepoints. In contrast to the Hilakivi-Clarke study (33), in our mammary gland development study we did not find a difference in terminal end bud number, mammary density, or ERα expression in mammary glands from alcohol-exposed animals compared to control animals at any of the developmental timepoints examined (Chapter 2). However, we did observe increased incorporation of bromodeoxyuridine (BrdU) in

mammary glands of alcohol-exposed animals compared to pair-fed controls at PND 20 and PND 40, indicating that fetal alcohol induces a hyperproliferative gland early in development (Chapter 2). Thus, the work of our lab (32, Chapter 2) and the Hilakivi-Clarke lab (33) indicates that moderate and high levels of alcohol exposure *in utero* increases susceptibility to carcinogen-induced mammary tumorigenesis in adulthood and that early changes in mammary gland development may be involved in the increased risk.

Fetal Alcohol and Epigenetics

Epigenetics involves heritable changes in gene expression that occur without an alteration in the primary nucleotide sequence of a gene. Epigenetic modifications to nuclear chromatin structure alter DNA, histones, and non-histone proteins. These modifications limit or enhance the accessibility and binding of the transcriptional machinery or recruit repressor complexes, resulting in changes in gene expression. Epigenetic mechanisms include DNA methylation of promoter and/or non-promoter CpG islands as well as CpG shores, covalent histone modifications (methylation, acetylation, phosphorylation, ubiquitination or sumoylation), microRNAs, and the more recently described long noncoding RNAs (137-140).

DNA methylation represents a major epigenetic regulatory pathway that is catalyzed by DNA methyltransferases (DNMTs). These enzymes add methyl groups from S-adenosylmethionines to carbon 5 positions of cytosines (141). Three important family members of DNMTs have been reported: DNMT1, DNMT3A, and DNMT3B. DNMT1 is considered the maintenance DNA methyltransferase, whereas DNMT3A and DNMT3B are primarily involved in *de novo* DNA methylation (137, 142). Covalent histone

modifications, including acetylation and methylation, are a second major pathway. Histone acetylation and deacetylation are regulated by histone acetyltransferases (HATs) and histone deacetylases (HDACs), respectively. Histone methylation and demethylation are regulated by histone methyltransferases (HMTs) and histone demethylases (HDMs), respectively (143). Lysine residues on histone tails can be regulated by both methylation and acetylation. Modifications of lysines on histone H3 can be repressive (e.g. H3K9 di- or trimethylation, H3K27 trimethylation) or activating (e.g. H3K9 acetylation, H3K4 trimethylation) (137, 143-145). Overall, hypomethylation of DNA and histone acetylation cause a more relaxed chromatin state, allowing easier interaction between the DNA and the transcriptional machinery, thus resulting in increased gene transcription. DNA hypermethylation and histone deacetylation result in condensed chromatin structure, causing a decrease in gene transcription (137).

The epigenome is particularly susceptible to environmental factors during fetal development as the DNA synthetic rate is high and the complex DNA methylation patterning and chromatin structure required for normal tissue development is established at this time (146). DNA methylation and histone modifying pathways cross-talk and both are necessary for normal genome imprinting during development (147). Epigenetic reprogramming involves genome-wide erasure and re-establishment of DNA methylation and histone modifications during normal mammalian development (immediately after fertilization until pre-implantation of the embryo and also during primordial germ cell development) (142, 144, 148-151). Aberrant epigenetic regulation is also implicated in cancer, whereby oncogenes are expressed, and tumor suppressor genes are silenced (145, 152).

In 1991, Garro et al. showed that administration of alcohol to pregnant mice on days 9 to 11 of pregnancy resulted in genome-wide hypomethylation in 11-day old whole fetuses. The effect was proposed to be mediated by acetaldehyde, a product of alcohol metabolism, which inhibits DNA methyltransferase *in vitro* (153). In the last few years numerous studies have confirmed that alcohol exposure *in utero* induces epigenetic alterations in the offspring. Some studies have employed the use of the Agouti mouse model for epigenetic analyses because differences can be easily identified by coat color. Gestational alcohol exposure was shown to change the expression of an epigenetically-sensitive allele, *Agouti viable yellow* (A^{vy}) in the offspring (154). Transcriptional silencing correlated with hypermethylation at A^{vy}. This study indicates that alcohol exposure during gestation can affect adult phenotype through epigenetic mechanisms (154). Microarray analysis of murine embryos exposed to alcohol on gestational day 9 shows altered expression of a subset of genes involved in methylation and chromatin remodeling (155). In support of this finding, analysis of whole-embryo murine cultures treated with alcohol show increased and decreased DNA methylation of 1,028 and 1,136 genes, respectively. Greater than 200 of these methylation alterations are found on chromosomes 7, 10, and X, which are chromosomes that contain many imprinted genes as well as genes prone to aberrant epigenetic silencing. Additionally, changes in DNA methylation correspond with actual changes in gene expression in 84 genes, suggesting that fetal alcohol can impact gene expression in the developing embryo through an epigenetic mechanism (156).

In addition to global methylation analyses, several studies have focused on methylation changes in specific genes. Exposure of mice to alcohol between gestational

days 10 and 18 affects methylation of the paternally imprinted H19 gene in the offspring's sperm, resulting in a 3% decrease in the number of methylated CpGs in this gene at 8 weeks of age. The CCCTC-factor DNA-binding sites of H19 play a role in regulating IGF-II expression (157). Due to the well-defined neurological consequences of developmental alcohol exposure, recent studies have focused on epigenetic regulators expressed specifically in the brain. Perinatal alcohol exposure (gestational day 1 through PND 10) induces gene expression changes in epigenetic regulators (DNMT1, DNMT3a, and methyl CpG binding protein 2) in the hippocampus as well as increases in DNMT activity (158). Alcohol exposure of fetal cerebral cortical neuroepithelial stem cells causes a decrease in trimethylation of H3K4 (H3K4me3) and H3K27 (H3K27me3) in developmental genes that play an integral role in regulating neural stem cells as well as neural differentiation (159). H3K4me3 is usually associated with gene activation, whereas H3K27me3 is considered a repressive histone mark (137, 159). Expression of epigenetic-modifying enzymes such as Dnmt1, Uhrf1, Ash2L1, Wdr5, Ehmt1, and Kdm1b are also observed (159). DNMT expression and histone modifications are also altered in the hypothalamus of offspring exposed to fetal alcohol. *In utero* alcohol exposure from gestational day 7 to 21 results in a decrease in H3K4 di- and trimethylation as well as H3K9 acetylation, and an increase in H3K9 dimethylation as well as expression of DNMT1, DNMT3a, and methyl-CpG-binding protein (160). These studies raise the possibility that alcohol exposure *in utero* will affect epigenetic regulators in other tissues as well, including the ovaries and mammary gland.

While epigenetic alterations induced by fetal alcohol exposure in the mammary gland have not been investigated to date, other *in utero* exposures cause epigenetic

modifications in the mammary gland. High-fat or ethinyl-oestradiol (EE2) exposure *in utero* increases DNMT1 expression in PND 50 rat mammary glands (134). Global methylation analysis of PND 50 mammary glands from EE2 exposed rats reveals 375 differentially methylated promoter regions, of which 21 are hypermethylated and 161 are hypomethylated (134). *In utero* exposure to DES or bisphenol-A (BPA) also induces epigenetic alterations in the adult mammary gland (161). DES exposure between gestational days 9 and 26 increases expression of the histone methyltransferase EZH2 in mammary glands of 6 week-old female mice. BPA or DES exposure also lead to increased histone H3K27 trimethylation, an EZH2 target, in the mammary gland indicating that EZH2 methyltransferase activity increases. Overexpression of EZH2 has been documented in breast cancer and is associated with aggressive forms of the disease (161). In summary, *in utero* exposures can cause epigenetic modifications specifically in the mammary gland and these epigenetic alterations can potentially affect the offspring's risk of mammary cancer.

The E2 signaling axis can also be epigenetically affected by *in utero* exposure. Treatment of mice with BPA during gestational days 9 to 16 leads to decreased DNA methylation in the homeobox gene *Hoxa10* in the uteri of 2 week old mice, subsequently resulting in increased *Hoxa10* mRNA and protein expression (162). The decrease in *Hoxa10* DNA methylation leads to increased binding of ER-α to the EREs located on the *Hoxa10* promoter. Furthermore, transfection of MCF-7 breast cancer cells with the unmethylated *Hoxa10* promoter increases luciferase activity in response to E2 compared to MCF-7 cells transfected with the methylated promoter, indicating that the unmethylated *Hoxa10* promoter is more estrogen responsive, leading to an increase in

ERE-driven gene expression (162). It is currently unknown whether other *in utero* exposures such as alcohol can have an epigenetic effect on the E2 signaling axis.

The studies outlined above indicate that prenatal alcohol exposure induces epigenetic modifications. Therefore, it is plausible that alcohol exposure *in utero* could affect epigenetic regulation of the E2/IGF system. Recent evidence has indicated that steroidogenic enzymes, nuclear receptors, and transcription factors involved in steroid hormone synthesis and action can be epigenetically regulated (163). It is therefore possible that alcohol exposure *in utero* can disrupt the normal epigenetic regulation of these key molecules involved in hormone signaling. Changes in the steroid signaling pathway induced by epigenetic modification could then interface with the IGF system as described above. Further studies will determine if fetal alcohol exposure induces epigenetic modifications in genes that can regulate hormone action at key phases of mammary development, ultimately leading to changes in susceptibility to carcinogens.

Objectives

Prenatal alcohol exposure can lead to fetal alcohol spectrum disorder, the most severe case being fetal alcohol syndrome. Despite warnings such as those issued by the U.S. Surgeon General, pregnant women continue to drink alcohol. Animal studies have shown that alcohol exposure *in utero* increases the offspring's susceptibility of mammary tumorigenesis. These data suggest that an additional adverse outcome of alcohol consumption during pregnancy could be that women born to these mothers have increased risk of developing breast cancer as adults.

The first objective of this work was to determine if alcohol exposure *in utero* alters normal mammary gland development and if these alterations involve changes in the insulin-like growth factor (IGF)/estradiol (E2) axis (Chapter 2). We hypothesized that fetal alcohol exposure may lead to enhanced expression of components of the E2 and IGF systems that would ultimately advance mammary gland development. To investigate this issue, we studied the IGF/E2 axis in mammary glands of rats exposed or not exposed to alcohol *in utero* at pre-pubertal, pubertal, and mature developmental time points.

Breast cancer is the most common form of cancer among women. It is of utmost importance to identify additional risk factors for breast cancer so that we can clearly distinguish which groups of women are at high risk for developing the disease. To further understand the effect of fetal alcohol on the offspring's susceptibility to mammary tumorigenesis, we studied tumors at 16 weeks after carcinogen administration, the time point at which maximal differences in tumor number were found between alcohol-exposed and control animals. The second objective of this work was to assess the

histological classification, receptor status (ERα, PR, HER2), and signaling molecule expression (E2/IGF pathway, EMT genes) of carcinogen-induced mammary tumors from animals exposed and not exposed to alcohol *in utero* at 16 weeks post-injection (Chapter 3).

Numerous studies have shown that alcohol exposure *in utero* induces epigenetic alterations in the offspring, while other *in utero* exposures have been shown to cause epigenetic modifications specifically in the mammary gland. We hypothesized that alcohol exposure in the fetal environment affects DNA methylation in the mammary gland and that changes in insulin-like growth factor binding protein-5 (IGFBP-5) and estrogen receptor (ER) α observed in our tissues might be due to these changes. Thus, the third objective of this work was to determine if alcohol *in utero* affects DNA methylation of the IGFBP-5 and ERα genes (Chapter 4).

Chapter 2

Alcohol Exposure *In Utero* Leads to Enhanced Prepubertal Mammary Development and Alterations in Mammary IGF and Estradiol Systems

Copyright and Permission Notice

Contributions to this Work

Conducted all aspects of the animal study with T.A. Polanco; Figures 1, 2, 3, 6; contributed to original manuscript; manuscript revisions

Abstract

Exposure to alcohol during fetal development increases susceptibility to mammary cancer in adult rats. This study determined if early changes in mammary morphology and the insulin-like growth factor (IGF)/estradiol axis are involved in the mechanisms that underlie this increased susceptibility. Pregnant Sprague-Dawley rats were fed a liquid diet containing 6.7% ethanol (alcohol), an isocaloric liquid diet (pair-fed), or rat chow *ad libitum* from days 11 to 21 of gestation. At birth, female pups were cross-fostered to *ad libitum* fed control dams. Offspring were euthanized at postnatal day (PND) 20, 40, or 80. Animals were injected with BrdU before euthanasia, then mammary glands, serum, and livers were collected. Mammary glands from animals exposed to alcohol *in utero* displayed increased epithelial cell proliferation and aromatase expression at PND 20 and 40. Mammary IGF-I mRNA was higher in alcohol-exposed animals relative to controls at PND 20, while mammary IGFBP-5 mRNA was lower in this group at PND 40. Hepatic IGF-I mRNA expression was increased at all time points in alcohol-exposed animals, however, circulating IGF-I levels were not altered. These data indicate that alcohol exposure *in utero* may advance mammary development via the IGF and estradiol systems, which could contribute to increased susceptibility to mammary cancer later in life.

Introduction

Exposure to alcohol *in utero* results in a range of adverse outcomes collectively referred to as fetal alcohol spectrum disorder, the most severe cases manifesting as fetal alcohol syndrome (FAS). Despite this information, the Centers for Disease Control reports that one in eight women drink and 1 in 50 women binge-drink while pregnant (164). This is substantiated by reports that 0.28-0.46% of newborns in the United States and Europe are diagnosed with FAS (165). In addition to the effects of alcohol exposure observed early in life, considerable evidence suggests that a sub-optimal *in utero* environment can increase an offspring's risk of disease in adulthood, such as diabetes, cardiovascular disease, and cancer (25, 166). Alcohol exposure *in utero* increases susceptibility to carcinogen-induced mammary tumors in rodent offspring (32, 33). In addition, these animals develop more tumors with phenotypic characteristics of poor-prognosis breast cancer (32). A recent epidemiological study showed that fetal alcohol exposure increases the risk for acute myeloid leukemia in children (34), which suggests that findings in animal models may be relevant to human disease.

Early developmental changes in the mammary gland could affect susceptibility to breast cancer later in life (167). Development of the mammary gland begins at day 10 of gestation in the rat. At birth, a primordial gland embedded in a fat pad precursor is observed. The gland undergoes isometric growth until puberty when growth becomes allometric. Terminal end buds (TEBs) lead ductal elongation through the fat pad creating a network of branching ducts decorated with alveolar buds (168). This process is regulated by estradiol (E2) and insulin-like growth factor-I (IGF-I), which are both necessary for normal mammary gland development (169) and play integral roles in breast

cancer etiology (170). We have previously shown that circulating E2 is higher in adult offspring that were exposed to alcohol *in utero* (32). In addition, Hilakivi-Clarke et al. (33) found that fetal alcohol exposure leads to increased estrogen receptor-α (ER-α) expression in the mammary glands of 22 week-old offspring. Since the E2 and IGF signaling systems exhibit cross-talk (114, 116), we predicted that fetal alcohol exposure might lead to enhanced expression of E2 and IGF system components that would ultimately advance mammary gland development. The current study was conducted to determine if alcohol exposure *in utero* alters normal mammary gland development through enhanced IGF and E2 action, which might contribute to increased susceptibility to mammary cancer in adulthood.

Materials and Methods

Animal Model

Pregnant Sprague Dawley rats were purchased from Charles River (Wilmington, MA) and housed in a controlled environment. Dams were acclimated to the environment for 2 days, then divided into 3 groups (n = 7) and fed a liquid diet containing ethanol (alcohol-fed; Bio-Serv, Frenchtown, NJ), an isocaloric liquid diet without ethanol (pair-fed; Bio-Serv), or *ad libitum* rat chow (ad lib; Purina Mills Lab Diet, St. Louis, MO) from days 7 to 21 of gestation. Alcohol-fed dams were acclimated to increasing amounts of ethanol (2.2% (v/v) days 7-8 and 4.4% (v/v) days 9-10) and began receiving 6.7% (v/v) alcohol on day 11 of gestation. Dams drinking 6.7% alcohol are expected to present with blood alcohol levels between 100 to 150 mg/dl (171, 172), which translates to approximately three to five drinks in 2 h in women (173). At birth, all female pups were cross-fostered to ad lib-fed dams and litters were normalized to eight pups per dam. Animals were weighed weekly until euthanasia. On post-natal day (PND) 20, offspring from each of the three *in utero* treatment groups were euthanized by rapid decapitation. The remaining pups were weaned at 21 days of age, fed rat chow *ad lib* for the remainder of the experiment, and euthanized on PND 40 or 80 (n = 9-13 offspring per treatment group per time point). Animals were injected intraperitoneally 2 and 4 h before euthanasia with BrdU (70 mg/kg body weight/injection; Acros Organics, Geel, Belgium). Animal care was performed in accordance with institutional guidelines and complied with National Institutes of Health policy.

Sample Collection

Livers, trunk blood, and mammary glands from the fifth inguinal gland were harvested from each animal. Half of each mammary gland was fixed in 10% neutral buffered formalin (NBF; Richard Alan Scientific, Kalamazoo, MI) for histological analyses. The liver and the remaining half of the mammary gland were frozen in liquid nitrogen and stored at -80°C for RNA and protein analyses. The contralateral fifth inguinal mammary gland was left adhered to the skin and fixed in 10% NBF for whole mount analysis.

Whole-Mount Analysis

After fixing in 10% NBF for 2 days, glands were dissected away from the skin, placed on slides, and allowed to air dry for 30 min. Glands were then rehydrated in 70%, 50%, and 25% ethanol for 15 min each, placed in H_2O for 5 min, and stained in carmine alum overnight. Carmine alum stain was made fresh by boiling 2 g carmine and 5 g aluminum potassium sulfate (Sigma-Aldrich, St. Louis, MO) in 800 ml H_2O for 20 min, filling to 1 L volume, and filtering through no. 1 Whatman paper. After staining, slides were dehydrated in 70% and 95% ethanol for 15 min each followed by xylene 2 x 30 min. PND 40 and 80 glands were cleared in toluene for 1 week after dehydration to remove excess fat. Glands were dried for 1 h before mounting in SealPAK pouches (Kapak, Minneapolis, MN) with cedarwood oil (Sigma-Aldrich). Mammary gland whole mounts were imaged at low magnification using a Nikon DS-Fi1 camera (Nikon, Melville, NY) with NIS Elements software (Nikon) to examine how the parenchyma changed across time. TEB number was determined by examining whole mounts under a

Nikon SMZ800 dissecting microscope (Nikon). Structures were defined as TEBs based on the criteria developed by Russo and Russo (174). Briefly, TEBs were defined as club-shaped structures located at the ends of rudimentary ductal structures. These were located at the periphery of the expanding parenchyma. High magnification images of TEBs were taken using a Nikon SMZ1000 dissecting microscope (x 8 magnification) with ACT-1 software (Nikon). Analysis of TEB size was performed using ImageJ (National Institutes of Health, Bethesda, Maryland, http://imagej.nih.gov/ij/). Mammary density was analyzed using Adobe Photoshop (San Jose, CA). Mammary gland length was measured with a ruler from the center of the lymph node to 3 different points on the leading edge of the gland.

Serum Analysis

Trunk blood was kept on ice for 4 h and spun at 5,000 rpm, and then the serum was collected and stored at -80°C. Serum IGF-I levels were detected using an ELISA (Immunodiagnostic Sytems, Fountain Hills, AZ; sensitivity = 63 ng/ml) as per kit instructions. The lack of treatment effect on serum IGF-I was verified using an RIA (data not shown) (175). Serum IGFBP-3 levels were detected by ligand blot analysis.

Immunohistochemistry

Fixed mammary gland tissue was dehydrated, cleared, embedded in Paraplast, and sectioned onto slides at the Histopathology Core of The Environmental Occupational Health Sciences Institute at Rutgers University. Slides were immuno-stained as previously described (32) using primary antibodies against BrdU (1:200; BD

Biosciences, San Jose, CA) and aromatase (1:100; AbD Serotec; Raleigh, NC). The ABC Elite Vectastain kit (Vector Labs, Burlingame, CA) was used for primary antibody detection. Slides were stained in 3,3'-diaminobenzidine (Sigma), counterstained with hematoxylin (Sigma) and mounted in Permount (Fisher Scientific, Pittsburgh, PA) as described previously (32). For BrdU analysis, epithelial cells and BrdU-positive cells were counted and presented as a percent of total epithelial cells stained for BrdU. For PND 20, all epithelial cells were counted for each gland, while up to 1,000 cells were counted for PND 40 and 80. Two sections from each gland were counted and the numbers were averaged. For aromatase analysis, three representative areas were counted and data were presented as the total number of aromatase-positive cells.

Apoptosis Analysis

Slides were prepared as described above and stained for DNA fragmentation using the *In Situ* Cell Death Detection kit (Roche, Basel, Switzerland) as per kit instructions. Sections were counterstained with Hoechst dye (Invitrogen, Carlsbad, CA) and imaged using an Olympus BX41 fluorescent microscope (Olympus, Center Valley, PA) with MetaMorph software (Molecular Devices, Sunnyvale, CA). For analysis, labeled cells in four fields were counted, and data were presented as the number of apoptotic cells per field.

Ligand Blot Analysis

Proteins in serum (4 μl) were separated under non-reducing conditions by SDS-polyacrylamide electrophoresis, transferred to nitrocellulose membranes, then ligand-

blotted with ^{125}I-IGF-I as previously described (176). Membranes were exposed to phosphorimaging screens and scanned using a Storm 860 (GE Healthcare, Piscataway, NJ). Densitometry was performed using ImageQuant 5.2 software (GE Healthcare). Bands were normalized to a calibrator sample which was run on each gel for comparison across gels.

RNA Analysis

Mammary tissue (100 mg) was homogenized in Trizol (Sigma) and RNA was isolated using an RNeasy kit (Qiagen, Valencia, CA) including DNase treatment according to the manufacturer's specifications. RNA quality was verified using the Agilent 2100 Bioanalyzer and the Agilent RNA 6000 Nano kit (Agilent Technologies, Santa Clara, CA). The High Capacity cDNA Reverse Transcription kit (Applied Biosystems (ABI), Foster City, CA) was used to reverse transcribe 2 µg of RNA. Primer sets for IGF-I (forward: 5'CTGTGCAGTTCGCCCATTGTTTGA3'; reverse: 5'ACATTTGGACACCCAGGCAGG TAT3'), IGFBP-5, and β-actin (32) were developed using PrimerQuest (IDT, Coralville, IA), purchased from Sigma-Aldrich, and validated as previously described (176). Quantitative real-time PCR was performed using Power SYBR Green PCR Master Mix (ABI) on 384 well plates (ABI) using an ABI 7900 HT Real-Time PCR system as described previously (32). For each experimental sample, fold-change relative to a calibrator sample was determined using the $2^{-\Delta\Delta ct}$ method with β-actin as the housekeeping gene. The calibrator sample was a pool of mammary gland RNA consisting of 2 RNA samples from each of the three treatment groups.

Statistical Analysis

Treatment differences were assessed using one-way or two-way ANOVA with a Newman-Keuls or Bonferroni post-hoc analysis at the level of $\alpha = 0.05$. GraphPad Prism 5 was used to perform statistical analysis.

Results

Mammary Gland Morphology

Mammary gland morphology was assessed by whole mount analysis at PND 20, 40, and 80, which correspond with pre-pubertal, postpubertal, and mature developmental time points, respectively. As shown in Fig. 1, the mammary epithelial tree occupied a relatively small portion of the mammary fat pad at PND 20, filled approximately half of the gland by PND 40, and had expanded to completely fill the mammary fat pad by PND 80. Overall, gross mammary gland morphology as determined by density of the mammary parenchyma and length of the ductal tree was not affected by treatment at any time point (data not shown). Structures defined as TEBs are illustrated in Fig. 2a. TEB numbers were highest at PND 20, and decreased at each consecutive time point (i.e. PND 40 and 80; Fig. 2b). However, TEB numbers per gland were not different between treatment groups at any time point. Treatment also had no effect of TEB size (data not shown).

Mammary Epithelial Cell Proliferation

Cell proliferation was determined by injecting BrdU prior to euthanasia (Fig. 3a). BrdU incorporation was greater in animals exposed to alcohol *in utero* compared to either control group at PND 20 and compared to pair-fed controls at PND 40, indicating that mammary epithelial cells were more proliferative in alcohol-exposed animals at these time points (Fig. 3b). There were no effects of treatment on proliferation at PND 80 (Fig. 3b). At PND 20, the apoptotic index was not affected by *in utero* alcohol exposure (Fig. 3c). Similar results were obtained at PND 40 (data not shown).

Systemic IGF-I Effects

As shown in Fig. 4a, hepatic IGF-I mRNA expression was significantly increased in animals exposed to alcohol *in utero* compared to both control groups at all time points. In contrast to the changes observed in hepatic mRNA levels, circulating IGF-I levels did not change with treatment, but did increase significantly with time (Fig. 4b). Ligand blot analysis indicated that circulating IGFBP-3 increased in a similar manner to IGF-I concentrations (Fig. 4c). There was no significant treatment effect on any of the IGFBPs detected by ligand blot analysis at any time point (data not shown). Similar to our previous study, alcohol-exposed animals weighed significantly less than either control group (Fig. 4d), although there was no effect on circulating IGF-I levels.

Mammary Gland IGF-I and IGFBP-5 mRNA Expression

At PND 20, IGF-I mRNA levels in the mammary gland were significantly higher in alcohol-exposed animals compared to control animals (Fig. 5a). In contrast, IGF-I mRNA levels did not change over time in the mammary glands of either control group (Fig. 5a). IGFBP-5 mRNA expression in the mammary gland increased between PND 20 and 40 in control animals (Fig. 5b). However, the rise in IGFBP-5 mRNA expression was delayed in alcohol-exposed animals, and at day 40, IGFBP-5 mRNA levels were lower in alcohol-exposed animals relative to pair-fed controls (Fig. 5b).

Mammary Gland Aromatase Expression

As shown in Fig. 6a, aromatase expression was localized to the stroma surrounding the ducts as well as to the adipocytes, in accordance with the work of others

(177, 178). At PND 20 and 40, there was significantly more aromatase expressed in mammary glands of alcohol-exposed animals compared to either control group (Fig. 6b). In the mammary gland, testosterone is converted to E2 by the P450 enzyme aromatase. Therefore, these data suggest that there may be more E2 in the local mammary gland environment in animals exposed to alcohol *in utero*.

Discussion

A sub-optimal fetal environment has been shown to contribute to a variety of adult diseases, including cancer (25, 26, 32, 34). However, the mechanisms that explain how early developmental exposure affects disease susceptibility in adulthood have not been determined. Many studies suggest that epigenetic alterations in gene expression early in life define the individual's response to later events that may enhance their risk for cancer, diabetes, or cardiovascular disease (179, 180). In terms of mammary gland development, fetal exposure to a wide variety of environmental chemicals such as diethylstilbestrol, genistein, nonylphenols, zearalenone, atrazine, and bisphenol-A, have been shown to affect mammary gland development postnatally (125-131). These endocrine disrupting compounds act by altering estrogen or androgen action. There is evidence that fetal alcohol exposure may also alter mammary gland development or cancer susceptibility by altering the estrogen system (32, 33). Since the estrogen system is intricately entwined with the IGF system, we hypothesized that fetal alcohol exposure might alter the IGF-E2 axis to affect early mammary gland development. These alterations might predispose the gland to enhanced susceptibility to carcinogenic exposure later in life.

Previously, Hilakivi-Clarke and colleagues (33) reported significant increases in TEB numbers at PND 21 and 42 in rats exposed to either low or moderate alcohol during fetal development. Only the moderate alcohol diet resulted in enhanced tumor multiplicity in response to DMBA in adult offspring. In contrast, in the present study, exposure to high alcohol *in utero* had no effect on TEB number at similar postnatal time points. The total number of TEBs was highest at PND 20 in all treatment groups and

decreased across time, in agreement with work by Russo and Russo (174). While total TEB number was not affected by *in utero* alcohol exposure, the proliferative index measured by BrdU incorporation in all epithelial structures was greater at PND 20 in mammary glands of alcohol-exposed offspring relative to either control group. This effect was lost by PND 80. The increase in proliferation could be a result of increased IGF-I activity since IGF-I mRNA expression in the mammary gland was elevated at PND 20 in alcohol-exposed offspring when BrdU incorporation was highest. This possibility is supported by studies in transgenic models that show enhanced mammary expression of IGF-I results in increased epithelial cell proliferation. For example, in a transgenic model where IGF-I expression in the mammary gland was driven by the MMTV promoter, IGF-I promoted enhanced alveolar budding in peripubertal virgin mice (103). Similarly, in a transgenic mouse model where tissue IGF-I was overexpressed in the myoepithelial cells adjacent to the ductal epithelium, mammary glands from transgenic mice exhibited enhanced alveolar budding as well as ductal hyperplasia (105). Total BrdU incorporation in epithelial cells was increased between 28 and 35 days of age, similar to the present findings. Conversely, transfer of embryonic mammary buds from IGFR -/- embryos into the cleared fat pad of 3-week old wild-type mice caused decreased ductal elongation and reduced epithelial cell proliferation compared to glands from IGFR +/+ littermates (104).

Interestingly, in the study reported in (105), the increase in total BrdU incorporation observed prior to puberty was lost after puberty, similar to the findings reported here. In spite of this, transgenic mice were more susceptible to carcinogen-induced tumorigenesis, as we have previously reported for rats with our *in utero* alcohol model (32). This suggests that early changes in mammary gland morphology may

correspond with biological outcomes later in life even though the mature gland is not morphologically altered. Additional support for this concept comes from studies with atrizine exposure *in utero*. This treatment led to a decrease in mammary length pre-pubertally that was lost postpubertally. Even though the change in mammary morphology was no longer detectable, the subsequent lactation was suboptimal resulting in stunted pup growth (131).

The availability of IGF-I in the mammary gland could also be increased by a decrease in IGFBP-5 expression, which was observed at PND 40 in alcohol-exposed animals. This could result in more unbound IGF-I available to activate the IGFR, which could contribute to the increased proliferation seen in fetal alcohol-exposed animals at this time point. Human breast cancer cells (MDA-MB-231) transfected with IGFBP-5 (MDA/BP5) exhibit decreased growth compared to cells transfected with a vector control (MDA/VEC) (181). In addition, nude mice injected with MDA/BP5 cells develop smaller tumors compared to mice injected with MDA/VEC cells (181). While a decrease in IGFBP-5 could also decrease apoptosis, terminal deoxynucleotidyl transferase-mediated dUTP nick-end labeling (TUNEL) staining was very low in the present study and was not altered by fetal alcohol exposure, suggesting that increased availability of IGF-I mainly influenced cell proliferation rather than apoptosis.

In addition to the increase in IGF-I and decrease in IGFBP-5 expression observed in alcohol-exposed offspring at early time points, increased aromatase activity was also observed at PND 20 and 40. Hilikivi-Clarke reported an increase in ER-α in mammary tissue of rat offspring exposed to moderate alcohol at 22 weeks of age, though no difference was detected at PND 56 (33). Together, these findings suggest that the E2

system may be altered in rat offspring exposed to alcohol during fetal development. The finding of increased aromatase expression is significant given the multiple mechanisms by which E2 may enhance cell proliferation, including both classical genomic effects as well as more recently recognized non-genomic effects that include cross-talk with the IGFR system (59, 170, 182). While the mechanism responsible for the increase in aromatase expression is unclear, it is interesting that IGF-I enhances aromatase expression in multiple cell types (183, 184). Therefore, it is possible that the increase in IGF-I activity is related to the increase in aromatase expression.

E2 and IGFBP-5 have been reported to be inversely related. For instance, in MCF-7 cells, E2 treatment decreased IGFBP-5 expression, while treatment with the anti-estrogen ICI 182780 increased IGFBP-5 expression (185, 186). These data support our finding at PND 40, where there was increased aromatase expression in the mammary gland, suggestive of higher levels of local E2 production, and decreased expression of IGFBP-5. We have also previously reported a significant increase in circulating E2 levels in alcohol-exposed animals and significantly lower levels of IGFBP-5 mRNA and protein in tumors which develop in these animals in response to a carcinogen (32). Therefore, our previous data together with the current study support the hypothesis that IGFBP-5 expression is altered in fetal alcohol-exposed animals possibly via alterations in E2, which could contribute to the changes observed in mammary gland development.

The changes in local mammary expression of IGF-I did not appear to correlate with changes in circulating IGF-I, which were not significantly altered at any time point. Fetal alcohol spectrum disorder is generally associated with uterine growth retardation in humans and animal models, with a reduced body weight typically observed at birth.

Several studies have looked at associations between stunted growth and the IGF axis. In rats, decreases in circulating IGF-I and hepatic IGF-I expression were observed in late gestation in both dams (187) and fetuses (188), while another study found a decrease in circulating IGF-II but no change in serum IGF-I in late-term fetuses exposed to alcohol (189). Interestingly, one study did report an increase in IGF-I mRNA in the lungs of alcohol-exposed fetal rats (190). In a study that looked at circulating IGF-I and hepatic IGF-I mRNA in alcohol exposed offspring at time points similar to the present work, circulating IGF-I was lower at PND 10 and 20 in alcohol-exposed offspring, but similar to controls at PND 40, which correlated with a catch-up in body weight. No differences were observed at PND 10 and 20 in hepatic IGF-I expression, but interestingly, hepatic IGF-I expression was significantly increased in alcohol-exposed offspring at PND 40 (191). A recent study has examined circulating IGF-I in FAS children. Children born with FAS displayed no difference in circulating IGF-I under the age of 2, while circulating IGF-I was higher in FAS children at 3-4 years of age. By age 5, the difference in circulating IGF-I was lost, while their heights were never significantly different (192). In the present study, an unexpected finding was that hepatic IGF-I mRNA was elevated in animals exposed to alcohol *in utero* at all time points without a corresponding increase in circulating IGF-I. An increase in hepatic IGF-I expression without an increase in circulating IGF-I could be due to the highly regulated homeostatic mechanisms that control circulating IGF-I and could potentially reflect increased uptake of IGF-I by tissues, including the mammary gland. Work with different genetic mouse models support roles for both circulating as well as local IGF-I in the development of the mammary gland (100, 101).

In conclusion, animals exposed to alcohol *in utero* displayed advanced pre-pubertal development of the mammary gland. This advanced development was demonstrated by an increase in epithelial cell proliferation in the glands of animals exposed to alcohol *in utero*. Changes in local expression of IGF-I, IGFBP-5, and aromatase in these animals corresponded with the enhanced proliferative state, supporting the hypothesis that changes in the IGF/E2 axis in early mammary gland development may contribute to the increase in susceptibility to mammary carcinogenesis observed in alcohol-exposed animals (32).

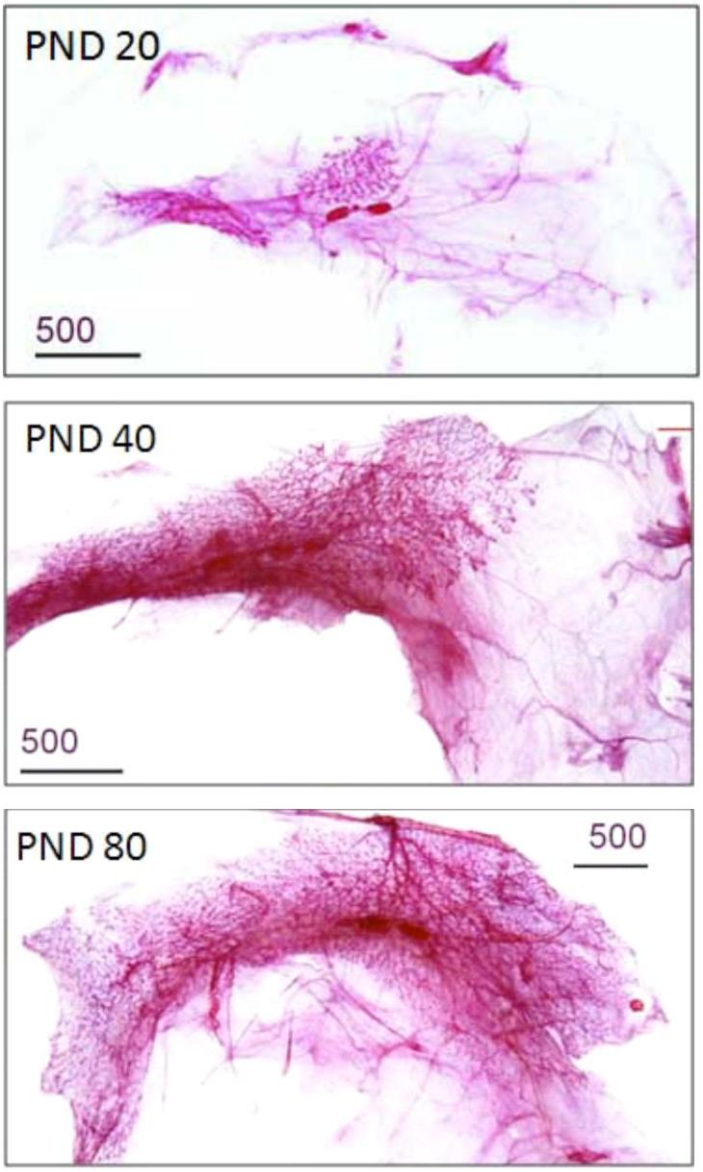

Figure 1. Gross mammary gland morphology is not affected by alcohol exposure in utero. Pups exposed to alcohol in utero and controls not exposed were euthanized at PND 20, 40, or 80. The fifth inguinal mammary gland was processed for whole-mount analysis. Mammary density and length of the ductal structure were not affected by treatment at any time point; therefore, representative whole mounts are shown without respect to treatment.

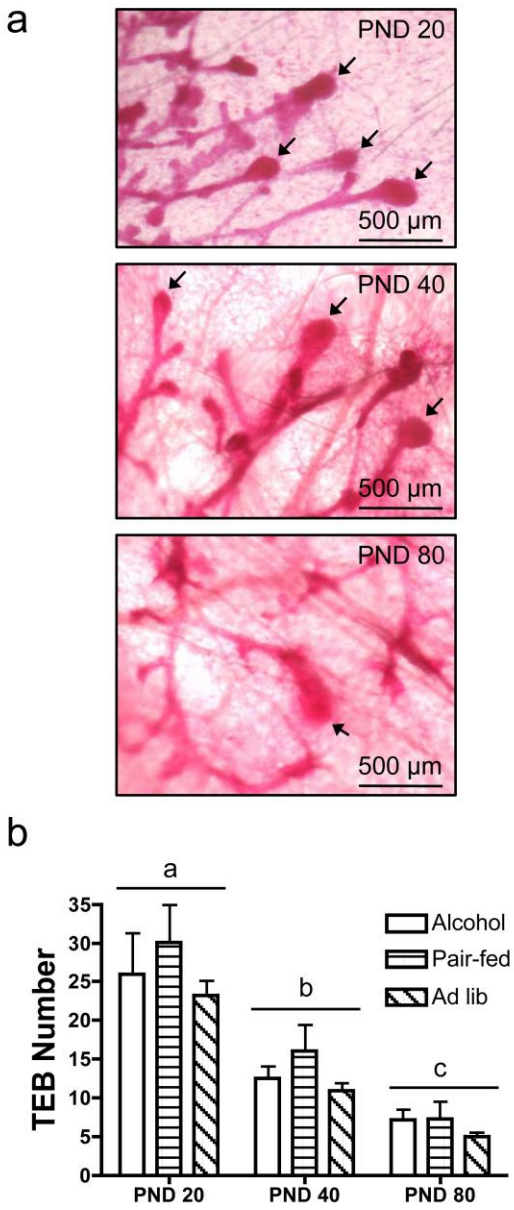

Figure 2. Terminal end bud (TEB) numbers decrease with time, but are not affected by in utero alcohol exposure. Pups exposed to alcohol in utero and controls not exposed were euthanized at PND 20, 40, or 80. The fifth inguinal mammary gland was processed for whole-mount analysis, and total TEBs were counted for each gland. **a** Digital images of whole mounts taken at x8 magnification. *Arrows* represent TEBs. **b** *Bars* represent mean±SEM of total TEBs per gland

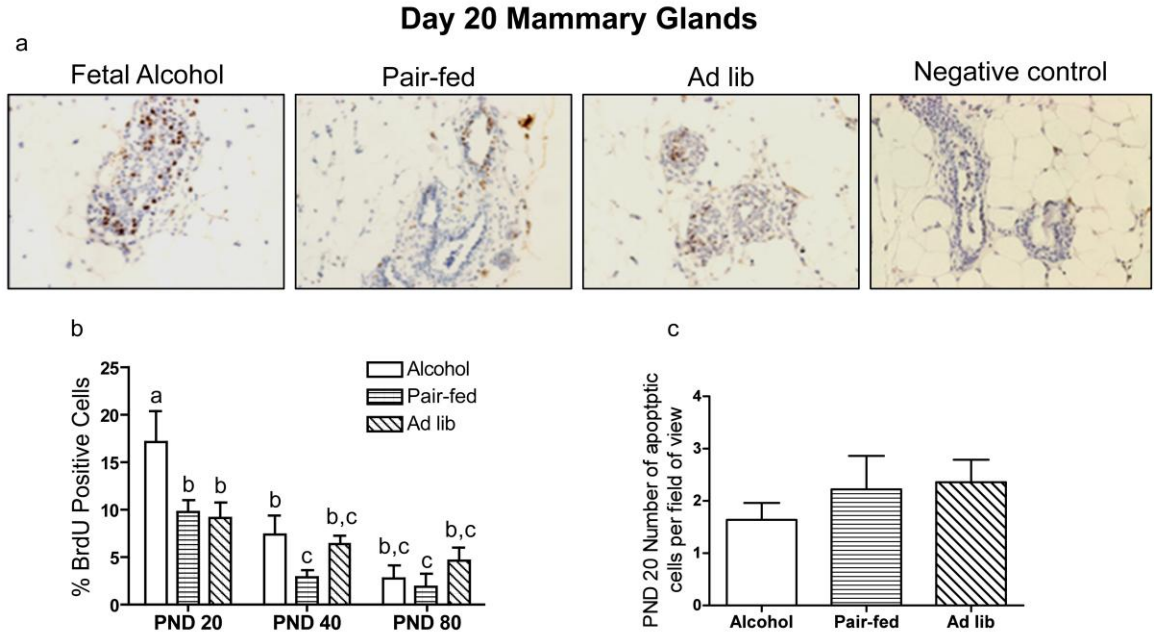

Figure 3. Epithelial cell proliferation is higher in animals exposed to alcohol in utero at PND 20 and 40. Mammary gland sections were prepared and stained for BrdU by immunohistochemistry as described in Materials and Methods. **a** Representative sections stained for BrdU. The negative control represents a section stained with an isotype IgG antibody. **b** BrdU incorporation was quantified by counting BrdU-stained cells and expressing them as a percent of total epithelial cells. For each mammary gland, two serial sections were counted and averaged. Total epithelial cells in each section were counted for PND 20, while up to 1,000 cells per section were counted for PND 40 and 80. *Bars* represent mean±SEM with different letters denoting a significant difference within each treatment group. A two-way ANOVA was performed with a Bonferroni post hoc test at the level of $\alpha = 0.05$ ($n = 10$, 9, and 13 for alcohol, pair-fed, and ad lib groups, respectively, at each time point). **c** Number of apoptotic cells per field of view

Figure 4. Hepatic IGF-I mRNA is increased in animals exposed to alcohol in utero, while serum IGF-I and IGFBP-3 increase over time in all treatment groups. Hepatic tissue and serum was collected from animals exposed to alcohol and controls not exposed and prepared as described in Materials and Methods. **a** Hepatic IGF-I mRNA expression was assayed by quantitative RT-PCR ($P<0.05$). **b** Circulating IGF-I levels were assayed by ELISA ($P<0.001$). **c** Serum IGFBP-3 levels were assayed by ligand blot ($P<0.0001$). **d** Weekly body weight recordings ($P<0.0001$). *Bars* represent mean±SEM with different letters denoting significant differences. A two-way ANOVA was performed in **a-c** with a Bonferroni post-test at the level of $\alpha = 0.05$ (n = 10, 9, or 13 for alcohol, pair-fed, and ad lib groups, respectively, at each time point). A repeated-measures one-way ANOVA was performed in **d** with a Newman-Keuls post-test at the level of $\alpha = 0.05$ (during weeks 1-4, n = 30, 28, and 40; during weeks 5 and 6, n = 20, 18, and 27; and during weeks 7 and 8, n = 10, 9, and 13 for alcohol, pair-fed, and ad lib groups, respectively).

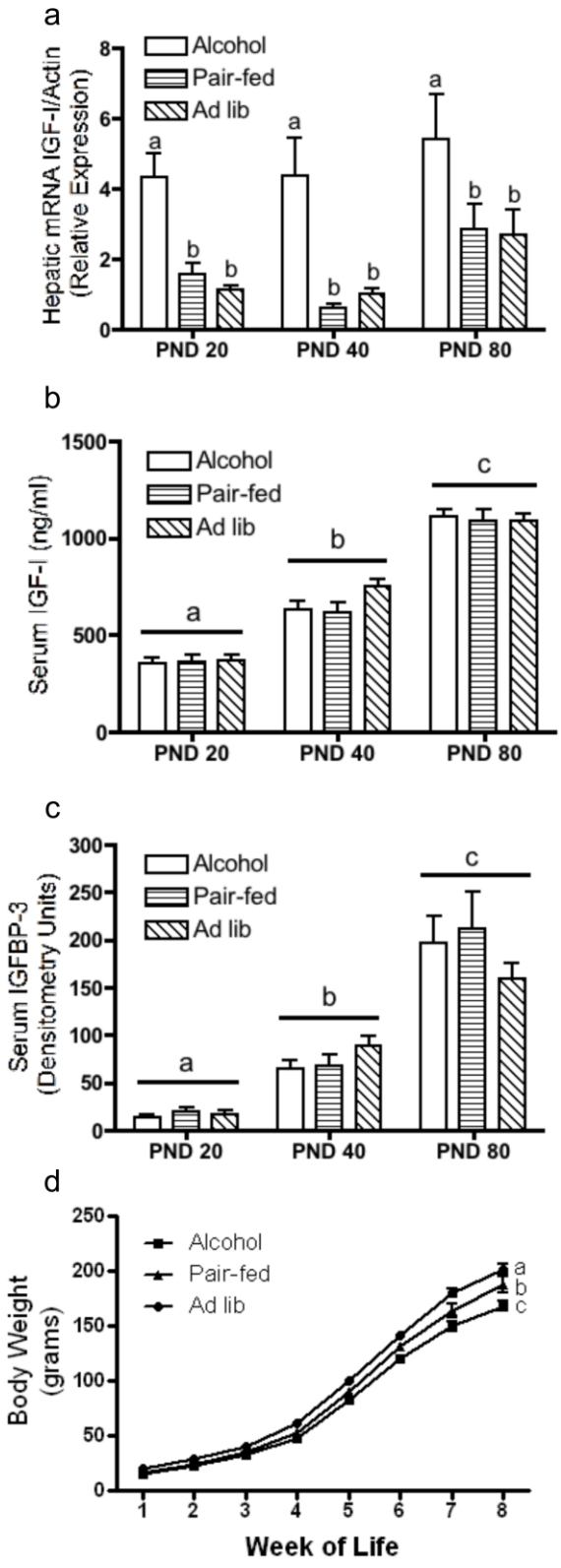
a
Hepatic mRNA IGF-I/Actin (Relative Expression)
Alcohol
Pair-fed
Ad lib
PND 20
PND 40
PND 80
b
Serum IGF-I (ng/ml)
c
Serum IGFBP-3 (Densitometry Units)
d
Body Weight (grams)
Week of Life

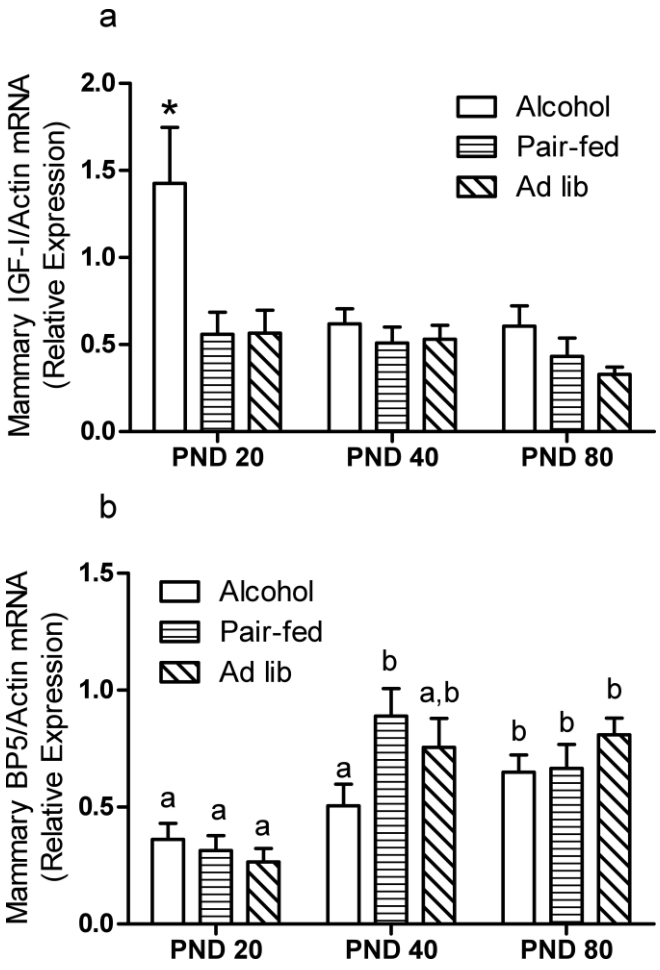

Figure 5. IGF-I mRNA is significantly higher at PND 20 and IGFBP-5 mRNA increased later in the mammary glands of alcohol-exposed animals. Mammary gland tissue was collected; RNA was isolated, and quantitative PCR was performed as described in Materials and Methods. **a** Mammary gland IGF-I mRNA expression with *asterisk* denoting significant difference ($P<0.001$). **b** Mammary gland IGFBP-5 mRNA expression with *different letters* denoting significant differences ($P<0.05$). *Bars* represent mean±SEM. A two-way ANOVA was performed with a Bonferroni post-test at the level of $\alpha = 0.05$ (n = 10, 9, or 13 for alcohol, pair-fed, and ad lib groups, respectively, at each time point).

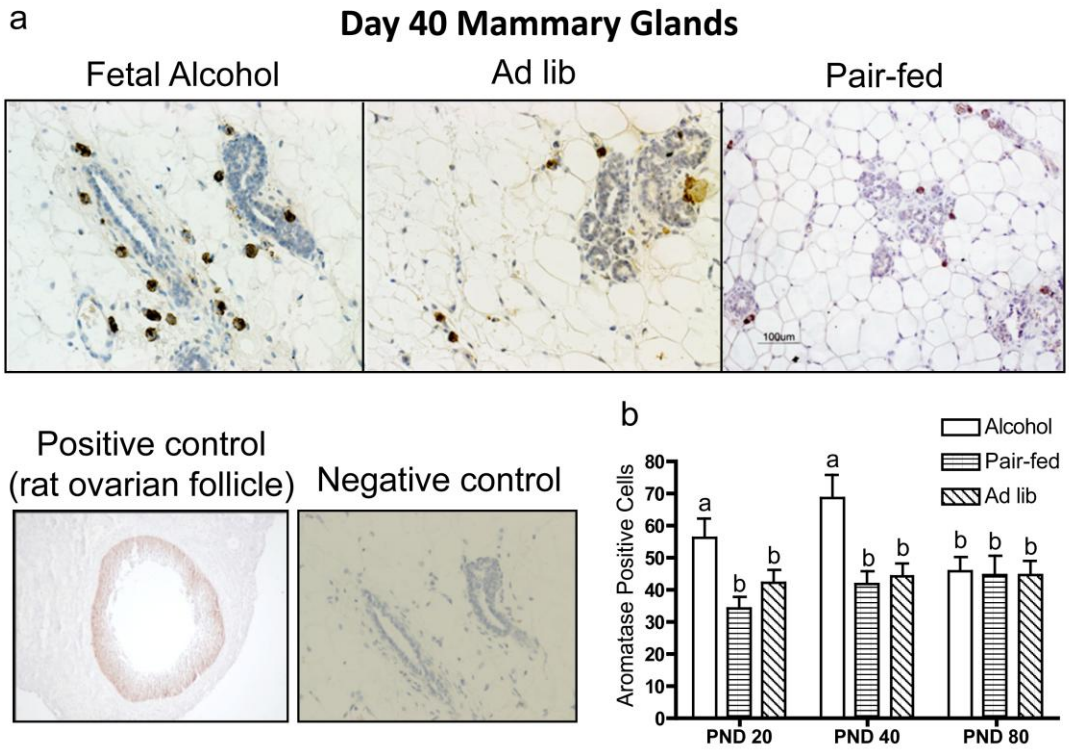

Figure 6. Aromatase expression is increased in the mammary glands of animals exposed to alcohol at PND 20 and 40. Mammary glands were prepared and stained for aromatase as described in Materials and Methods. **a** Representative sections of aromatase-stained cells. Negative control represents a section stained with an isotype IgG antibody. **b** Aromatase-positive cells were quantified by counting three fields of view and totaling the numbers for each section. *Bars* represent mean±SEM of aromatase-positive cells per gland with *different letters* denoting significant differences within a treatment group ($P<0.05$). A two-way ANOVA was performed with a Bonferroni post hoc text at the level of $\alpha = 0.05$ (n = 10, 9, or 13, for alcohol, pair-fed, and ad lib groups respectively, at each time point).

Chapter 3

Effects of Fetal Alcohol Exposure on Tumor Development and Gene Expression in Rats

Abstract

Alcohol exposure *in utero* increases susceptibility to carcinogen-induced mammary tumorigenesis in adult rats. However, the mechanisms underlying the enhanced susceptibility are not well understood. The current study was conducted to assess the histological classification, receptor status, and signaling molecule expression of NMU-induced mammary tumors from animals exposed and not exposed to alcohol *in utero* at 16 weeks post-NMU injection. Beginning on gestation day (GD) 7 until parturition, pregnant Sprague Dawley rats were fed either a liquid diet containing 6.7% ethanol (alcohol), an isocaloric liquid diet without ethanol (pair-fed), or rat chow *ad libitum* (ad lib). At birth, female F1 progeny were cross-fostered to control dams. Pups were weaned at postnatal day (PND) 21 and fed rat chow ad libitum for the remainder of the experiment. On PND 50, female offspring were administered a single intraperitoneal injection of 50 mg/kg body weight N-nitroso-N-methylurea (NMU) to induce mammary tumors. Mammary glands were palpated weekly and offspring were euthanized at 16 weeks post-NMU injection. Starting at 12 weeks post-NMU injection, the number of tumors rapidly increased in the alcohol group. However, this dramatic increase was not observed in either control group. At 16 weeks post-NMU injection, 45% of animals developed tumors in the alcohol group, whereas only 33% developed tumors in each of the pair-fed and ad lib groups. Overall, the alcohol group developed more tumors

compared to either control group. The alcohol group also developed more hyperplasias and adenocarcinomas compared to the control groups. Although tumor receptor status for ERα and HER2 did not differ among the treatment groups, the alcohol group developed more PR positive tumors compared to the pair-fed group. Alcohol-exposed animals exhibited increased Snail, IGF-II, and IGFBP-5, as well as decreased ERα tumor mRNA expression at 16 weeks post-NMU injection. Thus, the current study provides further evidence that alcohol exposure *in utero* enhances susceptibility to carcinogen-induced mammary tumorigenesis in adulthood. These data also indicate that alterations in IGF-II, IGFBP-5, ERα, PR, and Snail expression may be involved in the molecular mechanisms underlying the increased susceptibility to NMU-induced mammary tumors in the alcohol group. Additional studies should be aimed at these particular pathways to further delineate the mechanisms.

Introduction

It has long been recognized that prenatal alcohol exposure can lead to fetal alcohol spectrum disorder (FASD), the most severe case being fetal alcohol syndrome (FAS) (1). It is estimated that among younger school children FASD affects 20 to 50 per 1000 live births in the US and some Western European countries, while FAS affects 2 to 7 per 1000 live births in the US (5). In 2005 the U.S. Surgeon General issued an advisory stating that women who are pregnant or who are planning on becoming pregnant should abstain from drinking alcohol (6). Despite this warning, the Centers for Disease Control report that 51.5% of women who are of child-bearing age and 7.6% of pregnant women consume alcohol. Of pregnant women surveyed, 1.4% self-reported binge drinking in the U.S. (7). Of further concern is that worldwide, 41% of pregnancies are unplanned (8). Thus, prenatal alcohol exposure is likely to occur during the early critical stages of fetal development before a woman may even know that she is pregnant. Alcohol can rapidly diffuse across the placenta and within two hours of alcohol consumption the blood alcohol concentration (BAC) of the fetus is approximately equal to that of the mother. Elimination of alcohol from the blood is dependent on the mother's metabolism since metabolic capability of the fetus is limited. Furthermore, the continual re-uptake of the ethanol-containing amniotic fluid results in prolonged alcohol exposure causing a sustained BAC in the fetus even as the maternal BAC decreases (9).

Breast cancer is the most common form of cancer among women and the National Cancer Institute estimates that there were 232,340 new cases among women in the U.S. in 2013 (10). A newly emerging concept is that environmental exposures and lifestyle choices during pregnancy may affect the offspring's risk of disease in adulthood (25-28).

This has led to the idea that a woman's breast cancer risk may be pre-programmed prior to birth (29-31). In support of this hypothesis, moderate to high levels of alcohol exposure *in utero* increase susceptibility to carcinogen-induced mammary tumorigenesis in adulthood (32, 33). These studies suggest that an additional adverse outcome of alcohol consumption during pregnancy could be that women born to these mothers have increased risk of developing breast cancer as adults. Fetal exposure to alcohol has been shown to increase risk of childhood leukemia, suggesting that findings in rodent models may be relevant to human disease (34).

Estradiol (E2) plays an integral role in mammary gland development as well as breast cancer progression (193, 194). It acts via the estrogen receptor (ER) to initiate gene transcription (56, 59). ERα tumor expression has become a prognostic and predictive marker of breast cancer and it is utilized in the clinic to determine a patient's treatment regimen. The insulin-like growth factor (IGF) family is also a critical component of normal mammary gland development and breast cancer etiology (98). It consists of two ligands (IGF-I and IGF-II), two IGF receptors (IGF-IR and IGF-IIR), and six IGF-binding proteins (IGFBP-1 through IGFBP-6) that modulate the actions of IGFs (94, 95). IGF-I and IGF-II primarily act via the IGF-IR to initiate a downstream signaling cascade that ultimately activates the MAPK and PI3K/Akt pathways (96, 97). There is substantial evidence that the IGF and E2 signaling pathways crosstalk, particularly in normal mammary gland development as well as in breast cancer (97). Thus, although the mechanisms underlying the increased susceptibility to carcinogen-induced mammary tumors observed in alcohol-exposed animals are not well understood, we hypothesized that the E2 and IGF signaling pathways may be involved.

We have previously shown that at 23 weeks post NMU-injection, rats exposed to alcohol *in utero* develop more malignant tumors as well as more ERα negative tumors, and exhibit decreased tumor IGFBP-5 expression, while none of the other IGFBPs changed. These findings suggest that alterations in the IGF and E2 systems may play a role in the underlying mechanism (32). We have also shown that mammary glands from alcohol-exposed animals displayed increased epithelial cell proliferation and aromatase expression at PND 20 and 40, increased IGF-I expression at PND 20, and lower IGFBP-5 expression at PND 40 (Chapter 2). These data indicate that alcohol exposure *in utero* may advance mammary development via the IGF and E2 systems. Together the data from these two studies suggest that continued examination of the IGF and E2 systems is needed in order to further elucidate their potential roles in the underlying mechanisms of the increased susceptibility to carcinogen-induced mammary tumors observed in the fetal alcohol group.

We previously analyzed the effect of alcohol exposure *in utero* on carcinogen-induced mammary tumorigenesis at 23 weeks post-NMU injection. This is the timepoint at which tumor numbers had reached a plateau in all treatment groups (32). In that study, we found that at 16 weeks post-NMU injection, the alcohol group had significantly more tumors compared to the pair-fed and ad lib groups, which did not differ. The current study was conducted using a larger number of animals and terminated earlier as compared to our previous study with the goal of analyzing tumors at 16 weeks post-NMU injection, the time point at which maximal differences in tumor number were found between the three treatment groups (32). Our aim was to assess the histological classification, receptor status, and signaling molecule expression of NMU-induced

mammary tumors from animals exposed and not exposed to alcohol *in utero* at 16 weeks post-NMU injection.

Materials and Methods

Animal Study

Timed-pregnant Sprague-Dawley rats (CD IGS rat, strain code: 001) were purchased from Charles River (Wilmington, MA), received on gestation day (GD) 5, and individually housed in a controlled environment with a 12-hour light/dark cycle. Upon arrival, dams were weighed and divided into three groups (n = 7). Dams were acclimated to the environment for two days (GD 5 and 6). Beginning on GD 7 until parturition, dams were fed either a liquid diet containing ethanol (alcohol; Bio-Serv, Cat# F1258SP, Lieber DeCarli ’82 diet, Frenchtown, NJ), an isocaloric liquid diet without ethanol (pair-fed; Bio-Serv, Cat# F1259SP, Lieber DeCarli ’82 diet), or rat chow ad libitum (ad lib, Purina Mills Lab Diet, Cat# 5012, St. Louis, MO). Composition of the diets used for the three treatment groups is listed in Table 1. To acclimate the alcohol group to their diet, dams were given 2.2% (v/v) of ethanol in the diet on GD 7 and 8, 4.4% (v/v) on GD 9 and 10, and 6.7% (v/v) from GD 11 through parturition. Our lab has determined that dams drinking 6.7% ethanol have an average blood alcohol concentration (BAC) of 147.4 mg/dl (data not shown). This is in accordance with work of others who have shown that 6.7% ethanol results in BACs between 100 and 160 mg/dl (171, 172, 195, 196). This translates to approximately three to five drinks in two hours in women (173). The volume of liquid diet consumed by dams in the alcohol and pair-fed groups was recorded daily. The average volume consumed by the alcohol group was calculated on a daily basis and that amount was given to the pair-fed dams on the subsequent day. This was done in order to ensure that the liquid diets were isocaloric. Liquid diets were prepared according to the manufacturer’s specifications, mixed in a household blender, and given to dams

daily within 2 hours prior to the dark cycle. Dams were weighed every other day and weights were recorded. Entire litters were weighed at birth; hence the litter weight data collected was not segregated by sex. At birth, female F1 progeny were cross-fostered to control (pair-fed and ad lib) dams and litters were normalized to eight pups per dams. From 1 week after birth until study termination, individual female offspring were weighed weekly and weights were recorded. Pups were weaned at PND 21 and fed rat chow ad libitum for the remainder of the experiment (n = 31, 27, and 33 offspring for the alcohol, pair-fed, and ad lib groups, respectively). On PND 50, female offspring were administered a single intraperitoneal (I.P.) injection of 50 mg/kg body weight NMU (Sigma-Aldrich, St. Louis, MO) to induce mammary tumors. Mammary glands were palpated weekly to assess tumor latency. Offspring were euthanized by rapid decapitation at 16 weeks post-NMU injection. Mammary tumors and contralateral mammary glands were harvested from each animal. Half of each tissue was fixed in 10% Richard Allan Scientific™ neutral buffered formalin (NBF; ThermoScientific, Waltham, MA) for histological analysis. The remaining half of the tissue was snap-frozen in liquid nitrogen and stored at -80°C for RNA analysis. Animal care was performed in accordance with guidelines from the Rutgers Institutional Animal Care and Use Committee (IACUC) and complied with National Institutes of Health policy.

Histology

Fixed mammary gland or tumor tissue was dehydrated in increasing concentrations of ethanol, cleared in xylene, infiltrated with and embedded in Paraplast X-tra (Leica Biosystems, Buffalo Grove, IL), sectioned at 6 μm, and placed onto

Superfrost® Plus microscope slides (VWR, Radnor, PA) using facilities located in the Molecular Pathology Facility Core of the Environmental and Occupational Health Sciences Institute at Rutgers University. Slides were baked for 30 minutes at 60°C, deparaffinized in xylene, and rehydrated in decreasing concentrations of ethanol. Slides were stained with hematoxylin and eosin and mounted with Permount (Fisher Scientific, Pittsburgh, PA). Slides were read blindly by toxicological pathologist Dr. Kenneth Reuhl.

Immunohistochemistry (IHC)

For ERα IHC, samples were processed, sectioned, and placed onto slides as described above. Slides were baked in a hybridization oven at 60°C for 30 minutes, deparaffinized in xylene (Fisher Scientific), placed in xylene/100% ethanol (50:50), and rehydrated in decreasing concentrations of ethanol (100%, 95%, 90%, 80%, 70%, 50%) followed by water. Antigen retrieval was performed by boiling slides in 0.01 M sodium citrate buffer for 30 minutes. Timing was recorded once the sodium citrate buffer returned to boiling after the slides were placed in the buffer. Slides were cooled to 45°C in the buffer. After rinsing in 1X tris-buffed saline (TBS), endogenous peroxidase activity was blocked by adding 3% H_2O_2 to the slide for 10 minutes. After rinsing in 1X TBS, tissues were circled with a PAP pen (Life Technologies, Carlsbad, CA). Tissues were blocked in normal goat serum (Vector Laboratories, Burlingame, CA) for 20 minutes at room temperature. Each section of tissue was then incubated overnight at 4°C in a humidified chamber with either rabbit-ERα primary antibody (1:500; MC-20, Santa Cruz Biotechnology, Dallas, TX) made in PBS + 1% BSA (Amresco, Solon, OH) or rabbit primary antibody isotype control (Life Technologies), which served as a negative control

on each slide. The next day, slides were allowed to warm to room temperature, rinsed in 1X TBS, then incubated with biotinylated goat anti-rabbit secondary antibody (Vector Laboratories) for 40 minutes at room temperature. Slides were then rinsed in 1X TBS and incubated with the avidin and biotinylated horseradish peroxidase macromolecular complex (ABC) reagent from the Vectastain Elite ABC kit (Vector Laboratories) for 40 minutes at room temperature. After rinsing in 1X TBS, slides were placed in 0.1% 3,3'-diaminobenzidine (DAB, Sigma-Aldrich) made in 0.1 M Tris and 0.2% hydrogen peroxide for 7 minutes. Slides were placed in distilled H_2O to stop the reaction then counterstained with hematoxylin (Sigma-Aldrich), placed in water followed by increasing concentrations of ethanol (50%, 70%, 80%, 90%, 95%, 100%), xylene/100% ethanol (50:50), and xylene to dehydrate and clear the tissues. Finally, slides were mounted with Permount (Fisher Scientific). Positive staining was identified as a brown color. To determine ERα tumor status, three fields of view were selected for each tumor. The number of ERα positive cells and the total number of cells in each field of view were counted and the percentage of ERα positive cells for that field of view was calculated. The average percent of ERα positive cells from the three fields of view was calculated to determine the overall percent of ERα positive cells in that tumor. Two members of the lab independently performed the counting and calculations as described above and the average was used as the final ERα percentage.

Progesterone receptor (PR) IHC was carried out as described for ERα, with the following exceptions: after rehydration, slides were rinsed in 1X TBS and endogenous peroxidase activity was blocked with 3% H_2O_2 made in methanol for 10 minutes prior to antigen retrieval. Slides were blocked in 50% normal horse serum (Vector Laboratories)

for 1 hour at room temperature. Slides were incubated overnight at 4°C with either a mouse monoclonal primary antibody for PR (1:300, Thermo Scientific) or mouse primary antibody isotype control (Life Technologies). A biotinylated horse anti-mouse secondary antibody (Vector Laboratories) was used.

HER2 IHC was carried out as described above for ERα using a rabbit HER2/ErbB2 primary antibody (29D8, 1:300, Cell Signaling, Danvers, MA). For PR and HER2 tumor status, entire tissue sections were scanned at 10x and 20x magnifications under the microscope by two members of the lab. Tumors were considered PR or HER2 positive if ≥10% of the cells had positive staining.

RNA Analysis

Mammary tumor tissue or contralateral mammary gland tissue (20 - 40 mg) was homogenized in TRIzol Reagent (Life Technologies). RNA was isolated using the Nucleospin RNA II kit (Macherey-Nagel, Bethlehem, PA) according to the manufacturer's specifications. RNA concentration and quality was measured using the Nanodrop ND-1000 Spectrophotometer (Thermo Scientific). RNA integrity was verified using the Agilent 2100 Bioanalyzer and the Agilent RNA 6000 Nano kit (Agilent Technologies, Santa Clara, CA). RNA with an RNA integrity number (RIN) of greater than 6 was considered good quality RNA and was used for further analysis. The High Capacity cDNA Reverse Transcription kit (Life Technologies) was used to reverse transcribe 2 μg RNA using the GeneAmp® PCR System 9700 (Life Technologies). Primer sets were designed using either Primer Express 3.0 software (Life Technologies), Primer-BLAST (NCBI, www.ncbi.nlm.nih.gov/tools/primer-blast/), or PrimerQuest

(IDT, Coralville, IA), and purchased from Sigma-Aldrich. Primer sequences for all genes analyzed are listed in Table 2.

To validate each primer set, individual standard curves were established using serial dilutions (1:2 to 1:200,000) of either a mammary gland or tumor RNA pool consisting of samples from the three treatment groups. The slope and amplification efficiency of the standard curve for each primer set was determined. Amplification efficiencies between 90% and 110% were considered acceptable. Melt curves were evaluated to ensure that a single product was amplified. If the primers for the target and housekeeping genes amplify at the same rate, then the efficiency of these primers should be approximately equal. To determine this, ΔC_t ($C_{t\ target} - C_{t\ reference}$) was plotted for each dilution of the standard curve. As per the Applied Biosystems guidelines, if the absolute value of the slope for ΔC_t vs. log input amount of RNA is less than 0.1, then the primers for the target and housekeeping genes amplify at the same rate and the $\Delta\Delta C_t$ method can be used to analyze the data. If the absolute value of the slope for ΔC_t vs. log input amount of RNA is greater than 0.1, then the primers for the target and housekeeping genes amplify at different rates. In this case, the standard curve method is required for data analysis.

Quantitative reverse transcription PCR (qRT-PCR) was performed using Power SYBR Green PCR Master Mix (Life Technologies) on 384 well plates (Life Technologies) using a ViiA™7 Real-Time PCR system at RUCDR (Piscataway, NJ). β-actin was used as the housekeeping gene. Data were analyzed using the ViiA™7 software version 1.1 (Life Technologies). For primer sets where the target and housekeeping genes amplified at the same rate, the fold-change relative to a calibrator sample was determined

using the $\Delta\Delta C_t$ method as described by Applied Biosystems. For primer sets where the target and housekeeping genes did not amplify at the same rate, data were analyzed using the standard curve method. The calibrator sample was a pool of either mammary gland or tumor RNA consisting of RNA samples from each of the three treatment groups.

Statistical Analysis

Treatment differences between the alcohol, pair-fed, and ad lib groups were assessed using a one-way ANOVA with a Newman-Keuls post hoc analysis at the level of $\alpha = 0.05$. Treatment differences between the alcohol and pair-fed groups were analyzed using an unpaired t-test or an unpaired t-test with Welch's correction (if the variances were not equal). Tumor incidence (% of rats with tumors) was analyzed using a log-rank test at the level of $\alpha = 0.05$. GraphPad Prism version 4.0a (La Jolla, CA) was used to perform statistical analyses.

Results

Dam and Offspring Parameters

Throughout gestation alcohol and pair-fed dams gained less weight compared to ad lib dams (Figure 1A). At 21 days of gestation, average dam weight was 288.4 g, 241.0 g, and 380.7 g for the alcohol, pair-fed, and ad lib groups, respectively. At this time point there was also a significant difference in the weight of the alcohol and pair-fed dams (Figure 1A; one-way ANOVA for gestation day 21 $p < 0.0001$ with a Newman-Keuls post test, alcohol vs. pair-fed $p < 0.05$, alcohol vs. ad lib $p < 0.001$, and pair-fed vs. ad lib $p < 0.001$). All pair-fed and ad lib dams gave birth on gestation day 22 with the exception of one pair-fed dam which gave birth on gestation day 23. Two alcohol dams gave birth on gestation day 22 and the remaining five dams gave birth on gestation day 23 (Table 3). Litter size did not differ significantly among the three treatment groups, although litters tended to be smaller for dams fed the alcohol and pair-fed diets (Figure 1B). Entire litters were weighed at birth. It should be noted that litter weight was not segregated by sex. Average litter weight was 60.3 g, 48.0 g, and 74.0 g for the alcohol, pair-fed, and ad lib groups, respectively. Litters from alcohol and pair-fed dams weighed significantly less than litters from ad lib dams. Litters from pair-fed dams weighed less than litters from alcohol dams, but the difference was not statistically significant (Figure 1C, one-way ANOVA $p = 0.0062$ with a Newman-Keuls post test, alcohol vs. pair-fed $p > 0.05$, alcohol vs. ad lib $p < 0.05$, and pair-fed vs. ad lib $p < 0.01$). Beginning at cross-fostering, individual weights were recorded for female offspring at regular intervals until study termination (Figure 1D). Throughout the course of the study, offspring exposed to alcohol *in utero* and offspring born to pair-fed dams weighed less than offspring born to

ad lib dams (Figure 1D). At study termination, offspring born to alcohol and pair-fed dams weighed significantly less than the offspring born to ad lib dams, but no difference in weight of offspring was observed among the alcohol and pair-fed groups (Figure 1D, one-way ANOVA for data at study termination $p < 0.0001$ with a Newman-Keuls post test, alcohol vs. pair-fed $p > 0.05$, alcohol vs. ad lib $p < 0.001$, and pair-fed vs. ad lib $p < 0.001$). Average weight of offspring at study termination was 320.1 g, 308.0 g, and 350.2 g, for the alcohol, pair-fed, and ad lib groups, respectively. Although the alcohol and pair-fed dams themselves had significantly different weights at 21 days of gestation, litter size, litter weight, and weight of offspring at study termination did not differ between the two groups.

Tumor Parameters

The first mammary tumor was detected at 5 weeks post-NMU injection in the alcohol group, whereas the first tumor in the pair-fed and ad lib groups was detected at weeks 6 and 8, respectively (Figure 2D). Tumors were detected at various weeks throughout the study in the three treatment groups (Figure 2D). Starting at 12 weeks post-NMU injection, the number of tumors rapidly increased in the alcohol group. However, this drastic increase was not observed in either control group (Figure 2C). At 16 weeks post-NMU injection, tumor incidence (percent of animals with tumors) was higher in the alcohol group compared to the pair-fed and ad lib groups although the difference was not significant (Figure 2A, Kaplan-Meier survival curve with a log-rank test $p = 0.5794$). In the alcohol group 45% of animals developed tumors, whereas only 33% developed tumors in each of the pair-fed and ad lib groups. There were also several weeks

throughout the study when tumor incidence was greater in the alcohol group compared to the control groups. Tumor incidence was also highest in the alcohol group when the data were normalized by litter (data not shown). Tumor multiplicity representing the average number of tumors per tumor bearing animal also tended to be higher in the alcohol group compared to either control group (Figure 2B; one-way ANOVA $p = 0.0746$). As a result at 16 weeks post-NMU injection, the alcohol group developed more tumors overall compared to either control group (Figure 2C). The same results were obtained when the data were normalized by litter (data not shown).

Tumor Type

To determine tumor type, tumors were stained with hematoxylin and eosin and evaluated by a toxicological pathologist who was blinded to treatment. Ductal/cystic hyperplasia was defined by increased proliferation of benign glandular structures, with predominantly regular cells and nuclei. Adenomas were defined by a more solid-phase glandular structure with regular cells and nuclei predominating. Adenocarcinomas presented primarily as solid-phase lesions containing many atypical and anaplastic cells, a high mitotic rate (including numerous atypical mitoses), and observable zones of tumor necrosis. In general, tumors contained several different types of lesions and were classified by the most advanced type of lesion present in the tumor. It is important to note that many tumors were borderline in terms of their classification. In addition, many tumors exhibited extensive stromal inflammation. The alcohol group developed more hyperplasias and adenocarcinomas compared to the control groups. The majority of pair-fed animals developed adenomas. The ad lib group developed adenomas and

adenocarcinomas, but no hyperplasias (Figure 3). These data suggest that alcohol exposure *in utero* induces more atypia in the mammary gland as displayed by the fact that more hyperplasias were observed in this group compared to the control groups as early as 16 weeks post-NMU injection. In addition, not only did the alcohol group develop more tumors overall (Figure 2C), they also developed more adenocarcinomas (Figure 3), suggesting that fetal alcohol leads to a more malignant phenotype in response to a carcinogenic insult.

Tumor Receptor Status

Immunohistochemistry (IHC) was performed to determine ERα, PR, and HER2 receptor status of the tumors. Representative tumors classified as ERα positive and negative are shown in Figure 4A. The percentage of ERα positive cells varied widely in all treatment groups, with some tumors having little to no ERα expression and other tumors containing up to 30% ERα positive cells (Figure 4B). There was not a statistically significant difference in ERα expression among the treatment groups. Average percentage of ERα positive cells was 12.6% (alcohol), 15.6% (pair-fed), and 13.3% (ad lib). However, these data indicate that in general, NMU induces mammary tumors with a wide range of ERα positivity. PR positive and PR negative tumors developed in all three treatment groups (Figure 5). The majority of tumors in the alcohol and pair-fed groups were PR negative (66% and 92%, respectively), whereas the ad lib group had approximately equal numbers of PR positive and PR negative tumors (43% and 57%, respectively). Interestingly, the alcohol group developed more PR positive tumors (35%)

compared to the pair-fed group (8%). All tumors were HER2 negative across treatment groups (Figure 6).

Gene Expression of Tumors and Contralateral Mammary Glands

To identify genes that might be involved with increased tumorigenesis, pooled RNA samples from each treatment group were analyzed using a custom PCR array (SA Biosciences) that included genes involved in epithelial to mesenchymal transition (EMT), E2/ER signaling and tumorigenesis (Table 4). Results of this array identified Snail, Twist, and GATA3 as candidate genes. qRT-PCR was used to confirm these findings for individual tumor samples. Tumors from the alcohol group exhibited a 31% increase in Snail mRNA expression compared to the pair-fed group (Figure 7A; one way ANOVA for all treatment groups $p = 0.1648$, unpaired t-test with Welch's correction between the alcohol and pair-fed groups $p = 0.0414$). Adenomas from the alcohol group exhibited a 29% increase in Snail mRNA expression compared to the pair-fed group and adenocarcinomas from the alcohol group exhibited a 34% increase (Figure 7B). Snail expression among the hyperplasias could not be compared because there was not enough tissue from the one hyperplasia that developed in the pair-fed group to do both IHC and qPCR. Twist and GATA3 mRNA expression was not different among tumors from the three treatment groups (Figure 7C and 7D).

Previously, we found that mammary IGF-I mRNA was higher in offspring exposed to alcohol *in utero* relative to controls at PND 20, while mammary IGFBP-5 mRNA was lower in this group at PND 40. In addition, hepatic IGF-I mRNA expression was increased at PND 20, 40, and 80 in fetal alcohol-exposed animals (Chapter 2). These

data indicate that alcohol exposure *in utero* may advance mammary development via the IGF system, which could contribute to the increased susceptibility to mammary cancer later in life. For this reason, we sought to determine expression of signaling molecules in the IGF pathway in tumors of animals exposed and not exposed to alcohol *in utero*. There were no significant differences in IGF-I, IGFR, Akt1, or Akt2 mRNA expression among the three treatment groups (Figure 8). Although Akt1 and Akt2 mRNA expression was not altered in tumors of the alcohol group compared to the pair-fed group, it is possible that Akt1 and/or Akt2 activation (phosphorylation), rather than mRNA expression, is altered.

IGF-II mRNA expression was increased by 9.4-fold in tumors from the alcohol group compared to the pair-fed group (Figure 9A; one way ANOVA for all three treatment groups $p = 0.3173$, unpaired t-test with Welch's correction $p = 0.0352$ for alcohol and pair-fed groups). There was one value that was an outlier in each of the alcohol and ad lib groups, which accounts for the large standard error bars. When these data were analyzed by tumor type, IGF-II mRNA expression was increased in the adenomas (16.5 fold) and adenocarcinomas (5.3 fold) of the alcohol group compared to each tumor type in the pair-fed group (Figure 9B). The large standard error in the hyperplasias of the alcohol group is due to the same outlier as described above in Figure 9A. Tumors from the alcohol group exhibited a 70% increase in IGFBP-5 mRNA expression compared to tumors from the pair-fed group (Figure 9C; one way ANOVA for all treatment groups $p = 0.0944$, unpaired t-test with Welch's correction for alcohol and pair fed groups $p = 0.0085$). When these data were analyzed by tumor type, IGFBP-5 mRNA expression was increased in the adenomas (2.1-fold) and adenocarcinomas (1.6-

fold) from the alcohol group compared to each tumor type in the pair-fed group (Figure 9D). IGF-II and IGFBP-5 expression could not be compared across the hyperplasias for the same reason described above for Snail.

Tumors from the pair-fed group had 40% higher ER-α expression compared to the alcohol group (Figure 10A; a one-way ANOVA $p = 0.0209$ with a Newman-Keuls post test - alcohol vs. pair-fed $p < 0.05$, alcohol vs. ad lib $p > 0.05$, and pair-fed vs. ad lib $p > 0.05$). When these data were analyzed by tumor type, adenomas and adenocarcinomas from the alcohol group exhibited a 26% and 39% decrease, respectively, compared to this tumor type in the pair-fed group (Figure 10B).

Gene expression in the contralateral mammary glands was also analyzed. Mammary glands from the alcohol group had 23% increased Snail expression compared to the pair-fed group (Figure 11A; one-way ANOVA for all treatment groups $p = 0.0846$, unpaired t-test for alcohol and pair-fed groups $p = 0.1668$). IGF-II and DNMT1 mRNA expression in the mammary glands was not different among the three treatment groups (Figure 11B and 11C; one-way ANOVA $p = 0.3218$ for IGF-II, $p = 0.7305$ for DNMT1).

Discussion

In our previous work, tumor development in animals exposed to alcohol *in utero* was followed for 23 weeks post-NMU injection. Maximal differences in tumor number were found between the three treatment groups at 16 weeks post-injection, with the alcohol group developing more tumors compared to the control groups at this time point (32). For this reason, the current study was conducted using a larger number of animals and terminated earlier with the goal of analyzing tumors at 16 weeks post-NMU injection. The findings of this larger study support the findings of our previous study, indicating that overall tumor burden is greater in the offspring from the alcohol group compared to the pair-fed and ad lib groups. To date only one other group has studied mammary tumor susceptibility in an alcohol exposure model (33). In their study, pregnant Sprague Dawley rats were fed a liquid diet containing either low or moderate levels of alcohol from gestation days 7 to 19 or pair-fed an isocaloric liquid diet. The carcinogen 7,12-dimethylbenz(a)anthracene (DMBA) was administered to 47 day old offspring and the study was terminated at 17 weeks after DMBA administration. They found that offspring exposed to moderate, but not low, levels of alcohol developed more tumors as a group relative to the isocaloric pair-fed controls. Their data together with our previous and current studies indicate that moderate and high levels of alcohol exposure *in utero* increase susceptibility to carcinogen-induced mammary tumorigenesis in adult offspring.

Historically, ethanol was given to rodents in the drinking water. However, due to their natural aversion to ethanol, consumption was insufficient to result in sustained elevated blood alcohol concentrations (BAC). Therefore, Lieber and DeCarli developed

the technique of feeding ethanol in a liquid diet. With this diet, which contains 35.5% ethanol, rats consume sufficient amounts of ethanol, resulting in clinically relevant BACs (100 – 150 mg/dl; (196)). The liquid diet was formulated with 35% fat to mimic the Western diet. The Lieber-DeCarli diet was originally designed to determine if heavy alcohol consumption in the context of an adequate (Western) diet was associated with fatty liver disease. The ad lib diet was included to determine if the liquid diet alone shifted these baselines. An ad lib solid diet has continued to be included as a control group in many studies that use a liquid alcohol diet (195, 197-203). However, most of these studies do not list the composition (or even the source) of the diets, so we do not know if they used the Lieber-DeCarli liquid diet or if the fat and protein contents differ among liquid and ad libitum treatment groups.

In our study, the liquid Lieber-DeCarli diet used for the alcohol and pair-fed groups has higher fat and lower protein than the solid diet used for the ad lib group. Thus, of the two controls, the pair-fed group is a better control for the alcohol diet since the diets are isocaloric and the diet composition is similar except for the carbohydrates. The Institute of Medicine recommends that adults 19 and older should limit their fat intake to 20 - 35% (204). Therefore, the amount of fat in the liquid diet used in our study is at the upper limit of recommended fat intake for humans. While this diet mimics a typical American diet, it is not as high in fat as many of the rodent diets designed to specifically study a high fat diet, which contain between 42 and 60% fat (134, 205, 206). Although all of our analyses included the ad lib group, once we established that tumorigenesis was similar between the pair-fed and ad lib groups, our focus for the remaining parameters studied was on the comparison between the alcohol and pair-fed groups.

In this study, alcohol and pair-fed dams gained less weight throughout gestation than ad lib dams (Figure 1A) in accordance with work of others (195, 197, 207). It has been shown that pregnant rats on this liquid diet consume about 75 ml/day, which is nutritionally adequate for gestation (196). Furthermore, when the control liquid diet is given *ad libitum*, growth rates of non-pregnant rats are similar to or exceed the growth rate of animals fed solid rat chow (196). This indicates that the decreased weight gain in the alcohol rats is most likely due to decreased food intake, not a nutritional deficiency in the diet (196).

In this study the pair-fed dams weighed significantly less than the alcohol dams at 21 days of gestation. This difference is likely due to additional caloric restriction in the pair-fed dams. While the amount of control liquid diet fed to the pair-fed dams was based on the average amount the alcohol dams consumed, we have noticed in subsequent studies that the positioning of the feeding bottles in the cages prevents the pair-fed dams from completely consuming the total volume of the diet. In subsequent studies we have provided 20% more diet to the pair-fed group to account for this, which results in similar weights for the alcohol and pair-fed dams (data not shown). In spite of the differences in body weight between the alcohol and pair-fed dams, litter size, litter weight, and weight of offspring were not significantly different between these treatment groups.

All of the pair-fed and ad lib dams, except one pair-fed dam, gave birth on gestation day 22. In contrast, the alcohol dams tended to exhibit delayed parturition, with five of seven dams giving birth on gestation day 23 (Table 3). This trend was also observed in three other independent studies in our lab (data not shown). These data

indicate that alcohol consumption during pregnancy increases gestation length, in accordance with previously published work (207).

When female offspring were first weighed individually, those from the alcohol and pair-fed dams were 19% and 24% smaller, respectively, than the ad lib offspring. At study termination, the alcohol and pair-fed offspring were 8% and 12% smaller, respectively, than the ad lib offspring. Therefore, offspring from the alcohol and pair-fed groups weighed less initially, but exhibited catch up growth over time. Thus, they did not exhibit an additional postnatal growth deficit. However, the offspring from these two groups did ultimately remain smaller than offspring from the ad lib group. In studies reported in the literature offspring from the alcohol and pair-fed groups are consistently smaller than the ad lib group (195, 207). Other studies have similarly reported that the alcohol offspring are born smaller (188, 191, 197) and remain smaller than the control groups (197), although one study found no differences between the alcohol and pair-fed groups at 40 days of age (191). Although studies similarly report that the pair-fed offspring are born smaller, some studies, contrary to ours, indicate that the pair-fed group exhibits catch up growth as compared to the ad lib group (197). Together these data indicate that the liquid diet causes prenatal undernutrition in the alcohol and pair-fed groups, which in some cases is overcome postnatally by the pair-fed group, but not the alcohol group.

In terms of tumor phenotype, in the present study animals exposed to alcohol *in utero* developed more hyperplasias and adenocarcinomas than control groups. In our previous study at 23 weeks post-NMU injection, we also found that the alcohol group had more adenocarcinomas than control groups (32). The data from these two studies indicate

that fetal alcohol induces atypia in the mammary gland and leads to a more malignant phenotype in response to a carcinogenic insult. Histological analysis of tumors revealed a continuum of progression (hyperplasia, adenoma, and/or adenocarcinoma) within one tumor. Therefore, tumors were classified based on the most advanced stage observed within a single tumor. Future studies will be aimed at analyzing molecular markers to determine tumor phenotype to further classify the mammary tumors as luminal A, luminal B, or basal subtypes.

To classify tumor receptor status we performed immunohistochemistry (IHC) for ERα. A review of the literature revealed a lack of description as to how rodent tumors are classified as ERα positive or negative, particularly what should be used as the percentage cutoff. In the past, the clinical definition of an ERα positive tumor was that at least 10% of the cells expressed ERα, however recently the cutoff was changed to 1% (208). Classifying ERα receptor status in rodent tumors would be more accurate and reproducible across laboratories if a consensus were made as to what should be used as the cutoff in animal work as well as defining a method by which ERα positivity should be determined. For our analysis, the number of ERα positive cells in three fields of view were counted and expressed as a percentage of total cells. To the best of our knowledge this is the first time a comprehensive analysis of this nature has been performed to determine the percent of ERα positive cells in the NMU-induced mammary tumorigenesis model. From a comprehensive review of the literature, this is also the first time that HER2 status has been analyzed in NMU-induced mammary tumors.

Previously, we found that mammary tumors from the alcohol group collected at 23 weeks post-NMU injection were more ERα negative relative to tumors from control

groups (32). In the current study, tumors from all three treatment groups were ERα positive. Since tumors were collected at an earlier time point (i.e. 16 weeks), this suggests that tumors from fetal alcohol rats may lose ERα positivity more readily than tumors in control groups, which would lead to a poor prognosis if similar results were observed in women. Although we did not see a difference in the number of cells expressing ERα protein at this earlier time point, ERα mRNA expression was decreased in tumors of the alcohol group compared to the pair-fed group. qRT-PCR is more quantitative than IHC, especially when the colorimetric method is used for IHC. In addition, although we counted the number of ERα positive cells, we did not determine intensity, which may contribute to the discrepancy between the mRNA and protein data. Alternatively, it may be that changes observed at the mRNA level may not yet have translated to the protein level at this earlier time point. The mRNA data suggest that tumors in the alcohol group may be starting to lose ERα expression, which further supports the idea that fetal alcohol rats may lose ERα positivity over time. Future studies implementing the use of punch biopsies are needed to further clarify if tumors in the alcohol group start out as ERα positive and lose ERα positivity over time. Also, important to note is that in many of the NMU-induced tumors there were pockets of ERα positive cells along the periphery of the tumor whereas the center of the tumor was ERα negative. This pattern was seen in all treatment groups and may be an indication of tumor progression.

While ERα status was similar between the treatment groups, the alcohol group developed more PR positive tumors compared to the pair-fed controls. In our previous study, we found that alcohol-exposed animals had significantly increased circulating E2

(32). E2 induces PR expression in normal mammary glands as well as breast cancer cells (209, 210). Thus, it is possible that increased E2 in the alcohol animals is inducing PR. The progesterone (P4) signaling pathway plays a significant role in cell proliferation within the mammary gland (211, 212). Therefore, the increased PR observed in tumors of the alcohol group may be promoting cell proliferation. To determine if this is the case, future studies will involve the analysis of cell cycle/proliferation markers such as cyclin D1 and Ki67. The Wnt signaling pathway is involved in mammary gland development and certain *Wnt* genes are oncogenic in the rodent mammary gland (213-215). *Wnt-4* is downstream of PR in mammary epithelial cells and is essential for P4-induced ductal side branching during mammary gland development (213). In breast cancer cells, PR upregulates epidermal growth factor receptor (EGFR) and *Wnt-1*, which ultimately results in sustained activation of Erk1/2 MAPK leading to cell survival and proliferation (214). It would be interesting to determine if Wnt genes, particularly *Wnt-1* and *Wnt-4*, are expressed in our NMU-induced mammary tumors and if the expression of these genes is altered in tumors from the alcohol group. If so, the increased PR expression we see in the tumors of the alcohol group may be activating the Wnt signaling pathway to promote tumor cell survival and proliferation. Animal studies and clinical data indicate that the P4/PR signaling pathway is involved in initiation and development of mammary tumors (212, 216). Furthermore, studies of hormone replacement therapy (HRT) indicate that postmenopausal women on combination HRT including both estrogens and progestins have a greater risk of breast cancer than HRT with estrogen alone (212, 215, 217). These data suggest a critical role for the P4/PR signaling pathway in breast cancer development and progression. For this reason, if would be of great interest to focus future work on the

cause of the increased PR in tumors of the alcohol group as well as the downstream signaling effects of this elevated PR expression in order to extend our knowledge regarding the underlying mechanism for the increased susceptibility to carcinogen-induced mammary tumors in the alcohol group.

Snail is a transcription factor that promotes EMT (218). It plays a central role in cell migration during embryogenesis as well as tumor invasion and metastasis (218). In the present study, Snail mRNA expression was increased in the tumors from the alcohol group compared to the pair-fed group. A recent study found that constitutively activated IGF-IR induces Snail leading to EMT in MCF10A cells, an immortalized mammary epithelial cell line (219). In our study, we did not find a difference in IGF-IR mRNA expression among tumors from the three treatment groups. However, activation of IGF-IR in the tumors has yet to be analyzed. IGF-II expression was increased in tumors from the alcohol group (Figure 9A and 9B). A hypothesized model is that the increase in IGF-II leads to continued activation of the IGF-IR, which, in turn, results in increased Snail expression. Another recent study has provided further evidence for the connection between the IGF signaling pathway and EMT. MEMO1 is a protein that binds IRS-1, a major signaling molecule in the IGF pathway (220). In MCF10A cells, binding of MEMO1 to IRS-1 activates the PI3K/Akt pathway, resulting in increased Snail expression and induction of EMT (220).

In addition to its role in EMT, Snail has also been identified as a tumor progression gene. In human non-small cell lung cancer (NSCLC), Snail expression is increased and correlates with decreased patient survival (221). Using a Snail overexpression mouse model, this group also showed that upregulated Snail leads to

increased primary tumor burden and angiogenesis in the tumor (221). In an *in vitro* analysis of 35 cell lines as well as an analysis of 144 clinical breast samples, Snail was shown to play a role in breast cancer progression with Snail being expressed in both carcinoma cells as well as the stroma (222). Many studies have also shown that the role of Snail in tumor progression involves a de-differentiation step during the initial transformation process in which Snail promotes tumor cells to undergo EMT resulting in the generation of cancer stem cells (CSCs; (223-228)). Specifically, in transformed human mammary epithelial cells (HMLEN cells), Snail induces EMT and those cells that have undergone EMT exhibit the $CD44^{high}/CD24^{low}$ profile of breast CSCs as well as the CSC ability to form mammospheres (224). The same group has shown that these stem-like cells isolated from HMLEN cells as well as human breast tumors express EMT markers such as Snail (224). Therefore, it is possible that the increased Snail expression observed in tumors of the alcohol group is inducing those tumor cells to become CSCs. Also since stem cells have an EMT profile, it is possible that the increased Snail expression observed in tumors of the alcohol group is due to an increase in CSCs.

As previously mentioned, IGF-II expression was increased in tumors of the alcohol group compared to the pair-fed group (Figure 9A and 9B). This means there is more IGF-II available to stimulate cell proliferation via the IGF pathway. In breast cancer IGF-II is expressed mostly in the stroma as well as in malignant epithelial cells and it serves as a potent mitogen, inducing cell proliferation (229-233). There are several potential mechanisms by which IGF-II expression can be altered. In our previous study, we found that alcohol-exposed animals had significantly increased circulating E2 (32). E2 has been shown to upregulate IGF-II mRNA and protein expression in breast cancer

cells (229, 230, 234). It is possible that since E2 is increased in alcohol-exposed animals, E2 is causing the increase in IGF-II observed in tumors from this group. E2 also downregulates mannose-6-phosphate receptor/IGF-IIR mRNA and protein expression in breast cancer cells (235). Thus, a second possibility is that the increased E2 in alcohol-exposed animals downregulates the IGF-IIR. This would lead to increased IGF-II (since less IGF-II would be binding) and therefore more IGF-II would be available to activate IGF-IR. Fibroblasts derived from malignant breast tumors have increased IGF-II expression compared to fibroblasts derived from benign tumors or normal breast (232, 233). Furthermore, in the rat NMU-induced mammary tumor model, IGF-II expression has been shown in the stroma of the tumors and ovariectomy followed by hormone repletion increased IGF-II expression, supporting a role for IGF-II in NMU-induced mammary tumor growth (236). We have shown that the alcohol group exhibits increased tumor IGF-II expression and develops more malignant tumors (adenocarcinomas). It is plausible that in the alcohol group the tumors consist of malignant epithelial cells and fibroblasts associated with these malignant tumors that are expressing higher levels of IGF-II and the increased IGF-II is driving tumor growth.

IGF-II is an imprinted gene whereby it is expressed on the paternal allele and epigenetically silenced on the maternal allele by DNA methylation (237). Loss of imprinting (LOI) is commonly observed in many types of tumors, which results in gene expression on both paternal and maternal alleles (238-240). LOI of IGF-II has been found in endometrial carcinosarcoma, uterine leiomyosarcoma, cervical cancer, prostate cancer, Wilms' tumor, normal epithelium of the colon in patients at risk for colorectal cancer as well as those with colorectal cancer, and breast cancer (237, 239-244). Thus, a potential

mechanism is that tumors from the alcohol group exhibit LOI of IGF-II leading to increased IGF-II expression, which may be involved in tumor progression in fetal alcohol animals. A study examining carcinomas of breast cancer patients found a strong relationship between IGF-II mRNA expression and PR positivity (245). It is intriguing that we see both increased number of PR positive tumors and IGF-II mRNA expression in tumors of the alcohol group, suggesting that these molecules may work in concert to promote cell proliferation within tumors of this treatment group.

Another gene that was increased at 16 weeks post-NMU injection in alcohol-exposed offspring was IGFBP-5. This protein has been shown to have IGF-independent effects in breast cancer cells by inhibiting ceramide-induced apoptosis and promoting cell proliferation (246, 247). Our data suggest that IGFBP-5 may be acting via an IGF-independent mechanism in tumors of the alcohol group at 16 weeks post-NMU injection to inhibit apoptosis and/or promote cell proliferation. In the MCF-7 breast cancer cell line, E2 has been shown to upregulate IGFBP-5 mRNA expression (248). It is possible that since E2 is increased in fetal alcohol animals (32), it is responsible for the increased IGFBP-5 in tumors of the alcohol group. Interestingly, in our previous work, where we terminated the study at 23 weeks post-NMU injection, IGFBP-5 was decreased in tumors of the alcohol group (32). Therefore IGFBP-5 may act via an IGF-independent mechanism to promote cell proliferation/prevent apoptosis early on (at 16 weeks post-NMU injection) when the tumor is developing and progressing, but perhaps later on (at 23 weeks post-NMU injection), the tumor suppresses IGFBP-5 expression to increase IGF-I availability thus switching to an IGF-dependent mechanism. A clinical study has

shown that IGFBP-5 may contribute to the development of breast cancer and that IGFBP-5 mRNA is a prognostic factor for the disease (249).

IGF-II and IGFBP-5 mRNA expression in the tumors of the alcohol group decreased as the tumors became more malignant (comparing hyperplasia to adenoma to adenocarcinoma; Figure 9B and 9D). Enhanced IGF-II and IGFBP-5 expression in the hyperplasias may have promoted proliferation, but as the tumor progressed to adenoma or adenocarcinoma it may have switched its mechanism of signaling, resulting in decreased expression of these genes. Tumors are heterogeneous, thus each tumor and each tumor stage is comprised of different cell types. Thus, another possibility is that there was a shift in cell type during the progression from hyperplasia to adenoma to adenocarcinoma. This shift in cell type/phenotype might have caused the decrease in IGF-II and IGFBP-5 expression in the different tumor types.

In conclusion, this study provides further evidence that alcohol exposure *in utero* enhances susceptibility to carcinogen-induced mammary tumorigenesis. Fetal alcohol animals develop more malignant tumors and may lose ERα positivity more readily than tumors in control groups, which would lead to a poor prognosis if similar results were observed in women. Alcohol-exposed animals exhibit more PR positive tumors as well as increased Snail, IGF-II, and IGFBP-5 tumor expression at 16 weeks post-NMU injection. These data provide insights into the potential molecular mechanisms underlying the enhanced susceptibility to NMU-induced tumors in the alcohol group. Additional studies will be aimed at these particular pathways to further delineate the mechanism.

Diet	Company Cat #	Protein	Fat	Carbohydrate	Ethanol
Alcohol Alcohol liquid diet, Lieber DeCarli '82	Bio-Serv Cat# F1258SP	18.0%	35.0%	11.5%	35.5%
Pair-fed Control liquid diet, Lieber DeCarli '82	Bio-Serv Cat# F1259SP	18.0%	35.0%	47.0%	-
Ad lib Solid Rat Chow	Purina/Lab Diet Cat# 5012	27.1%	13.2%	59.7%	-

Table 1. Comparison of diet composition for the diets used for the alcohol, pair-fed, and ad lib groups. Percent of calories derived from protein, fat, carbohydrate, and ethanol are listed.

Gene	Accession #	Primer Sequence (5' to 3')	Product Length
Snail (Snai1)	NM_053805.1	F: GCCGGAAGCCCAACTATAGC R: AGGGCTGCTGGAAGGTGAA	63
Twist (Twist1)	NM_053530.2	F: AGTCGCTGAACGAGGCATTT R: GGTCTGAATCTTGCTCAGCTTGT	80
GATA3	NM_133293.1	F: ATCCAGACCCGAAACCGTAA R: AGCGCATCATGCACCTTTTT	65
IGF-I	NM_001082477.2 (transcript variant 1) NM_178866.4 (transcript variant 2) NM_001082478.1 (transcript variant 3) NM_001082479.1 (transcript variant 4)	F: ATCTGAGGAGGCTGGAGATGTACT R: GGATGGAACGAGCTGACTTTGT	63
IGFR	NM_052807	F: AGAGCGAGCTTCCTGTGAAAGTGA R: TGCCACGTTATGATGATGCGGTTC	81
Akt1	NM_033230.2	F: GAACGACGTAGCCATTGTGAAG R: GCCGCCAGGTTTTAATATATTCC	68
Akt2	NM_017093.1	F: CCCTTCAAACCTCAGGTCACTT R: GGCGGTGAATTCATCATCAAA	63
IGF-II	NM_031511.2 (transcript variant 1) NM_001190162.1 (transcript variant 2) NM_001190163.1 (transcript variant 3)	F: AAGAGCTCGAAGCGTTCAGAGA R: CTTTGGGTGGTAACACGATCAG	63
IGFBP-5	NM_012817.1	F: TTGAGGAAACTGAGGACCTCGGAA R: CCTTCTCTGTCCGTTCAACTTGCT	110
ERα	X61098	F: TCGGGAATGGCCTTGTTG R: AGCTGCGGGCGATTGA	65
DNMT1	NM_053354.3	F: ACCTGGGGCCAATCAATCAG R: TTGGTGCATACTCTGGGCTG	123
β-actin	NM_031144	F: CCATTGAACACGGCATTGTC R: GCCACACGCAGCTCATTGTA	82

Table 2. Primer sequences used for gene expression analysis by qRT-PCR. The forward primer (F) is listed first and the reverse primer (R) is listed second.

Treatment Group	Number of Dams that Gave Birth on Gestation Day 22	Number of Dams that Gave Birth on Gestation Day 23
Alcohol	2	5
Pair-fed	4	1
Ad lib	7	0

Table 3. Number of dams that gave birth on gestation days 22 and 23 from each treatment group

Gene Classification	Gene Name
Epithelial to Mesenchymal Transition	Slug
	Snail
	Twist
	p63
	E-cadherin
Estradiol/Estrogen Receptor Signaling	Aromatase (Cyp19)
	GATA3
Tumorigenesis	p53
	p21
	c-myc
	Smooth muscle actin
Housekeeping genes	β-actin
	Rplp1

Table 4. List of genes analyzed by a custom PCR array. Genes involved in epithelial to mesenchymal transition, estradiol/estrogen receptor signaling, and tumorigenesis were selected for a custom PCR array (SA Biosciences, Frederick, MD). qRT-PCR was performed for pooled samples from the three treatment groups. Data was analyzed using the RT^2 Profiler PCR Array Data Analysis Software (SA Biosciences) and candidate genes were identified**.**

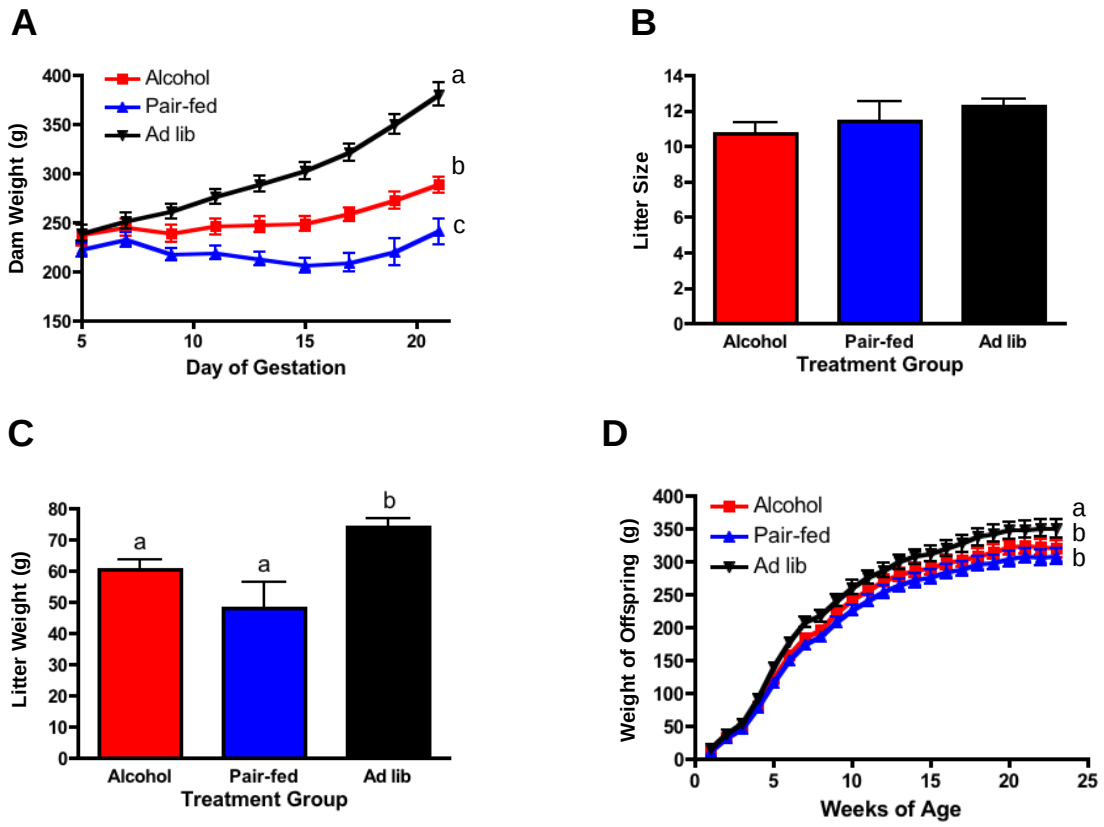

Figure 1. Dam and offspring parameters A) Weight of dams from gestation day (GD) 5 to 21; n = 7 (alcohol), 5 (pair-fed), and 7 (ad lib). Data for GD 21 were analyzed using a one-way ANOVA ($p < 0.0001$) with a Newman-Keuls post test (alcohol vs. pair-fed $p < 0.05$, alcohol vs. ad lib $p < 0.001$, and pair-fed vs. ad lib $p < 0.001$). B) Litter size. C) Litter weight at birth. Data were analyzed using a one-way ANOVA ($p = 0.0062$) with a Newman-Keuls post test (alcohol vs. pair-fed $p > 0.05$, alcohol vs. ad lib $p < 0.05$, and pair-fed vs. ad lib $p < 0.01$). D) Offspring were weighed each week until study termination; n = 31 (alcohol), 27 (pair-fed), and 33 (ad lib). Data at study termination were analyzed using a one-way ANOVA ($p < 0.0001$) with a Newman-Keuls post test (alcohol vs. pair-fed $p > 0.05$, alcohol vs. ad lib $p < 0.001$, and pair-fed vs. ad lib $p < 0.001$). Different letters denote significant differences.

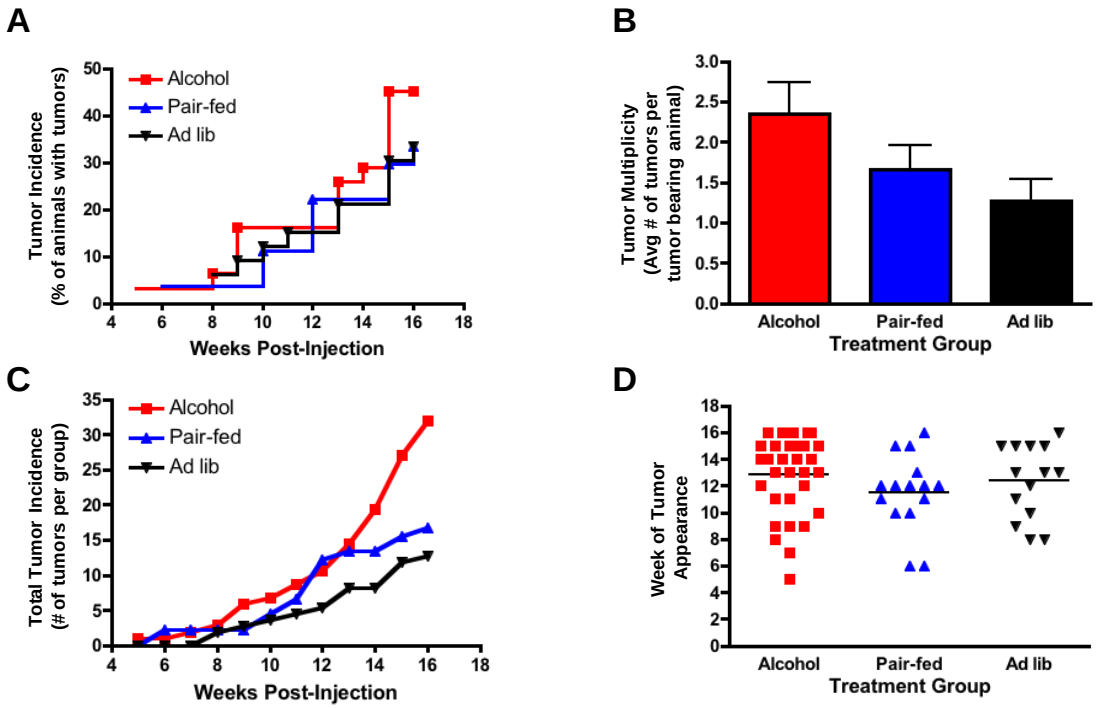

Figure 2. Alcohol exposure in utero enhances mammary tumorigenesis at 16 weeks post-NMU injection. A) Tumor incidence (% of animals with tumors) each week post-NMU injection; n = 31 (alcohol), 27 (pair-fed), and 33 (ad lib) animals; Kaplan-Meier survival curve with a log-rank test (p = 0.5794). B) Tumor multiplicity (average number of tumors per tumor bearing animal) at study termination; n = 14 (alcohol), 9 (pair-fed), and 11 (ad lib) tumor bearing animals. Data were analyzed using a one-way ANOVA (p = 0.0746). C) Total tumor incidence (number of tumors per treatment group) each week post-NMU injection. n = 31 (alcohol), 27 (pair-fed), and 33 (ad lib) animals. The data shown is standardized to 30 animals per group using the formula: (30 x total number of tumors per week)/number of animals per group. These data are shown to illustrate the differences among treatment groups and were not subjected to statistical analyses. D) Week of tumor appearance. Each data point represents an individual tumor; n = 33 (alcohol), 15 (pair-fed), and 14 (ad lib) tumors. The horizontal line represents the mean week of tumor appearance for that treatment group.

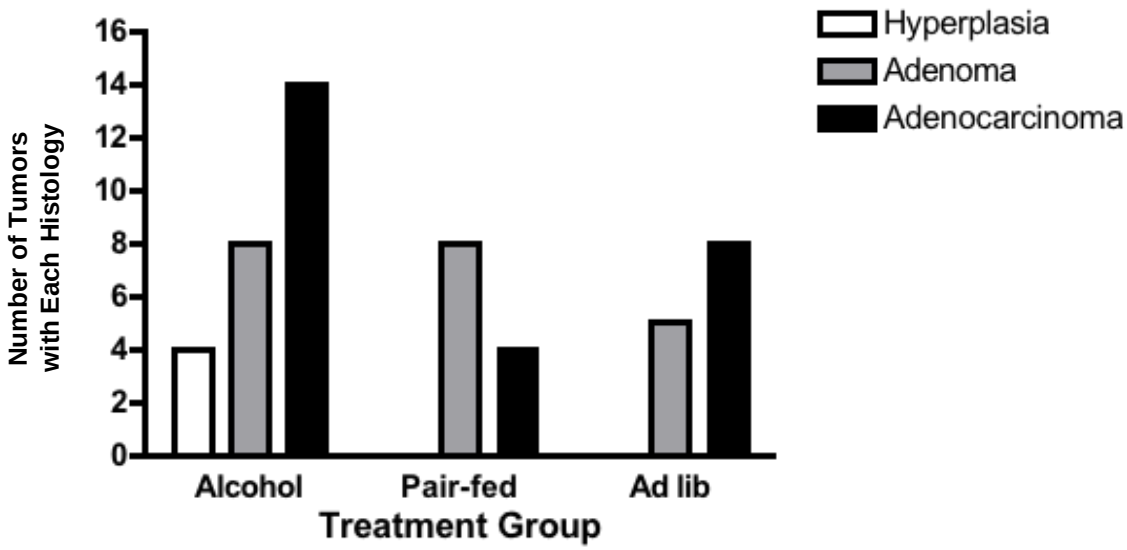

Treatment Group	Hyperplasia	Adenoma	Adenocarcinoma
Alcohol	4	8	14
Pair-fed	0	8	4
Ad lib	0	5	8

Figure 3. At 16 weeks post-NMU injection, animals exposed to alcohol *in utero* develop more hyperplasias and adenocarcinomas than control groups. Tumors were stained with hematoxylin and eosin and evaluated by a toxicological pathologist who was blinded to treatment. Tumors were classified by the most advanced type of lesion present in the tumor.

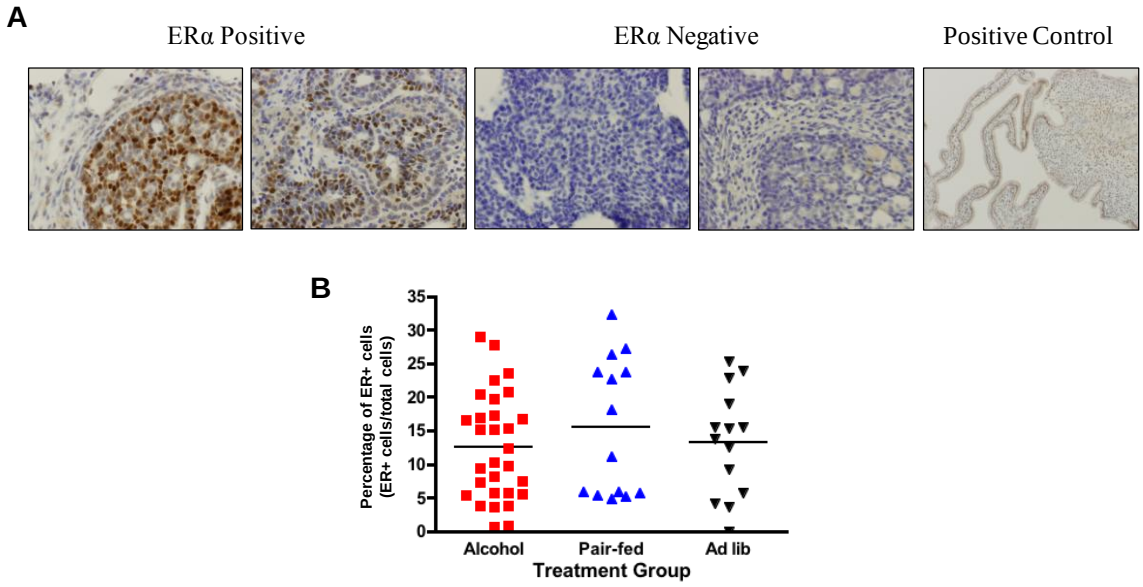

Figure 4. NMU induces mammary tumors with a wide range of ERα positivity. A) Representative images of ERα positive or negative tumors are shown. Rat oviduct was used as a positive control. B) Three fields of view were imaged per tumor. Two lab members counted ERα positive cells and total cells for each field of view to determine the percentage of ERα positive cells. Each point on the graph represents the average percentage of ERα positive cells from the two individual counts for each tumor. n = 30 (alcohol), 14 (pair-fed), and 14 (ad lib) tumors.

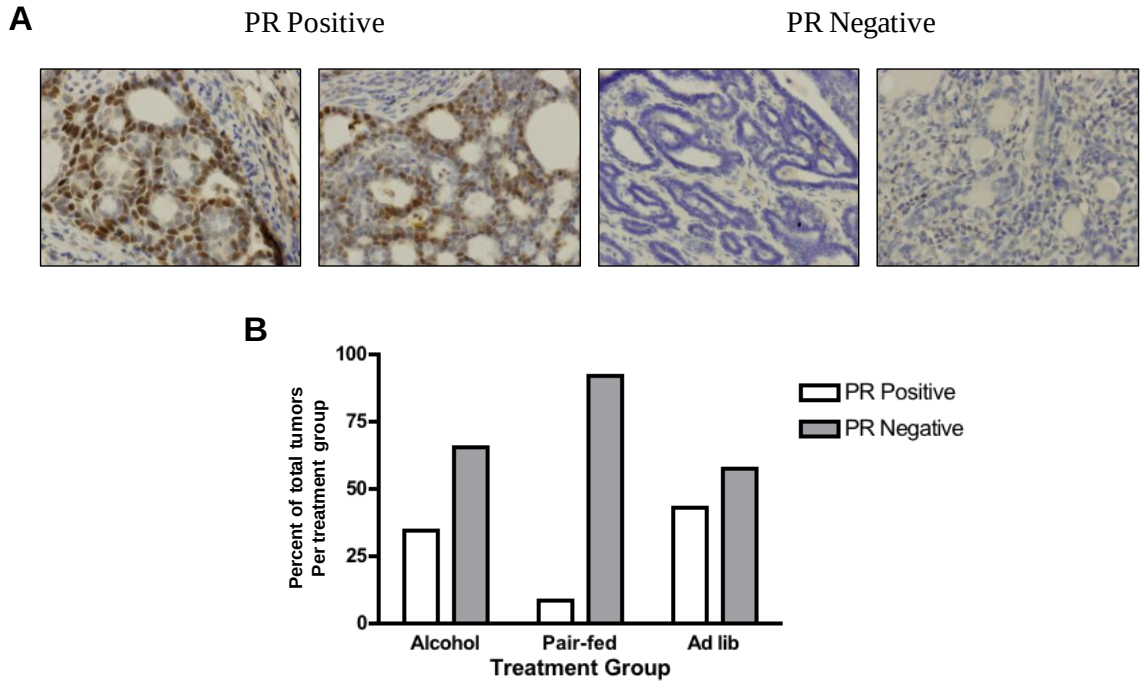

Figure 5. Animals exposed to alcohol *in utero* develop more progesterone receptor positive tumors. A) Representative images of PR positive or negative tumors are shown. B) Two members of the lab viewed all tumors blindly and classified them as positive or negative; n = 29 (alcohol), 12 (pair-fed), and 14 (ad lib) tumors.

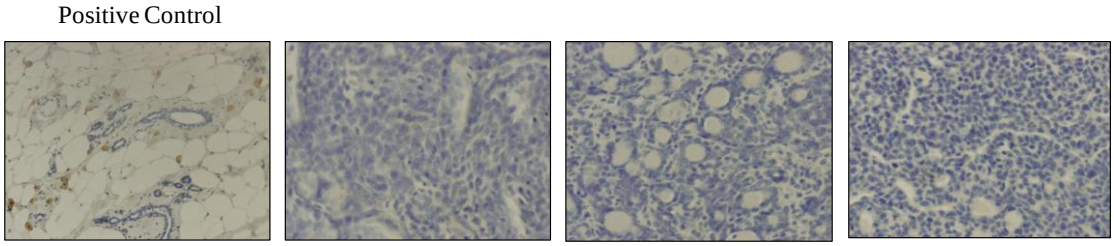

Figure 6. NMU-induced tumors in all treatment groups are HER2 negative. Representative images of HER2 negative tumors irrespective of treatment group. A rat mammary gland was used as a positive control.

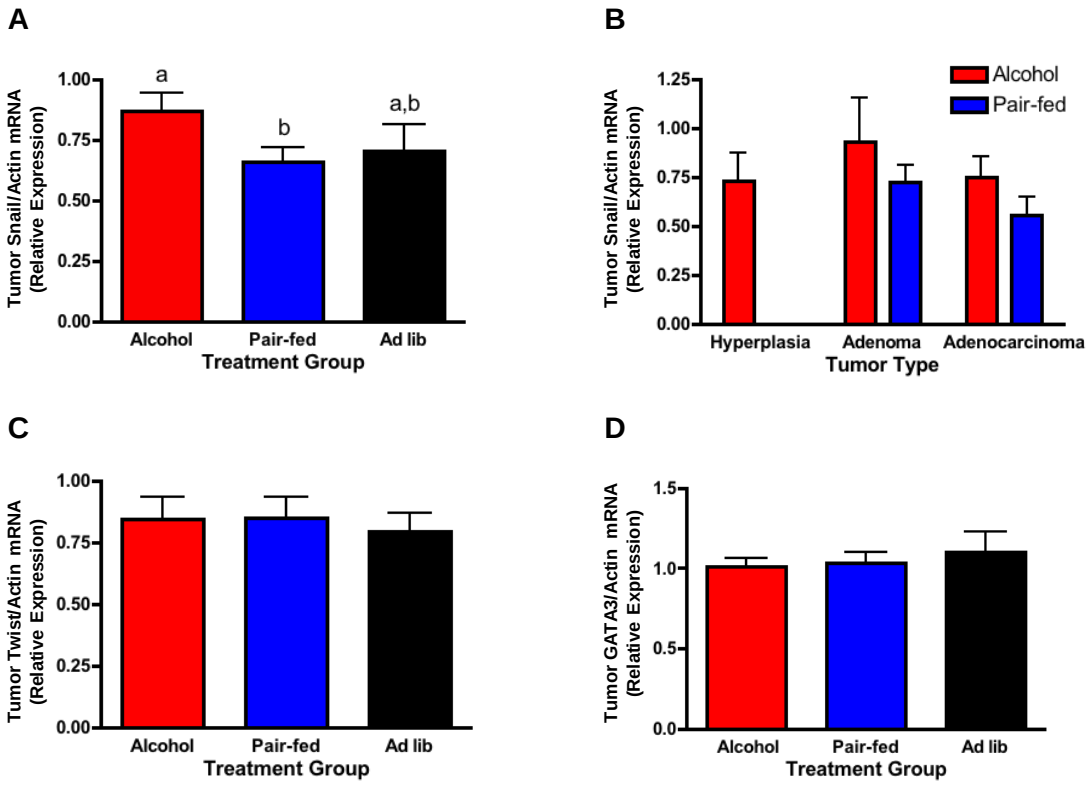

Figure 7. Snail, but not Twist or GATA3, mRNA expression is altered in tumors of fetal alcohol animals. mRNA expression of Snail (A and B), Twist (C), and GATA3 (D) in tumors from the three treatment groups was analyzed by qRT-PCR. n = 27 (alcohol), 12 (pair-fed), and 8 (ad lib) tumors. A) Data were analyzed by a one way ANOVA for all treatment groups ($p = 0.1648$) as well as an unpaired t-test with Welch's correction between the alcohol and pair-fed groups ($p = 0.0414$). Different letters denote significant differences. B) Snail mRNA expression was also analyzed by tumor type. n = 4 (alcohol) and 0 (pair-fed) tumors for hyperplasias, 6 (alcohol) and 6 (pair-fed) tumors for adenomas, 12 (alcohol) and 4 (pair-fed) tumors for adenocarcinomas.

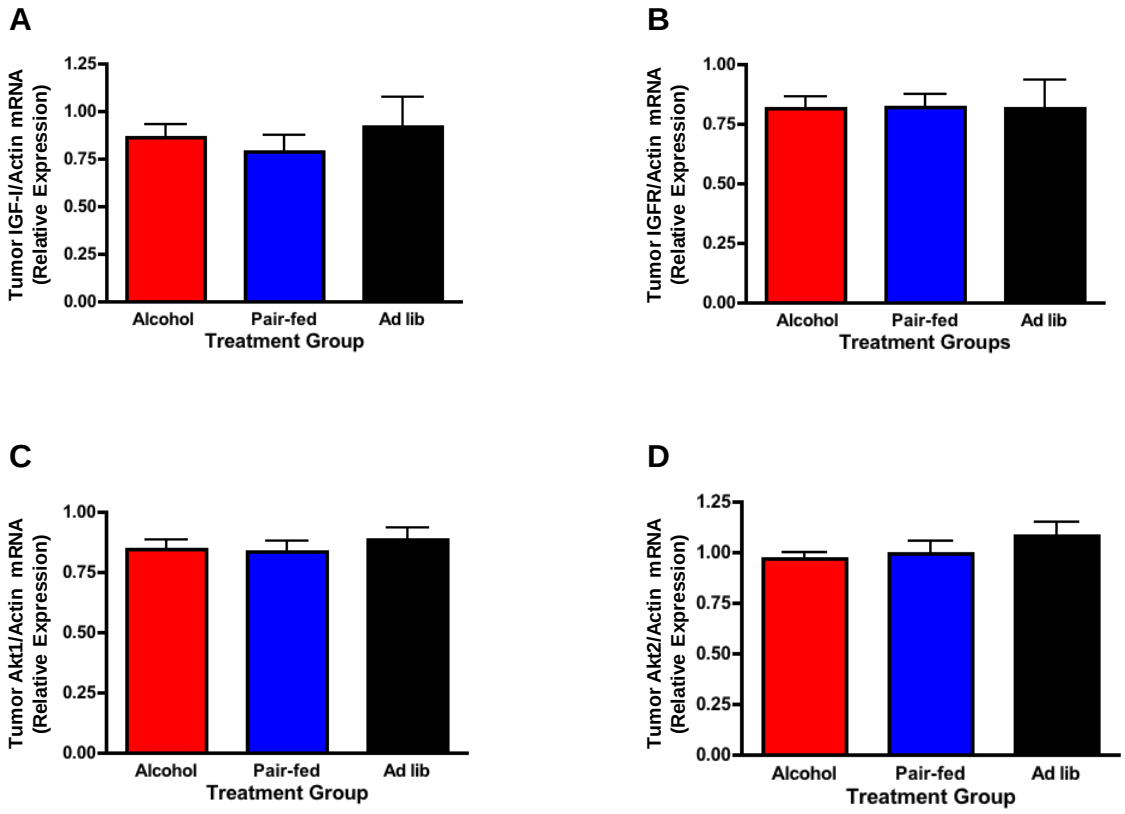

Figure 8. IGF-I, IGFR, Akt1, and Akt2 mRNA expression is not different among tumors from alcohol and pair-fed groups. mRNA expression of genes involved in the IGF signaling pathway were analyzed by qRT-PCR in tumors from the three treatment groups. A) IGF-I B) IGFR C) Akt1 and D) Akt2. Data were analyzed by a one-way ANOVA; n= 27 (alcohol), 12 (pair-fed), and 8 (IGF-II, IGFR, Akt1; ad lib) or 7 (Akt2; ad lib) tumors.

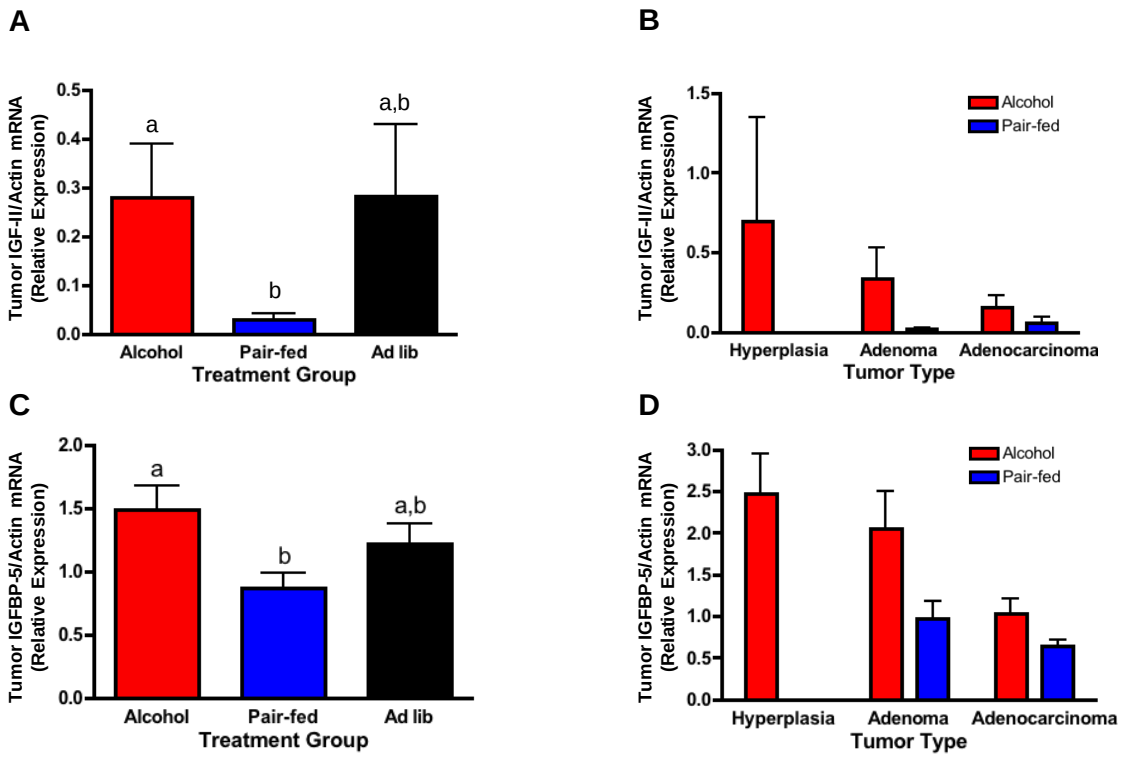

Figure 9. IGF-II and IGFBP-5 mRNA expression is increased in tumors from the alcohol group. mRNA expression was analyzed by qRT-PCR in tumors from the three treatment groups. A) IGF-II; n = 26 (alcohol), 11 (pair-fed), and 7 (ad lib) tumors. One way ANOVA for all treatment groups (p = 0.3173), unpaired t-test with Welch's correction for alcohol and pair-fed groups (p = p = 0.0352) B) IGF-II expression by tumor type; n = 4 (alcohol) and 0 (pair-fed) tumors for hyperplasias, 6 (alcohol) and 6 (pair-fed) tumors for adenomas, 11 (alcohol) and 3 (pair-fed) tumors for adenocarcinomas. C) IGFBP-5; n = 27 (alcohol), 12 (pair-fed), and 7 (ad lib) tumors. One way ANOVA for all treatment groups (p = 0.0944), unpaired t-test with Welch's correction for alcohol and pair-fed groups (p = 0.0085). D) IGFBP-5 expression by tumor type; n = 4 (alcohol) and 0 (pair-fed) tumors for hyperplasias, 6 (alcohol) and 6 (pair-fed) tumors for adenomas, 12 (alcohol) and 4 (pair-fed) tumors for adenocarcinomas.

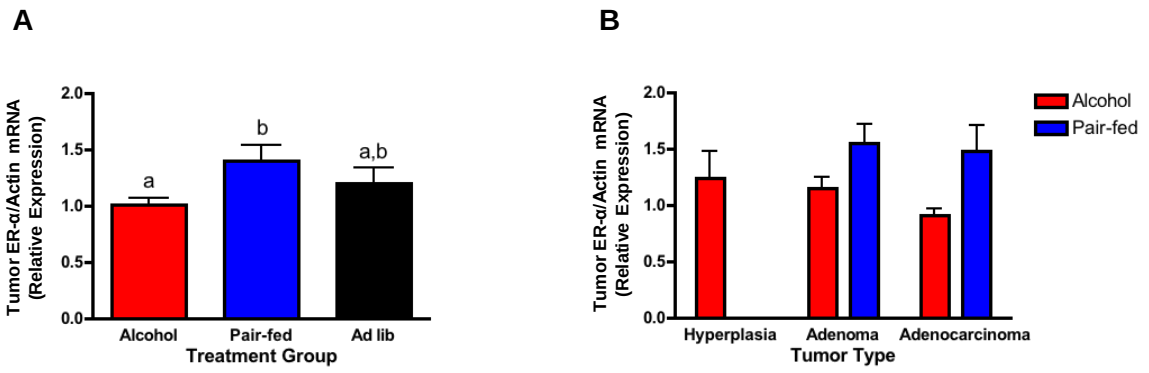

Figure 10. ERα mRNA expression is decreased in tumors of the alcohol group. ERα mRNA expression in tumors from the three treatment groups was analyzed by qRT-PCR A) ERα, Data were analyzed by a one-way ANOVA ($p = 0.0209$) with a Newman-Keuls post test (alcohol vs. pair-fed $p < 0.05$, alcohol vs. ad lib $p > 0.05$, and pair-fed vs. ad lib $p > 0.05$). Different letters denote significant differences; n = 29 (alcohol), 12 (pair-fed), and 10 (ad lib) tumors. B) ERα expression by tumor type; n = 4 (alcohol) and 0 (pair-fed) tumors for hyperplasias, 6 (alcohol) and 7 (pair-fed) tumors for adenomas, 13 (alcohol) and 4 (pair-fed) tumors for adenocarcinomas.

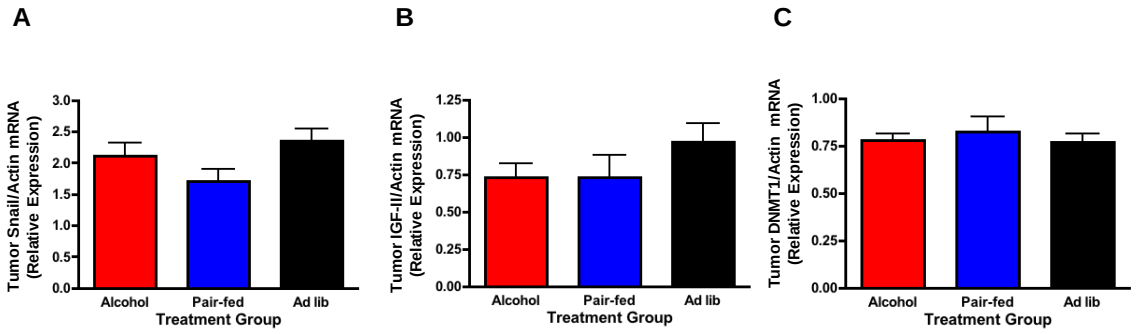

Figure 11. Snail, but not IGF-II or DNMT1, mRNA expression is increased in contralateral mammary glands from alcohol exposed animals. mRNA expression in contralateral mammary glands from the three treatment groups was analyzed by qRT-PCR A) Snail (one-way ANOVA for all treatment groups p = 0.0846, unpaired t-test for alcohol and pair-fed groups p = 0.1668). B) IGF-II (one-way ANOVA p = 0.3218) C) DNMT1 (one-way ANOVA p = 0.7305); n = 25 (Snail; alcohol) or 26 (IGF-II and DNMT1; alcohol), 25 (pair-fed), and 24 (Snail and DNMT1; ad lib) or 23 (IGF-II; ad lib).

Chapter 4

DNA Methylation Analysis of IGFBP-5 and ERα in Mammary Glands and Tumors of Rats Exposed to Alcohol *In Utero*

Abstract

Tumors and mammary tissue collected from animals exposed to alcohol *in utero* exhibit alterations in IGFBP-5 and estrogen receptor (ER) α expression relative to pair-fed controls. Since alcohol *in utero* induces epigenetic alterations in non-mammary tissues, the goal of this work was to determine if these changes resulted from alterations in DNA methylation of the IGFBP-5 and ERα genes. Using bisulfite DNA sequencing we analyzed an IGFBP-5 promoter CpG island, -310 to -211 from the transcription start site (TSS), in mammary tumors from female F1 offspring exposed to alcohol *in utero* collected at 23 weeks post-NMU injection. Methylation at only one or two CpG sites, if any, was observed in these tumors and the methylation that was seen was at different CpG sites, suggesting minimal methylation was present in these tumors. The first CpG island in IGFBP-5 exon I (+198 to +309 from TSS) was then analyzed by bisulfite DNA sequencing and methylation specific PCR (MSP) for DNA methylation in tumors from alcohol-exposed F1 offspring collected at 23 weeks post-NMU injection as well as PND 40 mammary glands. Results indicated partial methylation in almost all tissues analyzed. Since many tumors and mammary glands had some methylated DNA, we performed pyrosequencing to get a more quantitative analysis of the methylation in the 1st CpG island in IGFBP-5 exon I (+91 to +282 from TSS) in tumors and contralateral mammary glands from fetal alcohol animals collected at 16 weeks post-NMU injection as well as

PND 40 mammary glands of animals exposed to alcohol *in utero*. Analysis by this method revealed little to no DNA methylation in this region. MSP was also used to assess DNA methylation of the ERα promoter/exon I CpG island (-19 to +107) in NMU-induced mammary tumors from fetal alcohol animals collected at 23 weeks post-NMU injection. We found that these tumors exhibited partial methylation. Tumors from the alcohol group had slightly more methylated DNA than unmethylated DNA as compared to the pair-fed group. This study represents the first analysis of epigenetic alterations induced by fetal alcohol exposure in the mammary gland. We have also for the first time analyzed epigenetic modifications in NMU-induced mammary tumors of animals exposed to alcohol *in utero*. Further studies are needed to fully explore the possibility that changes in IGFBP-5 and ERα expression in tumors and mammary glands of fetal alcohol animals are due to DNA methylation.

Introduction

Epigenetics involves heritable changes in gene expression that occur without an alteration in the primary nucleotide sequence of a gene. Epigenetic modifications to nuclear chromatin structure alter DNA, histones, and non-histone proteins. These modifications limit or enhance the accessibility and binding of the transcriptional machinery or recruit repressor complexes, resulting in changes in gene expression. Epigenetic mechanisms include DNA methylation of promoter and/or non-promoter CpG islands, covalent histone modifications (methylation, acetylation, phosphorylation, ubiquitination or sumoylation), microRNAs, and the more recently described long noncoding RNAs (137-140).

DNA methylation represents a major epigenetic regulatory pathway that is catalyzed by DNA methyltransferases (DNMTs). These enzymes add methyl groups from S-adenosylmethionines to carbon 5 positions of cytosines (Figure 1; (141)). Three important family members of DNMTs have been reported: DNMT1, DNMT3A, and DNMT3B. DNMT1 is considered the maintenance DNA methyltransferase, whereas DNMT3A and DNMT3B are primarily involved in *de novo* DNA methylation (137, 142). Overall, hypomethylation of DNA causes a more relaxed chromatin state, allowing easier interaction between the DNA and the transcriptional machinery, thus resulting in increased gene transcription. DNA hypermethylation results in condensed chromatin structure, causing a decrease in gene transcription (137). DNA methylation of promoter CpG islands results in transcriptional silencing of that gene which can occur directly due to DNA methylation or due to chromatin conformational changes that inhibit transcription (250, 251). A recent genome-wide study analyzing the relationship between

DNA methylation and gene expression found a stronger link between DNA methylation in exon I (downstream of the transcriptional start site) and transcriptional silencing as compared to DNA methylation in the promoter region (252). These studies indicate that both promoter and non-promoter CpG islands can affect gene expression.

The gold standard of DNA methylation analysis is bisulfite DNA sequencing (253-255). In this process, genomic DNA is treated with sodium bisulfite, which results in the conversion of unmethylated cytosines to uracil (Figure 1). PCR is then performed during which cytosines that were converted to uracil during bisulfite treatment are recognized as thymines (Figure 1). This is followed by purification and cloning of the PCR products. Plasmid DNA from several clones per sample is then sequenced. Analysis of the sequence allows for identification of DNA methylation, whereby the presence of a thymine at a CpG site indicates the location of an unmethylated cytosine and a cytosine at a CpG site indicates the presence of a methylated cytosine (255-257). The advantage of bisulfite DNA sequencing is that it allows for examination of all CpG sites in the CpG island of interest (254, 256, 257).

Another commonly used method of DNA methylation analysis is methylation specific PCR (MSP; 258). As with bisulfite DNA sequencing, MSP is based on treatment of genomic DNA with sodium bisulfite. However, with MSP, the PCR following bisulfite treatment utilizes two sets of primers, the first, which recognizes methylated DNA and the second, which recognizes unmethylated DNA (259). PCR products are run on a gel and detection of bands at the correct molecular weight indicates the presence of unmethylated or methylated alleles. The advantage of MSP is that it is simpler, less time consuming, and less expensive than bisulfite DNA sequencing (258).

While both bisulfite DNA sequencing and MSP allow for detection of DNA methylation at specific CpG sites, neither method is quantitative. Pyrosequencing, on the other hand, allows for a quantitative analysis of DNA methylation at all CpG sites along the CpG island of interest (260). In this procedure, DNA samples are subjected to bisulfite modification and PCR is performed with one primer labeled with biotin. This biotin-labeled PCR primer is then immobilized on streptavidin-coated beads, which results in a single stranded PCR product. A complementary pyrosequencing primer is then hybridized to the single stranded PCR product and pyrosequencing is performed by sequentially adding individual nucleotides to the reaction. Incorporation of nucleotides results in the release of pyrophosphate, which results in the emission of light. Percent methylation of each CpG site within the CpG island is then calculated (260). Pyrosequencing is typically used once preliminary data suggests differential methylation and provides the advantage of quantitatively assessing large numbers of samples (260).

Our studies show that IGFBP-5 mRNA expression is decreased in mammary glands of alcohol-exposed animals at PND 40 relative to pair-fed controls (Chapter 2). Furthermore, when these offspring are exposed to NMU in adulthood, the resulting tumors express higher IGFBP-5 at week 16 post-injection, but lower IGFBP-5 at week 23. Tumor expression of ERα is also affected at both time points (Chapter 3, 32). Numerous studies have shown that alcohol exposure *in utero* induces epigenetic alterations in the offspring (153-160), while other *in utero* exposures have been shown to cause epigenetic modifications in the mammary gland (134, 161). Therefore, we hypothesized that changes in IGFBP-5 and ERα observed in our tissues might be due to

DNA methylation. Thus, the goal of the work presented in this chapter was to determine if alcohol *in utero* affects DNA methylation of the IGFBP-5 and ERα genes.

Materials and Methods

Animal Studies

Tissues collected during our previous studies were used for the epigenetic analyses described in this chapter. Diets used for each treatment group are listed in Table 1 of Chapter 3. For studies 1 and 3, female F1 offspring were administered a single intraperitoneal (I.P.) injection of 50 mg/kg body weight NMU on PND 50 and tumors as well as contralateral mammary glands were collected at 16 weeks post-NMU injection (study 3) or 23 weeks post-NMU injection (study 1; 32). For study 2, female F1 offspring were not injected with NMU and mammary glands were collected on PND 40, which corresponds with a postpubertal developmental time point (Chapter 2).

Genomic DNA Isolation

Mammary gland and tumor tissue (30 – 50 mg) was homogenized in 10 mM Tris-HCl/1 mM EDTA/0.5% SDS with Proteinase K (2 mg/ml; Roche, Basel, Switzerland). The homogenate was incubated overnight at 55°C with frequent agitation to allow for complete digestion. Genomic DNA was isolated by a phenol chloroform extraction method. Phenol:chloroform:isoamyl alcohol (25:24:1; Life Technologies, Carlsbad, CA) was added and the samples were vortexed for 2 minutes. Samples were centrifuged at 12,000 RPM for 10 minutes at room temperature. The upper aqueous phase was removed, an equal volume of chloroform (Fisher Scientific, Pittsburgh, PA) was added, and samples were centrifuged at 12,000 RPM for 10 minutes at room temperature. The upper aqueous phase was removed and ice cold 100% ethanol was added. The sample was mixed by inversion and placed at -20°C for 20 minutes to allow for precipitation.

Samples were spun at 12,000 RPM for 5 minutes at room temperature and the supernatant was removed. 75% ethanol was added and the sample was again spun at 12,000 RPM for 5 minutes at room temperature. The supernatant was removed and the 75% ethanol washing step was repeated a second time. The supernatant was removed and pellets were allowed to air dry at room temperature for 1 hour. TE buffer (10 mM Tris-HCl, 1 mM EDTA) was added and the samples were re-suspended by gentle shaking at room temperature for a few hours. Genomic DNA concentration and purity was determined using the Nanodrop ND-1000 Spectrophotometer (Thermo Scientific, Waltham, MA). Genomic DNA integrity was determined by running samples on a 1% agarose gel.

CpG Island Identification and Primer Design

MethPrimer (http://www.urogene.org/methprimer/) was used (261) to identify IGFBP-5 and ERα CpG islands. Primer design programs for standard PCR cannot be used to design primers for DNA methylation analysis because of the changes in the DNA sequence caused by bisulfite treatment as well as the constraints for bisulfite-conversion DNA primer design and type of region analyzed. MethPrimer is a program based on Primer3 that is specifically used for designing PCR primers for methylation analyses (261). Bisulfite conversion-based PCR primers were designed using MethPrimer for the IGFBP-5 promoter CpG island, 1st CpG island in IGFBP-5 exon I, and the CpG island spanning ERα promoter/exon I. A summary of the CpG islands analyzed by the different DNA methylation analysis methods is listed in Table 1. Primer sequences used for DNA

analysis of these CpG islands by bisulfite DNA sequencing and methylation specific PCR are listed in Table 2. Primers were purchased from Sigma-Aldrich.

Bisulfite Treatment

Genomic DNA (5 μg) was digested overnight at 37°C with RsaI (New England Biolabs, Ipswich, MA) to make the DNA accessible to bisulfite treatment. Digested DNA was then treated with sodium bisulfite using the EZ DNA Methylation™ Kit (Zymo Research, Irvine, CA) according to the manufacturer's instructions. During bisulfite treatment, unmethylated cytosines are converted to uracil, while methylated cytosines remain as cytosines. A universal methylated DNA standard (Zymo Research) was used as a positive control to assess the efficiency of the bisulfite-mediated conversion of DNA. The universal methylated DNA standard consisted of pUC19 DNA isolated from a methylation-negative bacteria strain. All CpG sites of this standard were enzymatically methylated by M. SssI methyltransferase. The bisulfite-treated DNA was then used as a template for bisulfite DNA sequencing and methylation specific PCR.

Bisulfite DNA Sequencing

Bisulfite-treated DNA was used as a template for PCR using ZymoTaq™ Premix (Zymo Research) and primers designed to amplify the CpG island of interest (Table 3). Any unmethylated cytosines that were converted to uracil during bisulfite treatment were detected as thymine during PCR. PCR conditions were: initial denaturation at 95°C for 10 min, followed by 40 cycles of denaturation at 94°C for 30 sec, annealing at 55°C for 30 sec, and extension at 72°C for 1 min; final extension at 72°C for 7 min. PCR product

verification was performed by running samples on a 1% or 2% agarose gel. The resulting PCR product was purified using the QIAquick PCR Purification Kit (Qiagen, Valencia, CA). For analysis of IGFBP-5 CpG islands, nested PCR was performed to further amplify the region of interest (see primers in Table 2) and PCR purification was repeated as described above. PCR products were cloned using the pGEM®-T Easy Vector System (Promega, Fitchburg, WI). Positive clones were selected using a blue/white color screening. Plasmid DNA was isolated from positive clones using the QIAprep Spin MiniPrep Kit (Qiagen). Plasmid DNA (3 µl) was digested with the restriction enzyme EcoRI (Promega) for 3 hours at 37°C and digested products were run on a 1% agarose gel to confirm the presence of the insert. Plasmid DNA was sequenced using T7 (5' TAATACGACTCACTATAGGG 3') and SP6 (5' GATTTAGGTGACACTATAG 3') sequencing primers (GeneWiz, South Plainfield, NJ) to determine the methylation status of each CpG site in the CpG island. Sequencher® software version 4.10.1 (Gene Codes Coporation, Ann Arbor, MI) was used to align the sequences of all clones from the same tissue sample as well as clones from tissue samples from different animals to identify differences in conversion of cytosine to thymine at each CpG site.

Methylation Specific PCR

Bisulfite-treated DNA was used as a template for methylation specific PCR (MSP) using ZymoTaq™ Premix (Zymo Research) and primers designed to amplify the CpG island of interest (Table 2). Primers used for MSP specifically amplify either methylated or unmethylated DNA (Herman et al. 1996). For this reason, PCR was performed for each sample in duplicate with the first replicate containing primers that

recognize methylated DNA and the duplicate sample containing primers that recognize unmethylated DNA. Any unmethylated cytosines that were converted to uracil during bisulfite treatment were detected as thymine during PCR. PCR conditions were: initial denaturation at 95°C for 10 min, followed by 40 cycles of denaturation at 94°C for 30 sec, annealing at 55°C for 30 sec, and extension at 72°C for 1 min; final extension at 72°C for 7 min. PCR product verification was performed by running samples on a 2% agarose gel. The presence of a PCR product at the expected size indicated the presence of either unmethlated or methylated alleles. Bands detected with both primer sets indicated that either one or both alleles of the gene were methylated (259).

Pyrosequencing

Genomic DNA (1 μg at 20 ng/μl) from tumors and contralateral mammary glands (study 3) as well as PND 40 mammary glands (study 2) from the three treatment groups was sent to EpigenDx (Hopkinton, MA) for pyrosequencing. The 1st CpG island in the IGFBP-5 exon I (+282 to +91 from TSS, -468 to -659 from ATG) was analyzed. This was similar to the region we analyzed by bisfulfite DNA sequencing and MSP (+198 to +309), but slightly different due to assay design constraints. In order for the assay design to work over the entire area of interest, which encompassed 12 CpG sites, two separate pyrosequencing assays were conducted (assay #1: +283 to +226, assay #2: +127 to +92) and the data were combined to assess DNA methylation over this entire region. The PCR product size was 296 bp. EpigenDx in-house control DNA was used for assay development, which involved optimization of bisulfite modification, PCR, and pyrosequencing for the CpG island of interest. At EpigenDx, in-house control DNA (200

– 500 ng) was subjected to bisulfite modification using the EZ DNA Methylation™ Kit (Zymo Research) followed by PCR amplification using HotStar Taq Polymerase (Qiagen). PCR cycling conditions were: 95°C for 15 min, 45 cycles of 95°C 15 sec, 62°C for 30 sec, 72°C for 30 sec; and 72°C for 5 min. The in-house control assay passed quality control with an R^2 of 0.9377. After confirmation that the assay design was successful, genomic DNA samples were subjected to bisulfite modification and PCR as described above, followed by pyrosequencing. Briefly, one of the PCR primers was biotin labeled and was immobilized on streptavidin-coated beads, which resulted in a single stranded PCR product. A complementary pyrosequencing primer was then hybridized to the single stranded PCR product and pyrosequencing was performed by sequentially adding individual nucleotides to the reaction. Percent methylation of each CpG site within the CpG island was then calculated (260). Three positive controls (low, medium, and highly methylated DNA) as well as a negative control were included in the analysis. Ten samples were also run in duplicate to confirm accuracy of the assay.

Results

DNA Methylation of the IGFBP-5 Promoter CpG Island in Mammary Tumors and Mammary Glands of Animals Exposed to Alcohol *In Utero*

MethPrimer was used to identify CpG islands in the IGFBP-5 promoter. The only CpG island identified in the promoter was located between -211 and -310 from the transcription start site (TSS) and contained 10 CpG sites (Figure 2). DNA methylation was analyzed by bisulfite DNA sequencing in a small subset of NMU-induced mammary tumors from study 1 (Table 3). These tumors were all from animals exposed to alcohol *in utero* and were collected at 23 weeks post-NMU injection. Each of the clones obtained was confirmed by sequencing as the IGFBP-5 nested PCR product. A universal methylated DNA standard was used as a positive control to assess the efficiency of the bisulfite DNA sequencing reaction. The standard was also confirmed by sequencing and as expected, all CpG sites in the standard were shown to be methylated. Two tumors exhibited methylation, whereas the other two did not. One clone from one tumor had methylation at CpG sites 1 and 3. Two clones from a second tumor exhibited methylation at CpG site 2 or 5, respectively. Methylation at only one or two CpG sites, if any, was observed in these tumors and the methylation that was seen was at different CpG sites, suggesting minimal methylation was present in these tumors. Bisulfite DNA sequencing was also performed with mammary glands from PND 40 animals (study 2; Table 4). The majority of the mammary glands did not exhibit methylation at any of the CpG sites. CpG site 4 was methylated in one clone obtained from one pair-fed mammary gland and from one ad lib mammary gland. One clone from a second ad lib mammary gland exhibited

methylation at CpG sites 2 and 3. Collectively these analyses suggested that there was little to no DNA methylation in the IGFBP-5 promoter CpG island in tumors and mammary glands from animals exposed to alcohol *in utero*. For this reason, we decided to examine the 1st CpG island in IGFBP-5 exon I.

DNA Methylation of the 1st CpG Island in IGFBP-5 Exon I in Mammary Tumors and Mammary Glands of Animals Exposed to Alcohol *In Utero*

Bisulfite DNA Sequencing

MethPrimer was used to identify CpG islands in IGFBP-5 exon I. The 1st CpG island in exon I was located between +198 and +309 relative to the TSS and contained 12 CpG sites (Figure 3). DNA methylation for a small subset of NMU-induced mammary tumors from alcohol-exposed animals in study 1, where we terminated the study at 23 weeks post-NMU injection, were analyzed by bisulfite DNA sequencing (Table 5). All clones from each of the tumors were confirmed by sequencing as the IGFBP-5 PCR product. Methylation was observed in all clones from all tumors, except for two clones from one tumor. The majority of the methylation observed was at CpG sites 4 – 9. It must be noted that chromatogram quality was low for certain regions in some clones. These data suggested that there may be DNA methylation in the 1st CpG island in IGFBP-5 exon I in mammary tumors of animals exposed to alcohol *in utero,* thus warranting further investigation. For a more thorough analysis of the DNA methylation in this CpG island, it would have been necessary to analyze 10 or more clones per tumor and also sequence each clone in both directions to get a clean chromatogram over the entire CpG

island. Therefore, in order to get a general idea about whether or not there was methylation in the 1st CpG island in IGFBP-5 exon I, methylation specific PCR (MSP) was performed.

Methylation Specific PCR (MSP)

MSP was performed for the 1st CpG island in IGFBP-5 exon I (the same region analyzed by bisulfite DNA sequencing; Figure 4). NMU-induced mammary tumors (study 1; termination at 23 weeks post-NMU injection) and PND 40 mammary glands (study 2) from animals exposed and not exposed to alcohol *in utero* were analyzed. Almost all tumors (Figure 5) and mammary glands (Figure 6) from all treatment groups exhibited both methylated and unmethylated DNA, although no tumors or mammary glands exhibited only methylated DNA. There were a few mammary glands that exhibited only unmethylated DNA. Semi-quantitation of these data indicated no difference among treatment groups (tumors: one-way ANOVA $p = 0.5664$; mammary glands: one-way ANOVA $p = 0.0967$). Since many tumors and mammary glands had some methylated DNA, pyrosequencing was performed to obtain a more quantitative analysis of the methylation in the 1st CpG island in IGFBP-5 exon I.

Pyrosequencing

Pyrosequencing was performed to determine DNA methylation of the 1st CpG island in IGFBP-5 exon I. Analysis was performed on mammary tumors (Table 6) and contralateral mammary glands (Table 7) collected in study 3 (tissues collected at 16 weeks post-NMU injection) as well as normal mammary glands from PND 40 animals

(study 2; Table 8). Tumors from study 1 (tissues collected at 23 weeks post-NMU injection) were not analyzed by pyrosequencing because tissue was limited. There was little to no methylation in the 1st CpG island in IGFBP-5 exon I in all of the tissues analyzed. Some samples were run in duplicate (Tables 6, 7, and 8 - yellow highlight) for confirmation purposes. Although the percent methylation varied somewhat between duplicates, there was still overall low methylation in these samples. Positive controls exhibiting low, medium, and high levels of methylation were used as a reference. All CpG sites exhibited an overall percent methylation that was comparable to the low methylation positive control, which ranged from 0.9% to 4.9%, and had much lower methylation than the medium methylation positive control, which ranged from 30.1 to 42.7%.

DNA Methylation of Estrogen Receptor α Promoter/Exon I CpG Island in Mammary Tumors of Animals Exposed to Alcohol *In Utero*

MethPrimer was used to identify CpG islands within -346 and +264 relative to the TSS in the estrogen receptor α (ERα) gene. A CpG island was identified from -19 to +107 relative to the TSS, which spans the promoter/exon I (Figure 7). DNA methylation for a subset of NMU-induced mammary tumors from animals exposed and not exposed to alcohol *in utero* in study 1 were analyzed by MSP (Figure 8). All tumors from all treatment groups exhibited both methylated and unmethylated DNA. No tumors exhibited only methylated DNA. There was one alcohol tumor that clearly had more methylated DNA as compared to unmethylated DNA. A PND 40 mammary gland from an ad lib animal (study 2) was also analyzed (Figure 8). Some methylation was also observed in

the normal mammary gland as well. Semi-quantitation of these data indicated no differences among treatment groups (one-way ANOVA $p = 0.2153$). However, it should be noted that tumors in the alcohol group tended to have more methylated DNA than unmethylated DNA as compared to the pair-fed group, which had equal amounts of methylated and unmethylated DNA.

Discussion

In the last few years numerous studies have shown that alcohol exposure *in utero* induces epigenetic alterations in the offspring (153-160). Although other *in utero* exposures have been shown to cause epigenetic modifications in the mammary gland (134, 161), this study represents the first analysis of epigenetic alterations in the mammary gland or in NMU-induced mammary tumors of animals exposed to alcohol *in utero*. DNA methylation of CpG islands in the promoter region of a gene results in transcriptional silencing which can occur directly due to DNA methylation or due to conformational changes in chromatin that inhibit transcription (250, 251). Therefore we first analyzed DNA methylation of the IGFBP-5 promoter CpG island in NMU-induced mammary tumors of animals exposed to alcohol *in utero* (23 weeks post-NMU injection) as well as in PND 40 mammary glands of alcohol-exposed and control animals. The tumor analysis was limited as we only analyzed four tumors from alcohol-exposed animals and only one to two clones per tumor. We chose to perform the analysis on tumors from the alcohol group only as that is the treatment group where we expected to see methylation. This was the first time our lab had ever performed bisulfite DNA sequencing so we chose to start with a small subset of tumors to determine if we could detect methylation at all. Since the data didn't seem promising, we decided not to analyze additional tumors or clones. The PND 40 mammary gland analysis consisted of two mammary glands per treatment group with anywhere from two to nine clones per tumor, again to get a general idea if there was any methylation. Although a limited number of tissues and clones was analyzed, we concluded from these data that the IGFBP-5 promoter CpG island was not methylated in response to alcohol exposure *in utero*.

A recent genome-wide study analyzing the relationship between DNA methylation and gene expression found a stronger link between DNA methylation in exon I (downstream of the TSS) and transcriptional silencing as compared to DNA methylation in the promoter region (252). We therefore decided to analyze DNA methylation in the 1st CpG island of IGFBP-5 exon I. Methylation was observed in mammary tumors of animals exposed to alcohol *in utero*. For a more thorough analysis of the DNA methylation in this CpG island using bisulfite DNA sequencing, it would have been necessary to analyze a larger number of tumors, 10 or more clones per tumor (262), and also sequence each clone in both directions to get a clean chromatogram over the entire CpG island. Although we did see some methylation and the data looked promising, this did not seem to be the most feasible option in terms of time and cost. Therefore, in order to get a general idea about whether or not there was methylation in the 1st CpG island of IGFBP-5 exon I, we decided to perform methylation specific PCR (MSP). Almost all tumors and mammary glands analyzed from all treatment groups exhibited partial methylation. However, we did not observe any samples that were completely methylated. There also did not seem to be a difference among treatment groups in the degree of methylation. A limitation of the MSP performed, as with any MSP, is that only two CpG sites are recognized by the forward primer and only one CpG site is recognized by the reverse primer. Therefore, these specific sites must be methylated to detect a methylated band. For a more thorough analysis of the DNA methylation differences in this region, CpG sites all along the entire CpG island should be analyzed. Since we did observe that many samples in the tumors and mammary glands had partial methylation, we decided to perform pyrosequencing in order to analyze all CpG sites in this CpG island and to get a

more quantitative analysis of the DNA methylation in this 1st CpG island of IGFBP-5 exon I.

Pyrosequencing analysis indicated low methylation in all samples at all CpG sites for NMU-induced mammary tumors and their contralateral mammary glands, as well as PND 40 mammary glands from all treatment groups. Previously we found that at 16 weeks post-NMU injection, tumor IGFBP-5 mRNA expression was increased in animals exposed to alcohol *in utero* compared to pair-fed animals (Chapter 3). Thus, we hypothesized that at this time point there would be decreased IGFBP-5 DNA methylation in alcohol-exposed group compared to the pair-fed group. However, pyrosequencing data showed that there was not a difference in DNA methylation among the alcohol and pair-fed groups. We also performed a side-by-side comparison of the DNA methylation results by MSP and pyrosequencing for a subset of samples (data not shown). MSP showed that there was a significant amount of methylation (50%) in these samples, however, by pyrosequencing they exhibited little to no methylation. Consultation with EpigenDx revealed that this is not the first time discrepancies have been observed between MSP and pyrosequencing data. They attributed the discrepancies to platform differences, but further analysis is needed to confirm that this is indeed the case. It is possible that the decrease in IGFBP-5 expression is due to DNA methylation of other CpG islands or CpG shores within the gene. Alternatively, other epigenetic modifications such as histone modifications (methylation, acetylation, phosphorylation, ubiquitination or sumoylation), microRNAs, or long noncoding RNAs may play a role. Lastly, there is also a possibility that IGFBP-5 expression is not altered by an epigenetic means.

The human ERα gene has a CpG island in its promoter and exon I which contains numerous sites for methylation-sensitive restriction endonucleases, making this gene highly susceptibility to DNA methylation and subsequent transcriptional inactivation (263). This raises the possibility that the increase in ERα negative tumors in alcohol-exposed animals at 23 weeks post-NMU (32) might arise through an epigenetic mechanism. Human ER negative breast cancer cells exhibit hypermethylation in a CpG island in the 5' region of the ER gene, which correlates with loss of ER expression. Demethylation of this region restores ER expression levels (263-265). Furthermore, in primary human breast tumors methylation of the 5' ER CpG island is also observed and it also correlates with loss of ER gene expression (266). Previous work analyzing ER DNA methylation in spontaneous and carcinogen-induced mammary tumors and contralateral mammary glands in the rat focused on an exon I CpG island (267). Another study analyzing ERα DNA methylation in rats analyzed a CpG island spanning the promoter/exon I (268). Using MethPrimer software, we searched for CpG islands in the rat ERα gene. We did not find any CpG islands within 3000 bp upstream of the TSS. When the first 2794 bp of the ERα gene was analyzed (with the first base as the TSS), three CpG islands were identified: the first spanning introns 1 and 2, the second spanning introns 1 and 2 as well as exon 2, and the third spanning exon 2 only (data not shown). These CpG islands did not correlate with the ERα CpG islands analyzed in the literature. For this reason, we then examined both regions together and found a CpG island that spans the promoter and exon I. In an effort to be consistent with the ERα CpG islands previously studied by other groups, we chose to analyze the ERα CpG island spanning the promoter/exon I. Tumors from all treatment groups were partially methylated. All of

the pair-fed tumors had equal amounts of methylated and unmethylated DNA. However, in the alcohol group three of the four samples had slightly more methylated DNA than unmethylated DNA. The fourth sample in the alcohol group clearly had greater methylated DNA than unmethylated DNA. It is interesting to point out that this particular tumor also had the lowest ERα mRNA expression of all the tumors analyzed for ERα MSP (data not shown). This suggests that there may be slightly more methylation in the tumors of the alcohol group compared to the pair-fed group and that extent of DNA methylation may correlate with ERα expression. DNA methylation analysis in an exon I ER CpG island found that 50% of DMBA-induced mammary tumors from Sprague Dawley rats exhibited hypomethylation (267). This may explain why we found low levels of methylation in our NMU-induced mammary tumors across all treatment groups. A limitation of this MSP analysis is that only one CpG site in the region where each primer binds was assessed. To get a more thorough analysis of whether or not there is differential DNA methylation in this region, CpG sites all along the entire CpG island should be analyzed. Thus, future studies should focus on other methodologies that are capable not only of determining methylation at each CpG site within the CpG island or CpG shores, but can also provide a quantitative means by which to assess DNA methylation. Since MSP analysis only detects methylation at the few CpG sites within the primer binding regions, future studies to determine if ERα methylation plays a role in the loss of ERα expression observed in alcohol-exposed animals should analyze all CpG sites in this CpG island.

Analysis Method	Gene	CpG Island Analyzed	Location Relative to Transcription Start Site (TSS)
Bisulfite DNA sequencing	IGFBP-5	Promoter	-310 to -211
	IGFBP-5	1st CpG island in IGFBP-5 Exon I	+198 to +309
Methylation Specific PCR	IGFBP-5	1st CpG island in IGFBP-5 Exon I	+198 to +309
	ERα	Promoter/Exon I	-19 to +107
Pyrosequencing	IGFBP-5	1st CpG island in IGFBP-5 Exon I	+91 to +282

Table 1. Summary list of DNA methylation analyses performed. The type of DNA methylation analysis performed for either IGFBP-5 or ERα is listed. The location of the specific CpG island analyzed in that gene is also indicated.

Analysis Method	Gene	CpG Island Analyzed	Primer Sequence (5' to 3')	Product Length
Bisulfite DNA Sequencing	IGFBP-5	Promoter	Outer PCR F: GAAAATGTGATTTTTAATAGTTAGTGTT R: AACTACAATTTAAACTCCCCAACAC Nested PCR F: TTTATTGTGTTTATTTAGTTTTTGA R: CAAAAATACCAAAAAACTTTACAAC	316 bp 224 bp
Bisulfite DNA Sequencing	IGFBP-5	1st CpG island in Exon I	Outer PCR F: GTTGTAAAGTTGTTTGGGTTTTTT R: CCCACTTCTCTCAACTACCAACTAC Nested PCR F: GAGGTTTGAGTTTTTGTTTTTTTT R: CCACTTCTCTCAACTACCAACTAC	279 bp 128 bp
Methylation Specific PCR	IGFBP-5	1st CpG island in Exon I	Methylated F: GTATTTTTTTTCGGATTTTTTGC R: CACTTCTCTCAACTACCAACTACG Unmethylated F: TTTTTTTTGGATTTTTTGTGG R: CACTTCTCTCAACTACCAACTACACC	209 bp 205 bp
Methylation Specific PCR	ERα	Promoter/ Exon I	Methylated F: TTTGTAGAAGTTTAGTTGTCGCGT R: CCTACCCTACTAATTCAAAAACGTC Unmethylated F: TTTTGTAGAAGTTTAGTTGTTGTGT R: CCTACCCTACTAATTCAAAAACATC	244 bp 245 bp

Table 2. Primer sequences used for DNA methylation analyses. List of primer sequences used for the various DNA methylation analyses performed are indicated. The forward primer (F) is listed first and the reverse primer (R) is listed second.

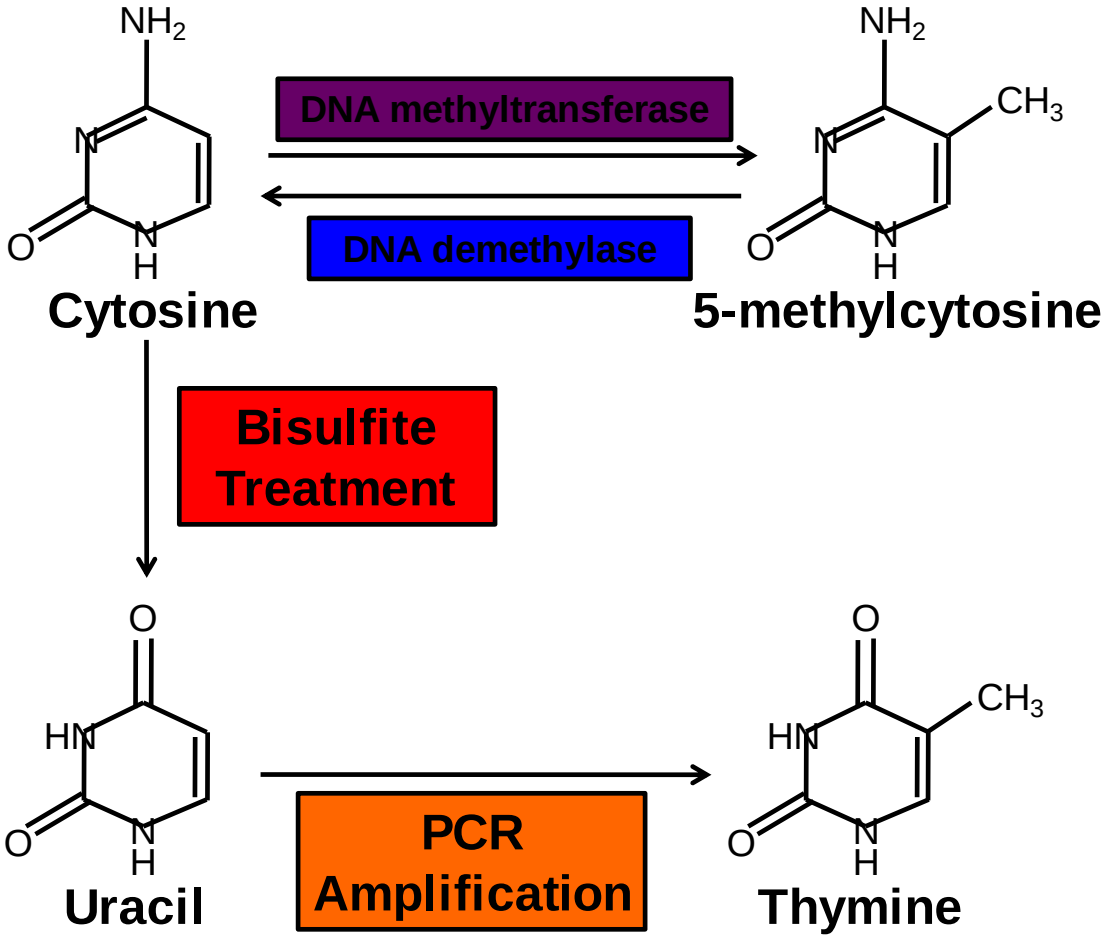

Figure 1. Schematic diagram of bisulfite DNA sequencing. DNA methylation occurs when DNA methyltransferases (DNMTs) add methyl groups from S-adenosylmethionines to carbon 5 positions of cytosines generating 5-methylcytosine. DNA demethylase can remove the methyl group converting 5-methylcytosine back to cytosine. Upon bisulfite treatment, unmethylated cytosines are converted to uracil through deamination. During PCR amplification, uracil is recognized as thymine. At the end of the bisulfite DNA sequencing process, unmethylated cytosines are recognized as thymines, whereas methylated cytosines remain as cytosines.

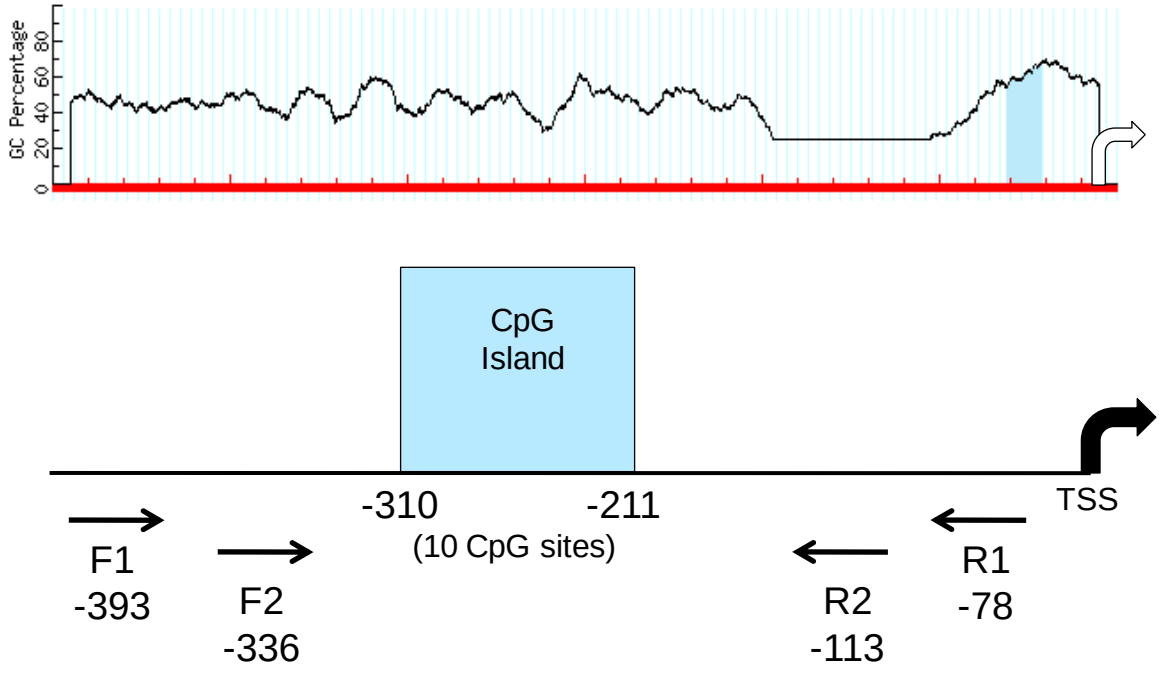

Figure 2. Schematic diagram of the IGFBP-5 promoter CpG island and primer locations for bisulfite DNA sequencing. MethPrimer was used to identify CpG islands in the IGFBP-5 promoter. The only CpG island identified in the promoter (blue) was located between -211 and -310 from the transcription start site (TSS) and contained 10 CpG sites. Locations (relative to the TSS) of the outer PCR primers (F1 and R1) and the nested PCR primers (F2 and R2) used for bisulfite DNA sequencing of this region are indicated.

Sample	Clone	Confirmed as IGFBP-5 Nested PCR Product?	CpG Sites Methylated
Tumor #1	1	Yes	None
	2	Yes	None
Tumor #2	1	Yes	None
	2	Yes	None
Tumor #3	1	Yes	#'s 1 & 3
Tumor #4	1	Yes	#2
	2	Yes	#5
Standard	-	Confirmed as standard	All (#'s 1 – 34)

Table 3. The IGFBP-5 promoter CpG island does not exhibit methylation in tumors from animals exposed to alcohol *in utero* collected at 23 weeks post-NMU injection (study 1). Bisulfite DNA sequencing was performed for the IGFBP-5 promoter CpG island to assess DNA methylation of this region in NMU-induced mammary tumors (23 weeks post-NMU injection) from animals exposed to alcohol *in utero*. This region contained 10 CpG sites total. Methylated CpG sites are indicated. A universal methylated DNA standard was used as a positive control to assess the efficiency of the bisulfite DNA sequencing reaction.

Sample	Clone	CpG Sites Methylated
Alcohol MG #1	1	None
	2	None
	3	None
	4	None
	5	None
	6	None
	7	None
	8	None
	9	None
Alcohol MG #2	1	None
	2	None
	3	None
	4	None
	5	None
Pair-fed MG #1	1	#4
	2	None
	3	None
	4	None
Pair-fed MG #2	1	None
	2	None
Ad lib MG #1	1	None
	2	#4
	3	None
	4	None
Ad lib MG #2	1	#'s 2 & 3
	2	None
	3	None
	4	None

Table 4. The IGFBP-5 promoter CpG island does not exhibit methylation in PND 40 mammary glands from animals exposed and not exposed to alcohol *in utero* (study 2). Bisulfite DNA sequencing was performed for the IGFBP-5 promoter CpG island to assess DNA methylation of this region in mammary glands from PND 40 animals that were and were not exposed to alcohol *in utero*. All nested PCR products were confirmed as IGFBP-5 and methylated CpG sites are indicated.

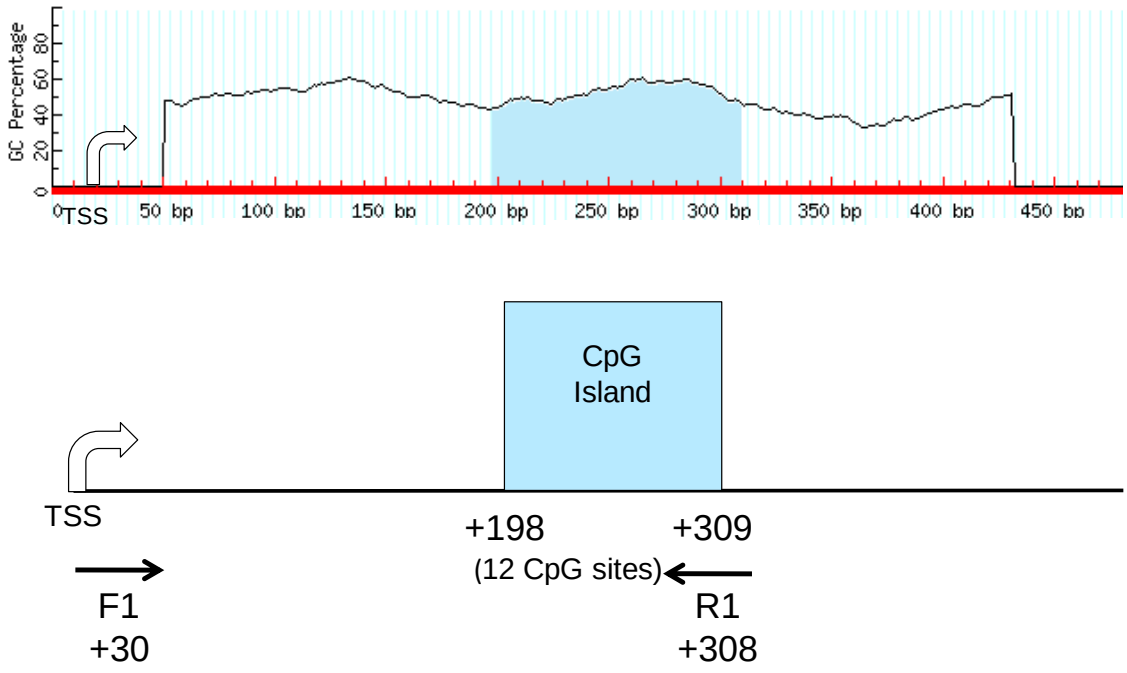

Figure 3. Schematic diagram of the 1st CpG island in IGFBP-5 exon I and primer locations for bisulfite DNA sequencing. MethPrimer was used to identify CpG islands in the IGFBP-5 gene. The 1st CpG island in exon I (blue) was located between +198 to +309 relative to the transcription start site (TSS) and contained 12 CpG sites. Locations (relative to the TSS) of the PCR primers used for bisulfite DNA sequencing of this region are indicated.

		CpG site											
Sample	**Clone**	**#1**	**#2**	**#3**	**#4**	**#5**	**#6**	**#7**	**#8**	**#9**	**#10**	**#11**	**#12**
Tumor #1	1			X		X	X	X	X	X	X		
	2					X							
Tumor #2	1												
	2					X							
	3												
Tumor #3	1			X	X								
	2			X	X								
	3					X	X	X	X				
Tumor #4	1	X	X		X		X	X					
	2					X	X	X	X	X			X
	3	X	X		X		X	X					
	4					X	X	X	X	X			X
	5					X	X	X	X	X	X		

Table 5. The 1st CpG island in IGFBP-5 exon I exhibits methylation in tumors from animals exposed to alcohol *in utero* collected at 23 weeks post-NMU injection (study 1). Bisulfite DNA sequencing was performed for the 1st CpG island in IGFBP-5 exon I to assess DNA methylation of this region in NMU-induced mammary tumors (23 weeks post NMU-injection) of animals exposed to alcohol *in utero*. Methylated CpG sites are indicated with an X (black = chromatogram quality is clean, red = chromatogram quality drops off).

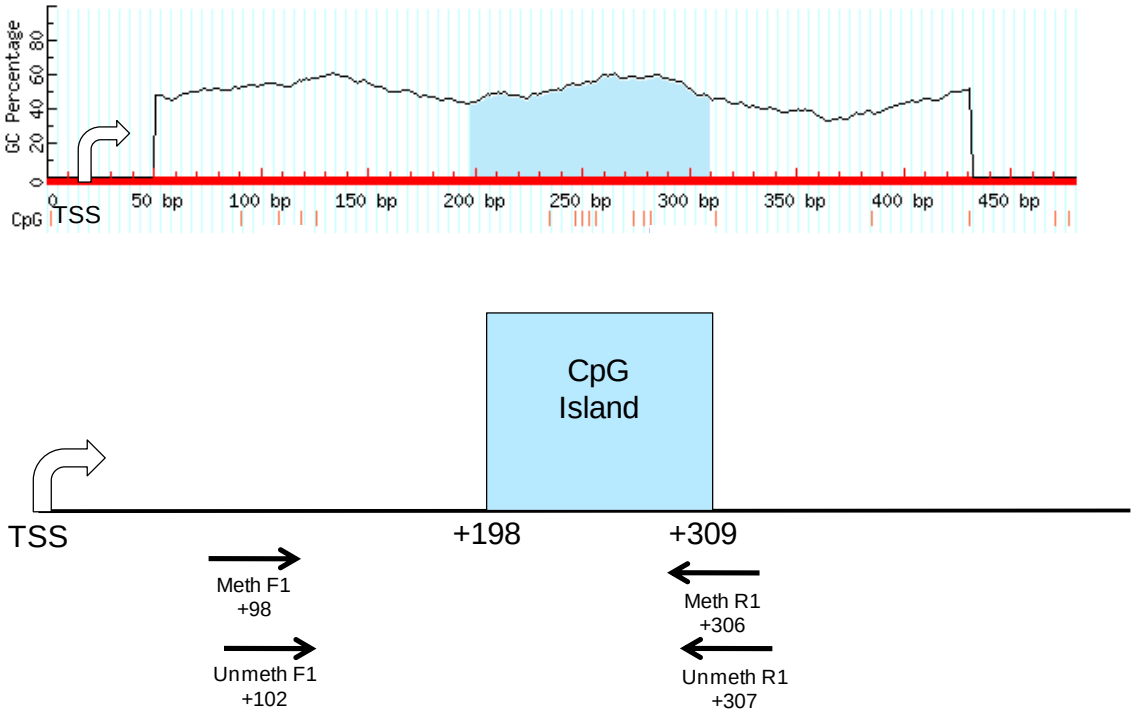

Figure 4. Schematic diagram of the 1st CpG island in IGFBP-5 exon I and primer locations for methylation specific PCR. MethPrimer was used to identify CpG islands in the IGFBP-5 gene. The 1st CpG island in exon I (blue) was located between +198 to +309 relative to the transcription start site (TSS). Locations of PCR primers (relative to the TSS) used to detect methylated (Meth F1, Meth R1) and unmethylated (Unmeth F1, Unmeth R1) DNA by methylation specific PCR are indicated.

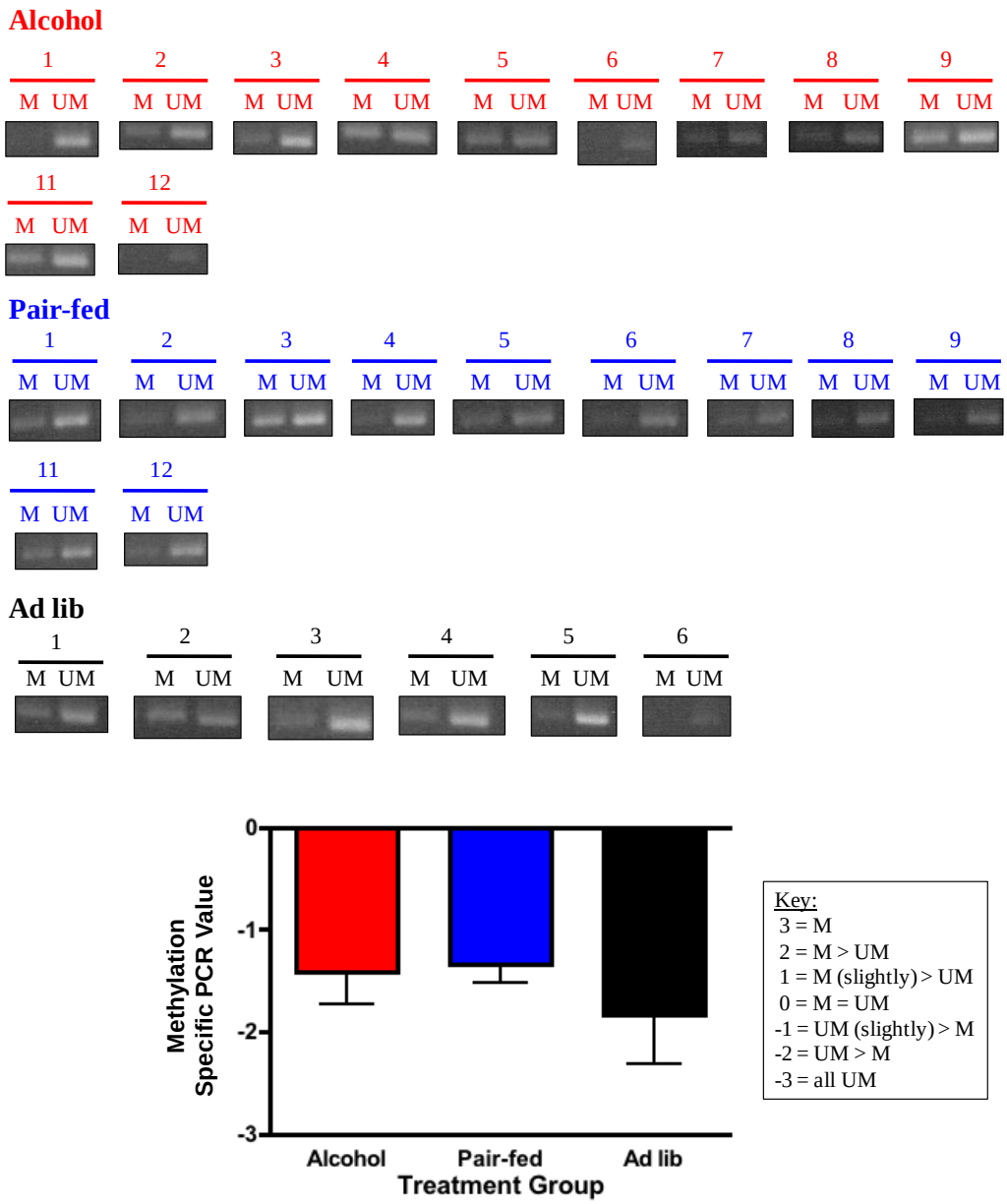

Figure 5. DNA methylation in the 1st CpG island of IGFBP-5 exon I in tumors from animals exposed and not exposed to alcohol *in utero* collected at 23 weeks post-NMU injection (study 1). Methylation specific PCR (MSP) was performed for the 1st CpG island in IGFBP-5 exon I to assess DNA methylation of this region in NMU-induced mammary tumors (23 weeks post NMU-injection) of animals exposed and not exposed to alcohol *in utero*. Each box of two bands represents methylated (M) and unmethylated (UM) DNA from each tumor. Semi-quantitation of MSP results (bottom); n =12 (alcohol), 12 (pair-fed), and 6 (ad lib) tumors. A key for how the scoring was performed is indicated (M = methylated, UM = unmethylated). Data were analyzed using a one-way ANOVA (p = 0.5664).

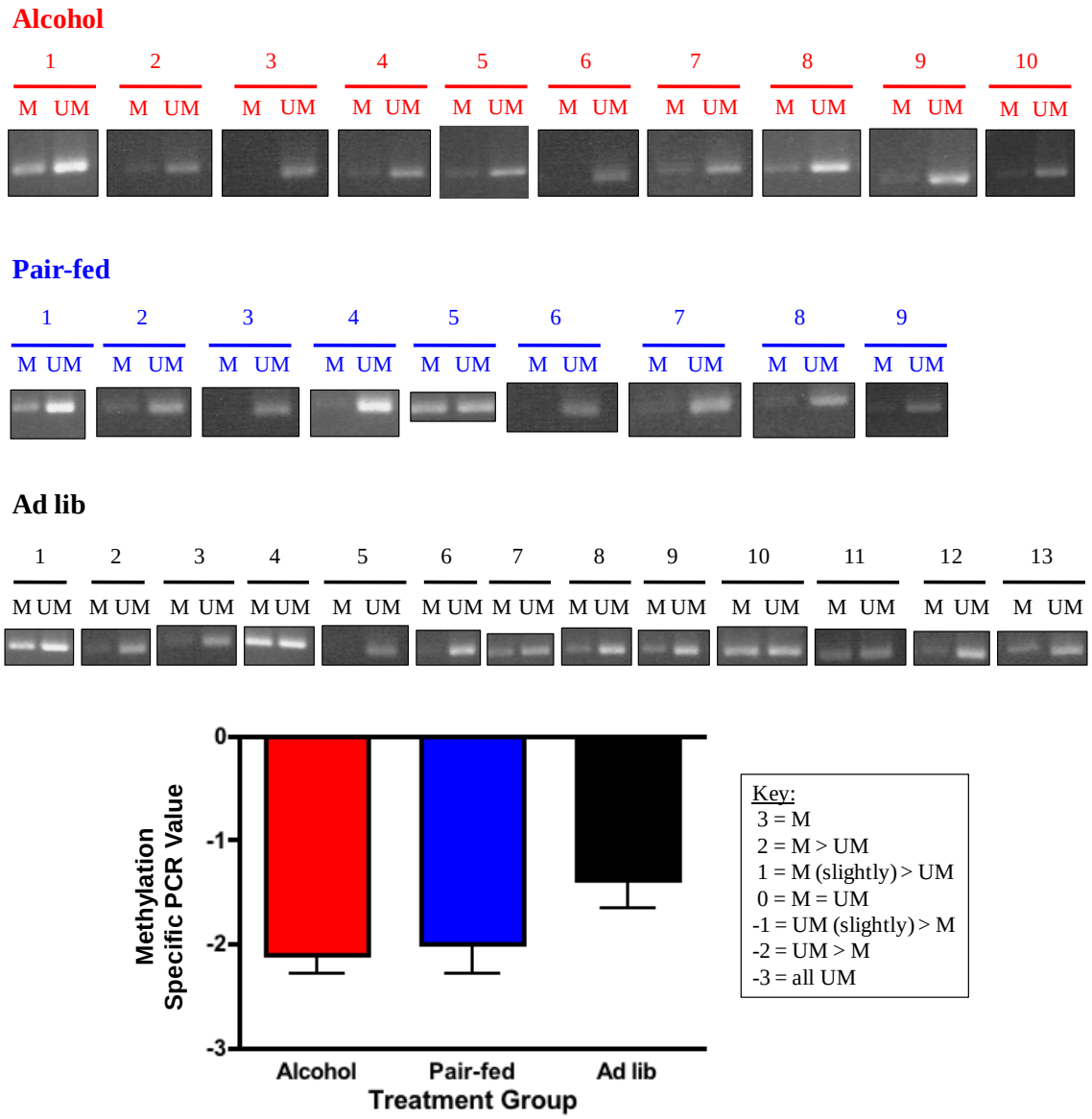

Figure 6. DNA methylation in the 1st CpG island of IGFBP-5 exon I in PND 40 mammary glands from animals exposed and not exposed to alcohol *in utero* (study 2). Methylation specific PCR (MSP) was performed for the 1st CpG island in IGFBP-5 exon I to assess DNA methylation of this region in mammary glands from PND 40 animals that were and were not exposed to alcohol *in utero*. Each box of two bands represents methylated (M) and unmethylated (UM) DNA from each mammary gland. Semi-quantitation of MSP results (bottom); n =10 (alcohol), 9 (pair-fed), and 13 (ad lib) mammary glands. A key for how the scoring was performed is indicated (M = methylated, UM = unmethylated). Data were analyzed using a one-way ANOVA (p = 0.0967).

Rat IGFBP-5 Methylation Analysis - Results in % Methylation																
TUMORS	**Assay #1**								**Assay #2**				**Overall Region**			
From ATG	-468	-471	-476	-494	-497	-500	-503	-515	-624	-631	-642	-659	-468 to -659			
From TSS	+283	+280	+275	+257	+254	+251	+248	+236	+127	+120	+109	+92	+283 to +92			
CpG site	**Pos #12**	**Pos #11**	**Pos #10**	**Pos #9**	**Pos #8**	**Pos #7**	**Pos #6**	**Pos #5**	**Pos #4**	**Pos #3**	**Pos #2**	**Pos #1**	**Mean**	**St Dev**	**Min**	**Max**
Alcohol #1	4.6	2.5	2.9	2.7	3.9	4.5	1.5	2.8	3.1	3.3	4.1	5.4	3.4	1.1	1.5	5.4
Alcohol #2	1.7	1.4	1.5	2.2	1.8	2.0	1.0	3.0	1.1	1.5	2.2	3.6	1.9	0.8	1.0	3.6
Alcohol #3	28.5	18.7	2.2	1.8	2.7	15.1	2.2	3.1	1.1	0.0	2.2	3.6	6.8	9.0	0.0	28.5
Alcohol #4	4.9	9.0	9.3	2.1	4.1	2.3	0.0	2.9	1.0	2.9	5.5	3.9	4.0	2.9	0.0	9.3
Alcohol #5	3.1	2.8	4.8	2.4	2.4	3.2	2.3	2.7	3.3	2.3	3.7	5.1	3.2	0.9	2.3	5.1
Alcohol #6	3.4	2.3	3.3	2.9	2.4	3.3	1.7	3.1	2.1	1.7	3.8	4.2	2.9	0.8	1.7	4.2
Alcohol #7	1.1	1.1	1.3	1.6	1.5	2.3	0.0	3.1	0.9	0.0	2.3	3.9	1.6	1.2	0.0	3.9
Alcohol #7 duplicate	1.6	1.5	2.5	2.4	2.6	2.5	0.0	3.2	1.1	2.0	2.7	10.3	2.7	2.5	0.0	10.3
Alcohol #8	3.0	2.1	1.9	1.5	2.2	2.8	1.7	3.8	8.2	7.3	9.0	4.5	4.0	2.7	1.5	9.0
Alcohol #9	3.7	2.2	3.6	0.0	4.2	2.6	0.0	3.3	3.3	1.7	4.4	4.5	2.8	1.5	0.0	4.5
Alcohol #10	4.9	2.6	2.7	0.0	1.4	1.4	1.9	2.2	0.8	0.0	2.6	3.6	2.0	1.4	0.0	4.9
Alcohol #11	0.0	2.4	1.9	1.8	1.2	2.2	0.0	2.7	1.0	0.0	3.1	3.4	1.6	1.2	0.0	3.4
Alcohol #11 duplicate	1.1	1.1	5.4	2.2	3.5	3.7	1.3	2.8	5.8	2.9	4.0	5.6	3.3	1.7	1.1	5.8
Alcohol #12	1.5	3.0	1.8	2.2	2.2	2.7	1.6	2.5	1.7	1.9	3.3	3.6	2.3	0.7	1.5	3.6
Pair-fed #1	1.3	1.1	4.4	3.3	2.3	3.6	3.6	5.2	5.2	2.7	4.6	4.6	3.5	1.4	1.1	5.2
Pair-fed #2	3.5	3.3	8.1	2.4	2.7	1.8	1.6	3.2	3.1	3.0	5.4	4.3	3.5	1.8	1.6	8.1
Pair-fed #3	3.7	4.5	4.5	4.1	2.2	11.4	1.2	3.0	0.8	2.0	2.1	3.7	3.6	2.7	0.8	11.4
Pair-fed #4	3.0	3.8	8.8	2.2	1.7	4.3	1.5	2.8	0.9	1.5	4.4	3.9	3.2	2.1	0.9	8.8
Pair-fed #5	4.4	5.4	6.1	3.1	3.3	3.7	2.9	2.9	2.5	2.3	2.8	4.1	3.6	1.2	2.3	6.1
Pair-fed #6	5.1	3.1	4.1	3.0	1.8	2.9	1.4	3.6	3.1	1.3	3.0	5.2	3.1	1.3	1.3	5.2
Pair-fed #7	2.7	6.5	0.0	0.0	2.2	1.4	0.0	2.7	1.2	0.0	4.0	3.9	2.0	2.0	0.0	6.5
Pair-fed #8	2.6	11.6	5.0	3.1	2.1	7.0	3.2	4.7	6.7	2.9	2.0	4.2	4.6	2.8	2.0	11.6
Pair-fed #9	5.1	6.5	6.8	2.1	2.2	1.4	0.0	2.6	2.4	0.0	5.9	3.8	3.2	2.4	0.0	6.8
Pair-fed #9 (duplicate)	6.9	5.1	5.5	2.5	3.4	4.8	1.9	4.0	2.6	2.1	6.4	5.5	4.2	1.7	1.9	6.9
Pair-fed #10	3.9	6.7	3.4	2.7	3.3	4.1	0.0	3.8	2.9	0.0	4.2	5.7	3.4	2.0	0.0	6.7
Ad lib #1	2.0	1.8	3.1	0.0	2.0	1.7	0.0	2.8	2.0	1.3	3.4	3.8	2.0	1.2	0.0	3.8
Ad lib #2	1.1	1.2	4.0	3.8	2.1	3.6	0.0	2.7	3.2	3.3	8.5	3.7	3.1	2.1	0.0	8.5
Ad lib #3	1.0	1.3	2.4	2.4	2.1	2.0	1.7	3.0	3.7	3.6	5.1	3.7	2.7	1.2	1.0	5.1
Ad lib #4	2.7	3.8	4.5	1.6	2.4	2.9	1.7	3.8	3.1	1.2	2.4	4.5	2.9	1.1	1.2	4.5
Ad lib #5	2.8	4.6	3.4	1.6	2.7	2.2	1.9	2.7	1.9	1.3	3.7	3.9	2.7	1.0	1.3	4.6
Ad lib #6	2.4	3.2	3.1	2.0	2.2	2.4	1.5	3.2	1.0	1.6	2.5	3.9	2.4	0.8	1.0	3.9
Ad lib #7	4.5	3.7	5.1	4.7	3.9	2.3	4.9	4.4	2.5	1.6	3.7	5.7	3.9	1.2	1.6	5.7
Ad lib #8	3.4	4.0	3.1	2.7	2.2	3.9	1.9	3.6	2.8	2.7	3.6	4.7	3.2	0.8	1.9	4.7
Ad lib #9	2.6	3.4	4.3	1.7	3.6	2.2	0.0	3.6	1.6	2.3	2.6	4.2	2.7	1.2	0.0	4.3
Ad lib #9 duplicate	3.1	4.1	0.0	0.0	2.9	5.4	1.6	2.6	2.1	0.0	3.1	3.5	2.4	1.7	0.0	5.4
Ad lib #10	1.4	5.4	0.0	1.4	1.1	1.9	2.9	2.6	2.2	0.0	2.8	5.3	2.2	1.7	0.0	5.4
Low Meth	3.0	2.2	2.5	2.1	3.1	2.7	1.0	4.1	0.9	2.1	4.0	4.9	2.7	1.2	0.9	4.9
Med Meth	38.6	41.1	42.7	41.1	38.3	37.3	30.1	39.5	41.2	40.2	37.6	37.3	38.7	3.3	30.1	42.7
High Meth	86.6	91.9	95.8	88.3	81.9	84.5	65.6	83.9	92.7	92.1	86.3	87.5	86.4	7.7	65.6	95.8
NTC																

Table 6. Pyrosequencing indicates that there is little to no methylation in the 1st CpG island of IGFBP-5 exon I in tumors from animals exposed and not exposed to alcohol *in utero* collected at 16 weeks post-NMU injection (study 3). Pyrosequencing was performed to determine DNA methylation of the 1st CpG island in IGFBP-5 exon I (+282 to +91 from the transcription start site) of tumors (16 weeks post-NMU injection) from animals that were and were not exposed to alcohol *in utero*. This region contained 12 CpG sites total. Percent methylation for each tumor at each CpG site is indicated. n = 12 (alcohol), 10 (pair-fed), and 10 (ad lib) tumors. Yellow highlight indicates samples that were run in duplicate. Percent methylation of positive controls exhibiting low, medium, and high levels of methylation are indicated at the bottom.

Rat IGFBP-5 Methylation Analysis - Results in % Methylation																
CONTRALATERAL MGS	**Assay #1**								**Assay #2**				**Overall Region**			
From ATG	-468	-471	-476	-494	-497	-500	-503	-515	-624	-631	-642	-659	-468 to -659			
From TSS	+283	+280	+275	+257	+254	+251	+248	+236	+127	+120	+109	+92	+283 to +92			
CpG site	**Pos #12**	**Pos #11**	**Pos #10**	**Pos #9**	**Pos #8**	**Pos #7**	**Pos #6**	**Pos #5**	**Pos #4**	**Pos #3**	**Pos #2**	**Pos #1**	**Mean**	**St Dev**	**Min**	**Max**
Alcohol #1	2.0	2.1	3.0	2.3	2.4	3.6	1.3	3.1	1.4	0.0	1.6	3.6	2.2	1.0	0.0	3.6
Alcohol #2	10.8	3.5	0.0	1.8	2.3	1.6	0.0	2.9	1.1	2.6	1.9	8.7	3.1	3.3	0.0	10.8
Alcohol #3	2.4	2.8	2.4	1.8	2.5	2.0	1.5	2.4	1.4	0.0	1.7	4.3	2.1	1.0	0.0	4.3
Alcohol #4	3.9	1.6	2.1	2.2	2.1	2.3	0.0	3.5	1.9	2.7	2.6	3.4	2.4	1.0	0.0	3.9
Alcohol #5	2.1	2.4	2.3	1.8	3.5	3.3	1.6	3.1	1.8	1.9	3.3	3.3	2.5	0.7	1.6	3.5
Alcohol #6	2.0	2.3	2.9	2.3	2.5	3.1	0.0	3.3	1.5	3.0	2.7	4.3	2.5	1.1	0.0	4.3
Alcohol #7	2.5	2.4	3.1	2.6	2.2	2.7	1.6	2.7	1.6	1.8	4.2	3.5	2.6	0.8	1.6	4.2
Alcohol #7 duplicate	1.8	1.9	2.3	0.0	2.4	2.8	0.0	3.1	0.3	0.0	2.0	3.6	1.7	1.3	0.0	3.6
Alcohol #8	1.7	1.5	7.6	2.1	2.4	2.9	1.8	3.0	1.2	1.4	2.5	3.7	2.6	1.7	1.2	7.6
Alcohol #9	2.5	3.2	2.7	2.6	2.7	3.4	1.7	4.8	1.6	2.1	2.8	3.7	2.8	0.9	1.6	4.8
Alcohol #10	2.1	6.9	4.5	2.9	3.6	3.8	3.1	4.6	3.8	2.4	3.5	4.5	3.8	1.3	2.1	6.9
Alcohol #11	2.7	6.5	5.4	5.3	5.5	5.1	2.3	4.5	3.4	2.8	7.1	3.9	4.5	1.5	2.3	7.1
Alcohol #11 duplicate	4.7	3.3	4.4	2.1	2.6	6.2	2.4	4.0	2.0	1.9	4.4	4.5	3.5	1.4	1.9	6.2
Alcohol #12	11.4	1.9	2.2	2.5	2.3	2.5	1.7	3.5	0.9	1.7	4.7	3.6	3.2	2.8	0.9	11.4
Pair-fed #1	1.3	0.0	1.6	0.0	14.8	3.0	0.0	3.0	1.1	0.0	2.1	3.9	2.6	4.1	0.0	14.8
Pair-fed #2	6.5	6.6	3.8	0.0	6.2	1.7	0.0	2.8	3.2	4.9	2.2	3.7	3.5	2.3	0.0	6.6
Pair-fed #3	2.7	3.3	1.3	0.0	2.3	3.5	0.0	2.5	2.8	0.0	3.9	3.9	2.2	1.5	0.0	3.9
Pair-fed #4	1.6	3.2	2.1	0.0	1.5	8.9	0.0	3.2	0.9	0.0	2.2	3.9	2.3	2.5	0.0	8.9
Pair-fed #5	0.0	2.2	0.0	0.0	3.5	1.7	0.0	3.2	0.0	0.0	3.2	2.8	1.4	1.5	0.0	3.5
Pair-fed #6	1.7	0.0	1.9	0.0	3.4	1.6	0.0	3.2	2.0	0.0	1.6	3.6	1.6	1.4	0.0	3.6
Pair-fed #7	3.7	2.6	3.8	2.0	2.4	4.0	1.7	3.0	1.2	2.0	3.6	4.0	2.8	1.0	1.2	4.0
Pair-fed #8	1.9	3.0	3.5	1.8	2.4	2.4	2.0	2.8	0.8	1.9	2.2	4.4	2.4	0.9	0.8	4.4
Pair-fed #9	6.3	1.8	1.5	2.9	1.8	4.9	1.8	2.5	2.5	3.7	4.1	4.4	3.2	1.5	1.5	6.3
Pair-fed #9 duplicate	1.7	4.7	4.4	3.0	4.1	3.6	1.6	3.2	1.0	2.0	2.3	4.6	3.0	1.3	1.0	4.7
Pair-fed #10	7.5	2.5	2.1	1.5	1.9	2.7	1.7	2.5	2.5	2.2	4.5	5.7	3.1	1.8	1.5	7.5
Ad lib #1	1.8	2.4	2.6	1.9	3.2	2.1	2.7	3.1	1.0	3.1	2.3	3.8	2.5	0.7	1.0	3.8
Ad lib #2	3.3	3.0	3.8	2.9	3.4	3.6	1.9	2.6	1.3	1.7	2.6	3.5	2.8	0.8	1.3	3.8
Ad lib #3	3.3	0.0	1.5	0.0	2.4	2.5	0.0	3.0	1.5	0.0	2.6	3.7	1.7	1.4	0.0	3.7
Ad lib #4	0.0	3.4	0.0	0.0	3.2	1.5	0.0	2.7	0.2	0.0	2.6	3.6	1.4	1.5	0.0	3.6
Ad lib #5	0.0	2.0	3.2	0.0	4.4	1.5	0.0	2.6	0.0	0.0	1.8	2.8	1.5	1.5	0.0	4.4
Ad lib #6	1.9	1.9	0.0	0.0	2.8	3.6	0.0	2.1	0.2	0.0	1.9	3.8	1.5	1.4	0.0	3.8
Ad lib #7	2.8	2.8	3.1	2.4	2.7	3.4	0.0	3.3	1.3	2.4	2.3	3.9	2.5	1.0	0.0	3.9
Ad lib #8	3.5	2.2	6.5	0.0	2.2	4.8	1.9	4.3	2.1	1.8	2.4	6.0	3.1	1.9	0.0	6.5
Ad lib #9	1.3	4.5	3.2	1.9	22.1	4.1	1.0	3.0	2.3	1.8	3.5	5.9	4.5	5.7	1.0	22.1
Ad lib #9 duplicate	2.2	3.9	1.8	2.2	2.2	4.4	1.2	2.7	1.2	1.2	3.2	3.8	2.5	1.1	1.2	4.4
Ad lib #10	2.3	1.7	2.0	2.2	2.6	3.3	1.7	3.0	2.4	2.8	3.1	4.0	2.6	0.7	1.7	4.0
Low Meth	3.0	2.2	2.5	2.1	3.1	2.7	1.0	4.1	0.9	2.1	4.0	4.9	2.7	1.2	0.9	4.9
Med Meth	38.6	41.1	42.7	41.1	38.3	37.3	30.1	39.5	41.2	40.2	37.6	37.3	38.7	3.3	30.1	42.7
High Meth	86.6	91.9	95.8	88.3	81.9	84.5	65.6	83.9	92.7	92.1	86.3	87.5	86.4	7.7	65.6	95.8
NTC																

Table 7. Pyrosequencing indicates that there is little to no methylation in the 1st CpG island of IGFBP-5 exon I in contralateral mammary glands from animals exposed and not exposed to alcohol *in utero* collected at 16 weeks post-NMU injection (study 3). Pyrosequencing was performed to determine DNA methylation of the 1st CpG island in IGFBP-5 exon I (+282 to +91 from the transcription start site) of contralateral mammary glands (MGs) from animals that were and were not exposed to alcohol *in utero*. This region contained 12 CpG sites total. Percent methylation for each tumor at each CpG site is indicated. n = 12 (alcohol), 11 (pair-fed), and 10 (ad lib) mammary glands. Yellow highlight indicates samples that were run in duplicate. Percent methylation of positive controls exhibiting low, medium, and high levels of methylation are indicated at the bottom.

Rat IGFBP-5 Methylation Analysis - Results in % Methylation																
PND 40 MGs	**Assay #1**								**Assay #2**				**Overall Region**			
From ATG	-468	-471	-476	-494	-497	-500	-503	-515	-624	-631	-642	-659	-468 to -659			
From TSS	+283	+280	+275	+257	+254	+251	+248	+236	+127	+120	+109	+92	+283 to +92			
CpG site	**Pos #12**	**Pos #11**	**Pos #10**	**Pos #9**	**Pos #8**	**Pos #7**	**Pos #6**	**Pos #5**	**Pos #4**	**Pos #3**	**Pos #2**	**Pos #1**	**Mean**	**St Dev**	**Min**	**Max**
Alcohol #1	2.8	2.7	2.3	1.3	1.9	2.0	1.1	2.7	1.0	0.0	3.4	3.7	2.1	1.1	0.0	3.7
Alcohol #2	1.4	2.5	1.3	2.7	1.9	1.4	0.0	2.6	1.5	0.0	2.8	3.8	1.8	1.1	0.0	3.8
Alcohol #3	2.3	2.8	1.8	2.1	2.2	4.4	1.9	2.6	0.9	2.3	2.0	3.6	2.4	0.9	0.9	4.4
Alcohol #4	5.1	4.6	2.9	1.8	3.4	3.6	2.0	2.8	1.0	0.0	3.9	5.0	3.0	1.6	0.0	5.1
Alcohol #4 duplicate	4.1	2.2	4.7	2.9	2.8	5.9	2.6	3.0	1.3	3.0	4.1	5.2	3.5	1.3	1.3	5.9
Alcohol #5	1.3	1.9	4.2	2.6	2.4	2.5	1.5	2.6	1.1	0.0	3.7	3.6	2.3	1.2	0.0	4.2
Alcohol #6	2.5	3.3	4.3	2.4	2.3	1.6	0.0	2.8	1.0	2.4	2.9	3.5	2.4	1.1	0.0	4.3
Pair-fed #1	6.2	1.2	3.2	3.0	2.0	2.4	1.5	2.8	1.3	1.7	2.2	4.6	2.7	1.4	1.2	6.2
Pair-fed #2	1.3	1.9	2.7	0.0	2.1	2.3	0.0	2.6	0.9	0.0	3.9	3.5	1.8	1.3	0.0	3.9
Pair-fed #3	6.9	5.3	2.0	1.5	3.7	4.4	1.4	2.8	1.4	6.2	2.4	3.9	3.5	1.9	1.4	6.9
Pair-fed #4	2.0	2.2	2.9	1.9	2.8	2.2	1.2	3.1	2.3	1.4	3.1	3.6	2.4	0.7	1.2	3.6
Pair-fed #5	2.0	1.2	1.5	0.0	1.6	4.2	0.0	2.9	1.1	1.5	2.3	3.5	1.8	1.3	0.0	4.2
Pair-fed #5 duplicate	2.6	0.0	1.7	0.0	1.2	1.3	0.0	6.2	0.8	1.8	2.3	3.5	1.8	1.8	0.0	6.2
Pair-fed #6	5.5	5.6	1.7	2.1	4.4	2.9	5.3	3.2	2.4	4.4	1.7	5.6	3.7	1.6	1.7	5.6
Ad lib #1	3.5	4.1	0.0	7.5	2.1	5.5	1.9	4.5	4.7	2.0	2.0	6.5	3.7	2.2	0.0	7.5
Ad lib #2	1.6	4.1	2.6	2.3	2.2	4.8	2.6	2.6	2.6	1.0	6.2	5.4	3.2	1.6	1.0	6.2
Ad lib #3	0.0	7.9	2.3	2.5	4.0	1.8	0.0	2.6	2.0	0.0	1.7	3.9	2.4	2.2	0.0	7.9
Ad lib #4	4.1	1.8	3.7	2.3	3.1	11.0	0.9	2.8	0.8	1.5	2.3	3.6	3.2	2.7	0.8	11.0
Ad lib #5	5.0	0.0	0.0	0.0	1.4	1.3	0.0	2.8	1.2	0.0	1.8	3.6	1.4	1.6	0.0	5.0
Ad lib #6	1.3	1.5	2.3	2.1	2.6	3.6	2.7	3.4	1.6	1.9	4.5	4.3	2.6	1.1	1.3	4.5
Low Meth	3.0	2.2	2.5	2.1	3.1	2.7	1.0	4.1	0.9	2.1	4.0	4.9	2.7	1.2	0.9	4.9
Med Meth	38.6	41.1	42.7	41.1	38.3	37.3	30.1	39.5	41.2	40.2	37.6	37.3	38.7	3.3	30.1	42.7
High Meth	86.6	91.9	95.8	88.3	81.9	84.5	65.6	83.9	92.7	92.1	86.3	87.5	86.4	7.7	65.6	95.8
NTC																

Table 8. Pyrosequencing indicates that there is little to no methylation in the 1st CpG island of IGFBP-5 exon I in PND 40 mammary glands from animals exposed and not exposed to alcohol *in utero* (study 2). Pyrosequencing was performed to determine DNA methylation of the 1st CpG island in IGFBP-5 exon I (+282 to +91 from the transcription start site) of postnatal (PND) 40 mammary glands (MGs) from animals that were and were not exposed to alcohol *in utero*. This region contained 12 CpG sites total. Percent methylation for each tumor at each CpG site is indicated. n = 6 for each treatment group. Yellow highlight indicates samples that were run in duplicate. Percent methylation of positive controls exhibiting low, medium, and high levels of methylation are indicated at the bottom.

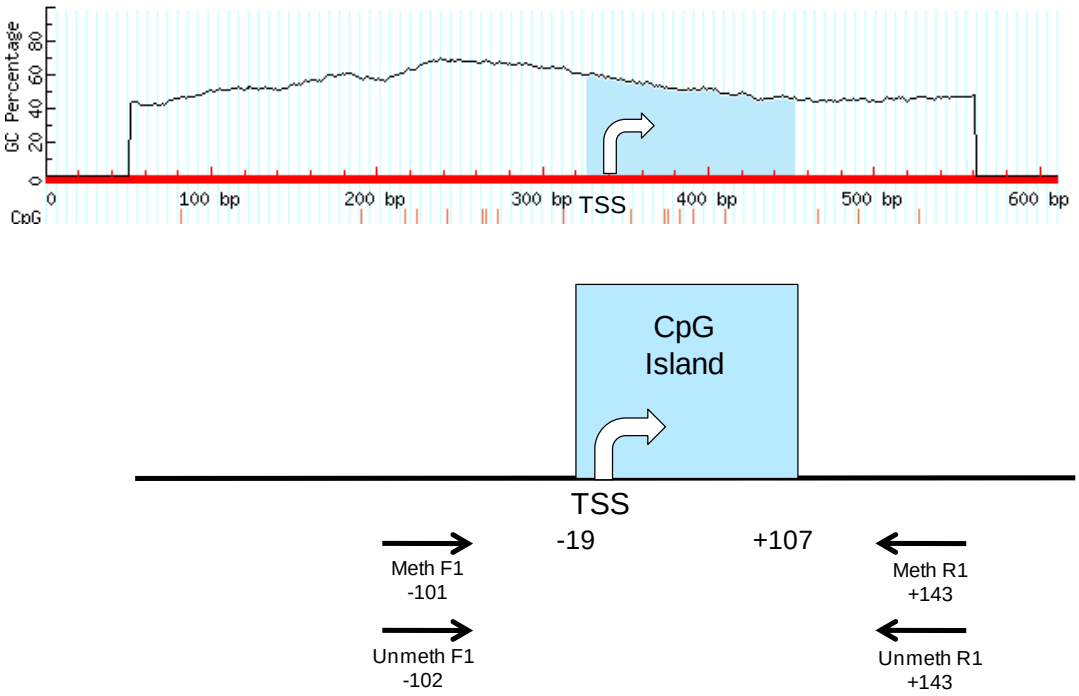

Figure 7. Schematic diagram of the ERα promoter/exon I CpG island and primer locations for methylation specific PCR. MethPrimer was used to identify CpG islands in the ERα gene from -346 to +264 relative to the transcription state site (TSS). The CpG island analyzed (blue) spanned the promoter and exon I and was located between -19 to +107 relative to TSS. Locations of PCR primers (relative to the TSS) used to detect methylated (Meth F1, Meth R1) and unmethylated (Unmeth F1, Unmeth R1) DNA by methylation specific PCR are indicated.

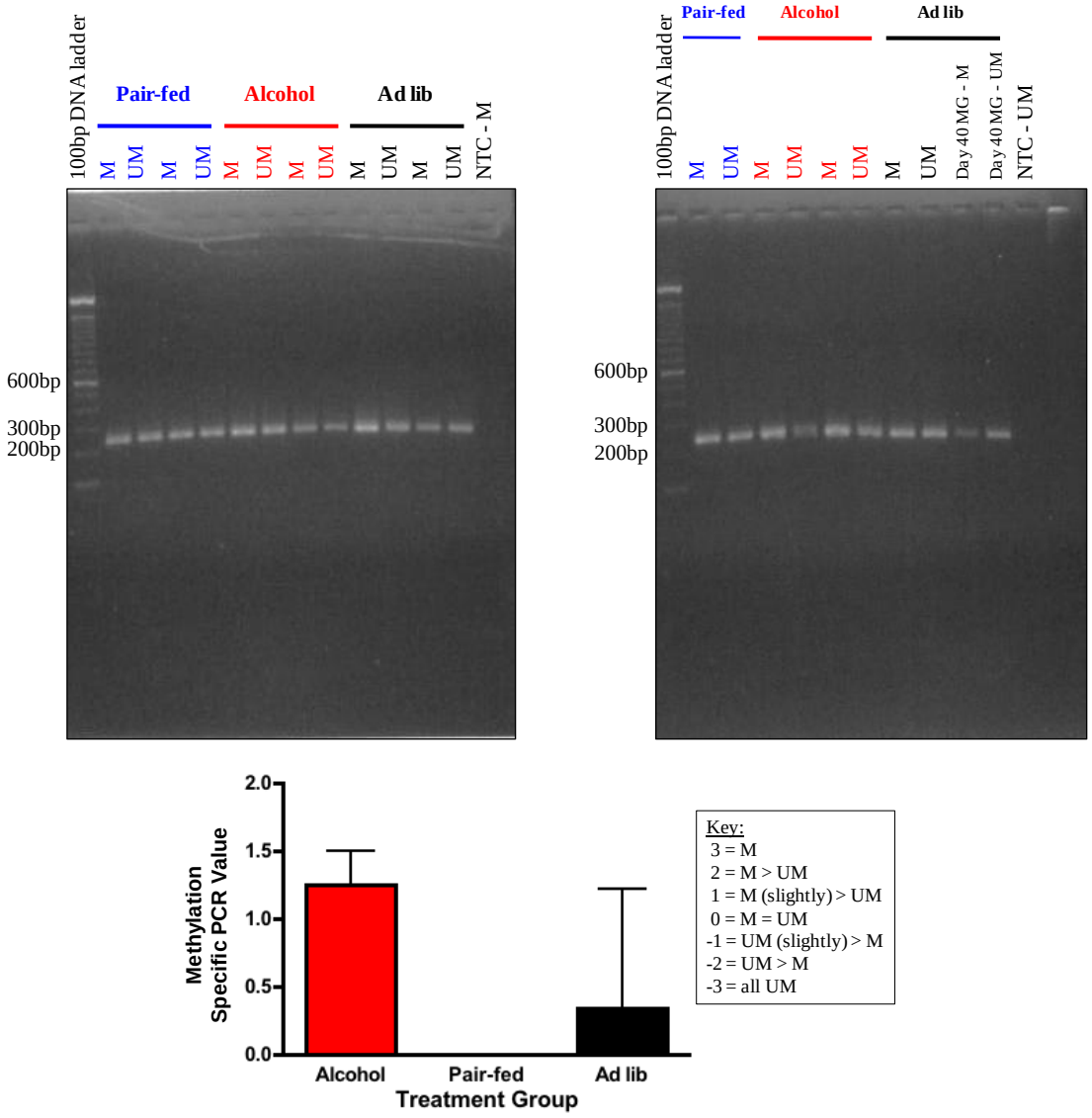

Figure 8. The ER promoter/exon I CpG exhibits DNA methylation in tumors from animals exposed and not exposed to alcohol *in utero* collected at 23 weeks post-NMU injection (study 1). Methylation specific PCR (MSP) was performed for the ER promoter/exon I to assess DNA methylation of this region in tumors (23 weeks post-NMU injection) from animals that were and were not exposed to alcohol *in utero*. Each set of methylated (M) and unmethylated (UM) bands represent methylated and unmethyled DNA from a tumor. A PND 40 mammary gland from an ad lib animal was also run, indicating that there is some DNA methylation in this region in the normal mammary gland as well. NTC – M = no template control using the methylated primers, NTC – UM = no template control using the unmethylated primers. Semi-quantitation of MSP results (bottom); n =4 (alcohol), 3 (pair-fed), and 3 (ad lib). A key for how the scoring was performed is indicated (M = methylated, UM = unmethylated). Data were analyzed using a one-way ANOVA for all treatment groups (p = 0.2153).

Conclusions and Future Directions

The data presented in this work provide additional evidence that alcohol exposure *in utero* leads to enhanced susceptibility to carcinogen-induced mammary tumorigenesis in offspring and our findings shed new light on potential molecular mechanisms that may be involved. For our alcohol exposure model we used the Lieber-DeCarli liquid diet. Determining an appropriate control for the liquid diet proved to be a challenge since two parameters differ between the pair-fed and ad lib control groups – nutrient composition and caloric intake. Therefore, data interpretation is difficult when endpoints differ between the two control groups. It has been reported that rats consuming the Lieber-DeCarli control liquid diet *ad libitum* exhibit growth rates that are fully comparable to or exceed the growth rates of rats on Purina rat chow, the diet used for the ad lib group. Thus, future studies in our lab should eliminate the solid rat chow diet and instead include an *ad libitum* liquid diet as a second control group. In this way, diet composition between the pair-fed and ad lib groups would be the same and the effects of caloric restriction in the pair-fed group can then be properly assessed.

Many studies have shown that early changes in the mammary gland in response to a suboptimal fetal environment may affect susceptibility to breast cancer later in life. This idea was investigated in Chapter 2. In this study, we showed that alcohol exposure *in utero* induces early changes in mammary morphology and the IGF/E2 axis. Therefore, alcohol exposure *in utero* may advance mammary development via the IGF and E2 systems, which could contribute to increased susceptibility to mammary cancer later in life.

Studies in Chapter 3 substantiate our previous work that alcohol exposure *in utero* enhances susceptibility to carcinogen-induced mammary tumorigenesis in adulthood and induces a worse tumor phenotype relative to control groups. In addition, alcohol-exposed animals exhibited more PR positive tumors and increased Snail, IGF-II, and IGFBP-5, as well as decreased ERα tumor expression at 16 weeks post-NMU injection. A review of the literature revealed numerous mechanisms by which these signaling molecules may interact to promote an advanced tumor phenotype in fetal alcohol animals as discussed in Chapter 3. The data described in Chapter 3 provides insights into the potential molecular mechanisms underlying the enhanced susceptibility to NMU-induced tumors in the alcohol group. Additional studies should be aimed at these particular pathways to further delineate the mechanism.

In addition to identifying key molecular pathways that may be altered by alcohol exposure *in utero*, we undertook a comprehensive analysis of the ERα/PR/HER2 status of the NMU-induced mammary tumorigenesis model. In general, NMU-induced mammary tumors are ERα positive and HER2 negative. Some tumors are PR positive while others are PR negative. In the current study, which was terminated at 16 weeks post-NMU injection, tumors from the three treatment groups were ERα positive. Previously, we found that mammary tumors from the alcohol group collected at 23 weeks post-NMU injection were more ERα negative relative to tumors from control groups. This suggests that tumors from fetal alcohol rats may lose ERα positivity more readily than tumors in control groups, which would lead to a poor prognosis if similar results were observed in women. Future studies implementing the use of punch biopsies are needed to further

clarify if tumors in the alcohol group start out as ERα positive and lose ERα positivity over time.

In the current study, where tumors were collected at 16 weeks post-NMU injection, we found that the alcohol group developed more PR positive tumors compared to the pair-fed controls. Since the P4 signaling pathway plays a significant role in cell proliferation within the mammary gland, the increased PR observed in the tumors of the alcohol group may be promoting cell proliferation. To determine if this is the case, future studies should include analysis of cell cycle/proliferation markers such as cyclin D1 and Ki67 in the PR positive tumors by Western immunoblot and/or immunohistochemistry. Animal studies and clinical data indicate that the P4/PR signaling pathway is involved in initiation and development of mammary tumors. It is interesting to speculate that the P4/PR signaling pathway may be involved in the underlying mechanisms for the increased susceptibility to carcinogen-induced mammary tumors observed in the alcohol group.

A study examining carcinomas of breast cancer patients found a strong relationship between IGF-II mRNA expression and PR positivity. It is intriguing that we see both increased number of PR positive tumors and IGF-II mRNA expression in tumors of the alcohol group, suggesting that these molecules may work in concert to promote cell proliferation within tumors of this treatment group. To gain further insights as to whether or not this is the case, additional analyses will determine if there is a correlation between PR positivity and IGF-II mRNA expression within a single tumor. If a positive association is found between PR positivity and IGF-II mRNA expression in the alcohol

group, this would suggest that the PR and IGF-II signaling pathways are working together to promote tumor progression in alcohol-exposed animals.

We also found that tumors from the alcohol group had increased Snail expression compared to the pair-fed control at 16 weeks post-NMU injection. Many studies have shown that the role of Snail in tumor progression involves a de-differentiation step during the initial transformation process in which Snail promotes tumor cells to undergo EMT resulting in the generation of progenitor cells. For this reason, it is possible that in our model the increased Snail expression in tumors of the alcohol group is promoting progenitor cell generation. To determine if this is the case, additional studies would be needed to assess CD44 and CD24 expression in the tumors. Flow cytometry can be utilized to determine if there is an increase in the population of cells exhibiting the $CD44^{high}/CD24^{low}$ profile that is characteristic of breast cancer stem cells.

In the studies described in both Chapters 2 and 3 changes were observed for IGFBP-5 and ERα. Since alcohol *in utero* induces epigenetic alterations in non-mammary tissues, the goal of this work was to determine if these changes resulted from alterations in DNA methylation of the IGFBP-5 and ERα genes. Methylation was not observed in the IGFBP-5 promoter CpG island. We also examined DNA methylation in the first CpG island in IGFBP-5 exon I. Analysis of this region by methylation-specific PCR revealed partial methylation in all tissues analyzed. However, pyrosequencing analysis indicated low methylation in these tissues. Further investigation is needed in order to clarify the discrepancy between results from these two techniques. A CpG island in ERα promoter/exon I was also analyzed as it has been shown that ER negative breast tumors have increased methylation, which is responsible for the loss of ER expression. In our

study, all tumors exhibited partial ERα methylation. The field of epigenetics is rapidly advancing and more powerful methods to assess DNA methylation are continuously being discovered. Thus, future studies should be aimed at analyzing all of the CpG sites in these CpG islands as well as additional CpG islands and CpG shores within the IGFBP-5 and ERα genes to more thoroughly clarify whether or not DNA methylation of these two genes is involved in the mechanisms underlying the increased susceptibility to NMU-induced tumors observed in the fetal alcohol group. As discussed in the literature review and Chapter 4, many studies have shown that alcohol exposure *in utero* can alter DNA methylation. It is likely that in our alcohol exposure model many genes may be epigenetically modified. One future direction is to perform methylated-DNA immunoprecipitation sequencing (MeDIP seq) using mammary glands from alcohol-exposed and control animals. Data from this analysis would provide insights into what genes in the mammary gland are being epigenetically modified due to alcohol *in utero*. The changes in DNA methylation of these genes could cause an altered response to the carcinogen, which could result in enhanced tumorigenesis.

One of the most exciting pieces of data we found was that at 16 weeks post-NMU injection, tumors of the alcohol group had significantly increased IGF-II expression compared to the pair-fed group. IGF-II is an imprinted gene and loss of imprinting (LOI) of IGF-II has been shown in several types of cancers including breast cancer. One of our working hypotheses is that tumors from the alcohol group exhibit LOI of IGF-II leading to increased IGF-II expression, which may be involved in tumor progression in fetal alcohol animals. As previously mentioned many studies have shown that alcohol exposure *in utero* can alter DNA methylation. LOI occurs when DNA methylation is lost

on the maternal allele. Thus, if LOI of IGF-II is occurring in tumors of the alcohol group, we anticipate that DNA methylation of IGF-II will be lost in these tumors. Since the IGF-II data was the most recent data obtained in this study, we have not yet had an opportunity to assess IGF-II DNA methylation. To determine if LOI is indeed occurring, future studies should involve such an analysis. It would also be interesting to compare DNA methylation status of IGF-II in tumors compared to contralateral mammary glands. It is possible that alterations in DNA methylation occur in the tumor and not in the contralateral mammary glands, therefore explaining why we observed a difference in IGF-II expression among the tumors from the two treatment groups, but not in the contralateral mammary glands.

Early detection of breast cancer is the best defense against the disease. For this reason, it is important to be able to identify subsets of women who are at higher risk for breast cancer. Thus, the identification of additional breast cancer risk factors, such as fetal alcohol exposure, is essential. If the findings of alcohol exposure *in utero* leading to enhanced risk of breast cancer extend to humans, then health professionals should be further encouraged to inform women of the numerous risks of alcohol consumption during pregnancy. Perhaps more importantly, women of alcoholic mothers should be informed that they may be at increased risk of breast cancer and encouraged to get regular mammograms at an early age.

References

1. **Nayak RB, Murthy P** 2008 Fetal alcohol spectrum disorder. Indian Pediatr 45:977-983

2. **Abel EL** 1982 Consumption of alcohol during pregnancy: a review of effects on growth and development of offspring. Human Biology 54:421-453

3. **Chaudhuri JD** 2000 Alcohol and the developing fetus--a review. Med Sci Monit 6:1031-1041

4. 2000 Prenatal exposure to alcohol. Alcohol Res Health 24:32-41

5. **May PA, Gossage JP, Kalberg WO, Robinson LK, Buckley D, Manning M, Hoyme HE** 2009 Prevalance and epidemiologic characteristics of FASD from various research methods with an emphasis on recent in-school studies. Dev Disabil Res Rev 15:176-192

6. **U.S. Department of Health and Human Services** 2005 US Surgeon General releases advisory on alcohol use in pregnancy. Available at http://www.surgeongeneral.gov/news/2005/02/sg02222005.html

7. **Centers for Disease Control and Prevention** 2012 Alcohol use and binge drinking among women of childbearing age - United States, 2006 - 2010. Morbidity and Mortality Weekly Report 61:534-538

8. **Singh S, Sedgh G, Hussain R** 2010 Unintended pregnancy: worldwide levels, trends, and outcomes. Stud Fam Plann 41:241-250

9. **Burd L, Blair J, Dropps K** 2012 Prenatal alcohol exposure, blood alcohol concentrations and alcohol elimination rates for the mother, fetus and newborn. J Perinatol 32:652-659

10. **Howlader N, Noone AM, Krapcho M, Garshell J, Neyman N, Altekruse SF, Kosary CL, Yu M, Ruhl J, Tatalovich Z, Cho H, Mariotto A, Lewis DR, Chen HS, Feuer EJ, Cronin KA (eds)** SEER Cancer Statistics Review, 1975-2010, National Cancer Institute. Bethesda, MD. http://seer.cancer.gov/csr/1975_2010/, based on November SEER data submission, posted to the SEER website April 2013

11. **McPherson K, Steel CM, Dixon JM** 2000 ABC of breast diseases. Breast cancer-epidemiology, risk factors, and genetics. BMJ 321:624-628

12. **Petri AL, Tjonneland A, Gamborg M, Johansen D, Hoidrup S, Sorensen TI, Gronbaek M** 2004 Alcohol intake, type of beverage, and risk of breast cancer in pre- and postmenopausal women. Alcohol Clin Exp Res 28:1084-1090

13. **Hamajima N, Hirose K, Tajima K, Rohan T, Calle EE, Heath CW, Jr., Coates RJ, Liff JM, Talamini R, Chantarakul N, Koetsawang S, Rachawat D, Morabia A, Schuman L, Stewart W, Szklo M, Bain C, Schofield F, Siskind V, Band P, Coldman AJ, Gallagher RP, Hislop TG, Yang P, Kolonel LM, Nomura AM, Hu J, Johnson KC, Mao Y, De Sanjose S, Lee N, Marchbanks P, Ory HW, Peterson HB, Wilson HG, Wingo PA, Ebeling K, Kunde D, Nishan P, Hopper JL, Colditz G, Gajalanski V, Martin N, Pardthaisong T, Silpisornkosol S, Theetranont C, Boosiri B, Chutivongse S, Jimakorn P, Virutamasen P, Wongsrichanalai C, Ewertz M, Adami HO, Bergkvist L, Magnusson C, Persson I, Chang-Claude J, Paul C, Skegg DC, Spears GF, Boyle P, Evstifeeva T, Daling JR, Hutchinson WB, Malone K, Noonan EA, Stanford JL, Thomas DB, Weiss NS, White E, Andrieu N, Bremond A, Clavel F, Gairard B, Lansac J, Piana L, Renaud R, Izquierdo A, Viladiu P, Cuevas HR, Ontiveros P, Palet A, Salazar SB, Aristizabel N, Cuadros A, Tryggvadottir L, Tulinius H, Bachelot A, Le MG, Peto J, Franceschi S, Lubin F, Modan B, Ron E, Wax Y, Friedman GD, Hiatt RA, Levi F, Bishop T, Kosmelj K, Primic-Zakelj M, Ravnihar B, Stare J, Beeson WL, Fraser G, Bullbrook RD, Cuzick J, Duffy SW, Fentiman IS, Hayward JL, Wang DY, McMichael AJ, McPherson K, Hanson RL, Leske MC, Mahoney MC, Nasca PC, Varma AO, Weinstein AL, Moller TR, Olsson H, Ranstam J, Goldbohm RA, van den Brandt PA, Apelo RA, Baens J, de la Cruz JR, Javier B, Lacaya LB, Ngelangel CA, La Vecchia C, Negri E, Marubini E, Ferraroni M, Gerber M, Richardson S, Segala C, Gatei D, Kenya P, Kungu A, Mati JG, Brinton LA, Hoover R, Schairer C, Spirtas R, Lee HP, Rookus MA, van Leeuwen FE, Schoenberg JA, McCredie M, Gammon MD, Clarke EA, Jones L, Neil A, Vessey M, Yeates D, Appleby P, Banks E, Beral V, Bull D, Crossley B, Goodill A, Green J, Hermon C, Key T, Langston N, Lewis C, Reeves G, Collins R, Doll R, Peto R, Mabuchi K, Preston D, Hannaford P, Kay C, Rosero-Bixby L, Gao YT, Jin F, Yuan JM, Wei HY, Yun T, Zhiheng C, Berry G, Cooper Booth J, Jelihovsky T, MacLennan R, Shearman R, Wang QS, Baines CJ, Miller AB, Wall C, Lund E, Stalsberg H, Shu XO, Zheng W, Katsouyanni K, Trichopoulou A, Trichopoulos D, Dabancens A, Martinez L, Molina R, Salas O, Alexander FE, Anderson K, Folsom AR, Hulka BS, Bernstein L, Enger S, Haile RW, Paganini-Hill A, Pike MC, Ross RK, Ursin G, Yu MC, Longnecker MP, Newcomb P, Kalache A, Farley TM, Holck S, Meirik O** 2002 Alcohol, tobacco and breast cancer--collaborative reanalysis of individual data from 53 epidemiological studies, including 58,515 women with breast cancer and 95,067 women without the disease. Br J Cancer 87:1234-1245

14. **Singletary KW, Gapstur SM** 2001 Alcohol and breast cancer: review of epidemiologic and experimental evidence and potential mechanisms. JAMA 286:2143-2151

15. **Smith-Warner SA, Spiegelman D, Yaun SS, van den Brandt PA, Folsom AR, Goldbohm RA, Graham S, Holmberg L, Howe GR, Marshall JR, Miller AB, Potter JD, Speizer FE, Willett WC, Wolk A, Hunter DJ** 1998 Alcohol and breast cancer in women: a pooled analysis of cohort studies. JAMA 279:535-540

16. **Howe G, Rohan T, Decarli A, Iscovich J, Kaldor J, Katsouyanni K, Marubini E, Miller A, Riboli E, Toniolo P, et al.** 1991 The association between alcohol and breast cancer risk: evidence from the combined analysis of six dietary case-control studies. Int J Cancer 47:707-710

17. **Longnecker MP** 1994 Alcoholic beverage consumption in relation to risk of breast cancer: meta-analysis and review. Cancer Causes Control 5:73-82

18. **Longnecker MP, Berlin JA, Orza MJ, Chalmers TC** 1988 A meta-analysis of alcohol consumption in relation to risk of breast cancer. JAMA 260:652-656

19. **Allen NE, Beral V, Casabonne D, Kan SW, Reeves GK, Brown A, Green J** 2009 Moderate alcohol intake and cancer incidence in women. J Natl Cancer Inst 101:296-305

20. **Hiatt RA** 1990 Alcohol consumption and breast cancer. Med Oncol Tumor Pharmacother 7:143-151

21. **Singletary K, Nelshoppen J, Wallig M** 1995 Enhancement by chronic ethanol intake of N-methyl-N-nitrosourea-induced rat mammary tumorigenesis. Carcinogenesis 16:959-964

22. **Grubbs C, Juliana M, Whitaker L** 1988 Effect of ethanol initiation of methylnitrosourea (MNU)- and dimethylbenz(a)anthracene (DMBA)-induced mammary cancers. Proc Am Assoc Cancer Res 29:148

23. **Singletary KW, McNary MQ, Odoms AM, Nelshoppen J, Wallig MA** 1991 Ethanol consumption and DMBA-induced mammary carcinogenesis in rats. Nutr Cancer 16:13-23

24. **Watabiki T, Okii Y, Tokiyasu T, Yoshimura S, Yoshida M, Akane A, Shikata N, Tsubura A** 2000 Long-term ethanol consumption in ICR mice causes mammary tumor in females and liver fibrosis in males. Alcohol Clin Exp Res 24:117S-122S

25. **Barker DJ** 2007 The origins of the developmental origins theory. J Intern Med 261:412-417

26. **Jones RH, Ozanne SE** 2007 Intra-uterine origins of type 2 diabetes. Arch Physiol Biochem 113:25-29

27. **Tang WY, Ho SM** 2007 Epigenetic reprogramming and imprinting in origins of disease. Rev Endocr Metab Disord 8:173-182

28. **Simmen FA, Simmen RC** 2011 The maternal womb: a novel target for cancer prevention in the era of the obesity pandemic? Eur J Cancer Prev 20:539-548

29. **Trichopoulos D** 1990 Hypothesis: does breast cancer originate in utero? Lancet 335:939-940

30. **Hilakivi-Clarke L, de Assis S** 2006 Fetal origins of breast cancer. Trends Endocrinol Metab 17:340-348

31. **Soto AM, Vandenberg LN, Maffini MV, Sonnenschein C** 2008 Does breast cancer start in the womb? Basic Clin Pharmacol Toxicol 102:125-133

32. **Polanco TA, Crismale-Gann C, Reuhl KR, Sarkar DK, Cohick WS** 2010 Fetal alcohol exposure increases mammary tumor susceptibility and alters tumor phenotype in rats. Alcohol Clin Exp Res 34:1879-1887

33. **Hilakivi-Clarke L, Cabanes A, de Assis S, Wang M, Khan G, Shoemaker WJ, Stevens RG** 2004 In utero alcohol exposure increases mammary tumorigenesis in rats. Br J Cancer 90:2225-2231

34. **Latino-Martel P, Chan DS, Druesne-Pecollo N, Barrandon E, Hercberg S, Norat T** 2010 Maternal alcohol consumption during pregnancy and risk of childhood leukemia: systematic review and meta-analysis. Cancer Epidemiol Biomarkers Prev 19:1238-1260

35. **Afonso N** 2009 Women at high risk for breast cancer--what the primary care provider needs to know. J Am Board Fam Med 22:43-50

36. **Robinson GW** 2007 Cooperation of signalling pathways in embryonic mammary gland development. Nat Rev Genet 8:963-972

37. **Daniel CW, Silberstein GB** 1987 Postnatal development of the rodent mammary gland. In: Nelville MC, Daniel CW eds. The Mammary Gland: Development, Regulation, and Function. New York: Plenum Press; 3-36

38. **Macias H, Hinck L** 2012 Mammary gland development. Wiley Interdiscip Rev Dev Biol 1:533-557

39. **Watson CJ, Khaled WT** 2008 Mammary development in the embryo and adult: a journey of morphogenesis and commitment. Development 135:995-1003

40. **Cowie AT, Folley SJ** 1949 Relative growth of the mammary gland in the normal, gonadectomized and adrenalectomized rat. J Endocrinol 6:vi

41. **Haslam S** 1987 Roles of Sex Steroid Hormones in Normal Mammary Gland Function. In: Neville MC, Daniel CW eds. The Mammary Gland: Development, Regulation and Function. New York: Plenum Press; 499-533

42. **Hovey RC, Trott JF, Vonderhaar BK** 2002 Establishing a framework for the functional mammary gland: from endocrinology to morphology. J Mammary Gland Biol Neoplasia 7:17-38

43. **Masso-Welch PA, Darcy KM, Stangle-Castor NC, Ip MM** 2000 A developmental atlas of rat mammary gland histology. J Mammary Gland Biol Neoplasia 5:165-185

44. **Gjorevski N, Nelson CM** 2011 Integrated morphodynamic signalling of the mammary gland. Nat Rev Mol Cell Biol 12:581-593

45. **Russo J, Russo IH** 1987 Development of the human mammary gland. In: Neville MC, Daniel CW eds. The Mammary Gland: Development, Regulation, and Function. New York: Plenum Press; 67-93

46. **Sakakura T** 1987 Mammary embryogenesis. In: Neville MC, Daniel CW eds. The Mammary Gland: Development, Regulation, and Function. New York: Plenum Press; 37-66

47. **Sakakura T, Kusano I, Kusakabe M, Inaguma Y, Nishizuka Y** 1987 Biology of mammary fat pad in fetal mouse: capacity to support development of various fetal epithelia in vivo. Development 100:421-430

48. **Hens JR, Wysolmerski JJ** 2005 Key stages of mammary gland development: molecular mechanisms involved in the formation of the embryonic mammary gland. Breast Cancer Res 7:220-224

49. **Rillema JA** 1994 Development of the mammary gland and lactation. Trends Endocrinol Metab 5:149-154

50. **Propper AY** 1978 Wandering epithelial cells in the rabbit embryo milk line. A preliminary scanning electron microscope study. Dev Biol 67:225-231

51. **Balinsky BI** 1950 On the prenatal growth of the mammary gland rudiment in the mouse. J Anat 84:227-235

52. **Russo J, Gusterson BA, Rogers AE, Russo IH, Wellings SR, van Zwieten MJ** 1990 Comparative study of human and rat mammary tumorigenesis. Lab Invest 62:244-278

53. **Sternlicht MD** 2006 Key stages in mammary gland development: the cues that regulate ductal branching morphogenesis. Breast Cancer Res 8:201

54. **Watson CJ** 2006 Involution: apoptosis and tissue remodelling that convert the mammary gland from milk factory to a quiescent organ. Breast Cancer Res 8:203

55. **Nandi S** 1958 Endocrine control of mammarygland development and function in the C3H/ He Crgl mouse. J Natl Cancer Inst 21:1039-1063

56. **Schiff R, Osborne CK** 2005 Endocrinology and hormone therapy in breast cancer: new insight into estrogen receptor-alpha function and its implication for endocrine therapy resistance in breast cancer. Breast Cancer Res 7:205-211

57. **Mosselman S, Polman J, Dijkema R** 1996 ER beta: identification and characterization of a novel human estrogen receptor. FEBS Lett 392:49-53

58. **Saji S, Jensen EV, Nilsson S, Rylander T, Warner M, Gustafsson JA** 2000 Estrogen receptors alpha and beta in the rodent mammary gland. Proc Natl Acad Sci U S A 97:337-342

59. **Fagan DH, Yee D** 2008 Crosstalk between IGF1R and estrogen receptor signaling in breast cancer. J Mammary Gland Biol Neoplasia 13:423-429

60. **Song RX, Barnes CJ, Zhang Z, Bao Y, Kumar R, Santen RJ** 2004 The role of Shc and insulin-like growth factor 1 receptor in mediating the translocation of estrogen receptor alpha to the plasma membrane. Proc Natl Acad Sci U S A 101:2076-2081

61. **Levin ER** 2005 Integration of the extranuclear and nuclear actions of estrogen. Mol Endocrinol 19:1951-1959

62. **Kahlert S, Nuedling S, van Eickels M, Vetter H, Meyer R, Grohe C** 2000 Estrogen receptor alpha rapidly activates the IGF-1 receptor pathway. J Biol Chem 275:18447-18453

63. **Song RX, Chen Y, Zhang Z, Bao Y, Yue W, Wang JP, Fan P, Santen RJ** 2009 Estrogen utilization of IGF-1-R and EGF-R to signal in breast cancer cells. J Steroid Biochem Mol Biol 118:219-230

64. **Prossnitz ER, Barton M** 2011 The G-protein-coupled estrogen receptor GPER in health and disease. Nat Rev Endocrinol 7:715-726

65. **Kang L, Zhang X, Xie Y, Tu Y, Wang D, Liu Z, Wang ZY** 2010 Involvement of estrogen receptor variant ER-alpha36, not GPR30, in nongenomic estrogen signaling. Mol Endocrinol 24:709-721

66. **Morelli C, Garofalo C, Bartucci M, Surmacz E** 2003 Estrogen receptor-alpha regulates the degradation of insulin receptor substrates 1 and 2 in breast cancer cells. Oncogene 22:4007-4016

67. **Tian J, Berton TR, Shirley SH, Lambertz I, Gimenez-Conti IB, DiGiovanni J, Korach KS, Conti CJ, Fuchs-Young R** 2012 Developmental stage determines estrogen receptor alpha expression and non-genomic mechanisms that control IGF-1 signaling and mammary proliferation in mice. J Clin Invest 122:192-204

68. **Simoncini T, Hafezi-Moghadam A, Brazil DP, Ley K, Chin WW, Liao JK** 2000 Interaction of oestrogen receptor with the regulatory subunit of phosphatidylinositol-3-OH kinase. Nature 407:538-541

69. **Sun M, Paciga JE, Feldman RI, Yuan Z, Coppola D, Lu YY, Shelley SA, Nicosia SV, Cheng JQ** 2001 Phosphatidylinositol-3-OH Kinase (PI3K)/AKT2,

activated in breast cancer, regulates and is induced by estrogen receptor alpha (ERalpha) via interaction between ERalpha and PI3K. Cancer Res 61:5985-5991

70. **Zeleniuch-Jacquotte A, Toniolo P, Levitz M, Shore RE, Koenig KL, Banerjee S, Strax P, Pasternack BS** 1995 Endogenous estrogens and risk of breast cancer by estrogen receptor status: a prospective study in postmenopausal women. Cancer Epidemiol Biomarkers Prev 4:857-860

71. **Daniel CW, Silberstein GB, Strickland P** 1987 Direct action of 17 beta-estradiol on mouse mammary ducts analyzed by sustained release implants and steroid autoradiography. Cancer Res 47:6052-6057

72. **Silberstein GB, Van Horn K, Shyamala G, Daniel CW** 1994 Essential role of endogenous estrogen in directly stimulating mammary growth demonstrated by implants containing pure antiestrogens. Endocrinology 134:84-90

73. **Nandi S** 1958 Hormonal control of mammary-gland development and function in the C3H/He Crgl mouse. J Natl Cancer Inst Monogr 21:1036-1063

74. **Korach KS, Couse JF, Curtis SW, Washburn TF, Lindzey J, Kimbro KS, Eddy EM, Migliaccio S, Snedeker SM, Lubahn DB, Schomberg DW, Smith EP** 1996 Estrogen receptor gene disruption: molecular characterization and experimental and clinical phenotypes. Recent Prog Horm Res 51:159-186; discussion 186-158

75. **Mallepell S, Krust A, Chambon P, Brisken C** 2006 Paracrine signaling through the epithelial estrogen receptor alpha is required for proliferation and morphogenesis in the mammary gland. Proc Natl Acad Sci U S A 103:2196-2201

76. **Krege JH, Hodgin JB, Couse JF, Enmark E, Warner M, Mahler JF, Sar M, Korach KS, Gustafsson JA, Smithies O** 1998 Generation and reproductive phenotypes of mice lacking estrogen receptor beta. Proc Natl Acad Sci U S A 95:15677-15682

77. **Forster C, Makela S, Warri A, Kietz S, Becker D, Hultenby K, Warner M, Gustafsson JA** 2002 Involvement of estrogen receptor beta in terminal differentiation of mammary gland epithelium. Proc Natl Acad Sci U S A 99:15578-15583

78. **Feng Y, Manka D, Wagner KU, Khan SA** 2007 Estrogen receptor-alpha expression in the mammary epithelium is required for ductal and alveolar morphogenesis in mice. Proc Natl Acad Sci U S A 104:14718-14723

79. **Bernstein L, Ross RK** 1993 Endogenous hormones and breast cancer risk. Epidemiol Rev 15:48-65

80. **Henderson B, Pike M, Bernstein L, Ross R** 1996 Breast Cancer. In: J SDaF ed. Cancer Epidemiology and Prevention. 2nd ed. ed. New York, NY: Oxford University Press; 1022-1029

81. **Key T, Appleby P, Barnes I, Reeves G** 2002 Endogenous sex hormones and breast cancer in postmenopausal women: reanalysis of nine prospective studies. J Natl Cancer Inst 94:606-616

82. **Kaaks R, Rinaldi S, Key TJ, Berrino F, Peeters PH, Biessy C, Dossus L, Lukanova A, Bingham S, Khaw KT, Allen NE, Bueno-de-Mesquita HB, van Gils CH, Grobbee D, Boeing H, Lahmann PH, Nagel G, Chang-Claude J, Clavel-Chapelon F, Fournier A, Thiebaut A, Gonzalez CA, Quiros JR, Tormo MJ, Ardanaz E, Amiano P, Krogh V, Palli D, Panico S, Tumino R, Vineis P, Trichopoulou A, Kalapothaki V, Trichopoulos D, Ferrari P, Norat T, Saracci R, Riboli E** 2005 Postmenopausal serum androgens, oestrogens and breast cancer risk: the European prospective investigation into cancer and nutrition. Endocr Relat Cancer 12:1071-1082

83. **Missmer SA, Eliassen AH, Barbieri RL, Hankinson SE** 2004 Endogenous estrogen, androgen, and progesterone concentrations and breast cancer risk among postmenopausal women. J Natl Cancer Inst 96:1856-1865

84. **Berrino F, Muti P, Micheli A, Bolelli G, Krogh V, Sciajno R, Pisani P, Panico S, Secreto G** 1996 Serum sex hormone levels after menopause and subsequent breast cancer. J Natl Cancer Inst 88:291-296

85. **Hankinson SE, Willett WC, Colditz GA, Hunter DJ, Michaud DS, Deroo B, Rosner B, Speizer FE, Pollak M** 1998 Circulating concentrations of insulin-like growth factor-I and risk of breast cancer. Lancet 351:1393-1396

86. **Toniolo PG, Levitz M, Zeleniuch-Jacquotte A, Banerjee S, Koenig KL, Shore RE, Strax P, Pasternack BS** 1995 A prospective study of endogenous estrogens and breast cancer in postmenopausal women. J Natl Cancer Inst 87:190-197

87. **Britt K** 2012 Menarche, menopause, and breast cancer risk. Lancet Oncol 13:1071-1072

88. **Henderson BE, Bernstein L** 1996 Endogenous and Exogenous Hormonal Factors. In: Harris JR MM, Lippman ME, Helman S ed. Diseases of the Breast. Philadelphia, PA: Lippincott-Raven Publishers; 185-200

89. **Key TJ, Appleby PN, Reeves GK, Roddam AW, Helzlsouer KJ, Alberg AJ, Rollison DE, Dorgan JF, Brinton LA, Overvad K, Kaaks R, Trichopoulou A, Clavel-Chapelon F, Panico S, Duell EJ, Peeters PH, Rinaldi S, Fentiman IS, Dowsett M, Manjer J, Lenner P, Hallmans G, Baglietto L, English DR, Giles GG, Hopper JL, Severi G, Morris HA, Hankinson SE, Tworoger SS, Koenig K, Zeleniuch-Jacquotte A, Arslan AA, Toniolo P, Shore RE, Krogh V, Micheli A, Berrino F, Barrett-Connor E, Laughlin GA, Kabuto M, Akiba S,**

Stevens RG, Neriishi K, Land CE, Cauley JA, Lui LY, Cummings SR, Gunter MJ, Rohan TE, Strickler HD 2011 Circulating sex hormones and breast cancer risk factors in postmenopausal women: reanalysis of 13 studies. Br J Cancer 105:709-722

90. **Dao T** 1981 The Role of Ovarian Steroid Hormones in Mammary Carcinogenesis. In: Pike MC SP, and Welsch CW ed. Hormones and Breast Cancer (Banbury REport no 8). Cold Spring Harbor, NY: Cold Spring Harbor Laboratory Press; 281-285

91. **Li SA, Weroha SJ, Tawfik O, Li JJ** 2002 Prevention of solely estrogen-induced mammary tumors in female aci rats by tamoxifen: evidence for estrogen receptor mediation. J Endocrinol 175:297-305

92. **Schiff R, Chamness GC, Brown PH** 2003 Advances in breast cancer treatment and prevention: preclinical studies on aromatase inhibitors and new selective estrogen receptor modulators (SERMs). Breast Cancer Res 5:228-231

93. **Beral V** 2003 Breast cancer and hormone-replacement therapy in the Million Women Study. Lancet 362:419-427

94. **Yu H, Rohan T** 2000 Role of the insulin-like growth factor family in cancer development and progression. J Natl Cancer Inst 92:1472-1489

95. **Lee AV, Yee D** 1995 Insulin-like growth factors and breast cancer. Biomed Pharmacother 49:415-421

96. **Wood TL, Yee D** 2000 Introduction: IGFs and IGFBPs in the normal mammary gland and in breast cancer. J Mammary Gland Biol Neoplasia 5:1-5

97. **Hawsawi Y, El-Gendy R, Twelves C, Speirs V, Beattie J** 2013 Insulin-like growth factor - oestradiol crosstalk and mammary gland tumourigenesis. Biochim Biophys Acta 1836:345-353

98. **Hadsell DL, Bonnette SG** 2000 IGF and insulin action in the mammary gland: lessons from transgenic and knockout models. J Mammary Gland Biol Neoplasia 5:19-30

99. **Ruan W, Kleinberg DL** 1999 Insulin-like growth factor I is essential for terminal end bud formation and ductal morphogenesis during mammary development. Endocrinology 140:5075-5081

100. **Cannata D, Lann D, Wu Y, Elis S, Sun H, Yakar S, Lazzarino DA, Wood TL, Leroith D** 2010 Elevated circulating IGF-I promotes mammary gland development and proliferation. Endocrinology 151:5751-5761

101. **Richards RG, Klotz DM, Walker MP, Diaugustine RP** 2004 Mammary gland branching morphogenesis is diminished in mice with a deficiency of insulin-like

growth factor-I (IGF-I), but not in mice with a liver-specific deletion of IGF-I. Endocrinology 145:3106-3110

102. **Powell-Braxton L, Hollingshead P, Warburton C, Dowd M, Pitts-Meek S, Dalton D, Gillett N, Stewart TA** 1993 IGF-I is required for normal embryonic growth in mice. Genes Dev 7:2609-2617

103. **Weber MS, Boyle PL, Corl BA, Wong EA, Gwazdauskas FC, Akers RM** 1998 Expression of ovine insulin-like growth factor-1 (IGF-1) stimulates alveolar bud development in mammary glands of transgenic mice. Endocrine 8:251-259

104. **Bonnette SG, Hadsell DL** 2001 Targeted disruption of the IGF-I receptor gene decreases cellular proliferation in mammary terminal end buds. Endocrinology 142:4937-4945

105. **de Ostrovich KK, Lambertz I, Colby JK, Tian J, Rundhaug JE, Johnston D, Conti CJ, DiGiovanni J, Fuchs-Young R** 2008 Paracrine overexpression of insulin-like growth factor-1 enhances mammary tumorigenesis in vivo. Am J Pathol 173:824-834

106. **Wu Y, Cui K, Miyoshi K, Hennighausen L, Green JE, Setser J, LeRoith D, Yakar S** 2003 Reduced circulating insulin-like growth factor I levels delay the onset of chemically and genetically induced mammary tumors. Cancer Res 63:4384-4388

107. **Peyrat JP, Bonneterre J, Hecquet B, Vennin P, Louchez MM, Fournier C, Lefebvre J, Demaille A** 1993 Plasma insulin-like growth factor-1 (IGF-1) concentrations in human breast cancer. Eur J Cancer 29A:492-497

108. **Shi R, Yu H, McLarty J, Glass J** 2004 IGF-I and breast cancer: a meta-analysis. Int J Cancer 111:418-423

109. **Belfiore A, Frasca F** 2008 IGF and insulin receptor signaling in breast cancer. J Mammary Gland Biol Neoplasia 13:381-406

110. **Peyrat JP, Bonneterre J** 1992 Type 1 IGF receptor in human breast diseases. Breast Cancer Res Treat 22:59-67

111. **Yang Y, Yee D** 2012 Targeting insulin and insulin-like growth factor signaling in breast cancer. J Mammary Gland Biol Neoplasia 17:251-261

112. **Pollak M** 2012 The insulin and insulin-like growth factor receptor family in neoplasia: an update. Nat Rev Cancer 12:159-169

113. **Hamelers IH, Steenbergh PH** 2003 Interactions between estrogen and insulin-like growth factor signaling pathways in human breast tumor cells. Endocr Relat Cancer 10:331-345

114. **Thorne C, Lee AV** 2003 Cross talk between estrogen receptor and IGF signaling in normal mammary gland development and breast cancer. Breast Dis 17:105-114

115. **Bartella V, De Marco P, Malaguarnera R, Belfiore A, Maggiolini M** 2012 New advances on the functional cross-talk between insulin-like growth factor-I and estrogen signaling in cancer. Cell Signal 24:1515-1521

116. **Lanzino M, Morelli C, Garofalo C, Panno ML, Mauro L, Ando S, Sisci D** 2008 Interaction between estrogen receptor alpha and insulin/IGF signaling in breast cancer. Curr Cancer Drug Targets 8:597-610

117. **Kato S, Endoh H, Masuhiro Y, Kitamoto T, Uchiyama S, Sasaki H, Masushige S, Gotoh Y, Nishida E, Kawashima H, Metzger D, Chambon P** 1995 Activation of the estrogen receptor through phosphorylation by mitogen-activated protein kinase. Science 270:1491-1494

118. **Lee AV, Weng CN, Jackson JG, Yee D** 1997 Activation of estrogen receptor-mediated gene transcription by IGF-I in human breast cancer cells. J Endocrinol 152:39-47

119. **Richards RG, DiAugustine RP, Petrusz P, Clark GC, Sebastian J** 1996 Estradiol stimulates tyrosine phosphorylation of the insulin-like growth factor-1 receptor and insulin receptor substrate-1 in the uterus. Proc Natl Acad Sci U S A 93:12002-12007

120. **Yee D, Lee AV** 2000 Crosstalk between the insulin-like growth factors and estrogens in breast cancer. J Mammary Gland Biol Neoplasia 5:107-115

121. **Yu Z, Gao W, Jiang E, Lu F, Zhang L, Shi Z, Wang X, Chen L, Lv T** 2013 Interaction between IGF-IR and ER induced by E2 and IGF-I. PLoS One 8:e62642

122. **Ruan W, Catanese V, Wieczorek R, Feldman M, Kleinberg DL** 1995 Estradiol enhances the stimulatory effect of insulin-like growth factor-I (IGF-I) on mammary development and growth hormone-induced IGF-I messenger ribonucleic acid. Endocrinology 136:1296-1302

123. **Lee AV, Jackson JG, Gooch JL, Hilsenbeck SG, Coronado-Heinsohn E, Osborne CK, Yee D** 1999 Enhancement of insulin-like growth factor signaling in human breast cancer: estrogen regulation of insulin receptor substrate-1 expression in vitro and in vivo. Mol Endocrinol 13:787-796

124. **Weroha SJ, Haluska P** 2008 IGF-1 receptor inhibitors in clinical trials--early lessons. J Mammary Gland Biol Neoplasia 13:471-483

125. **Vandenberg LN, Maffini MV, Wadia PR, Sonnenschein C, Rubin BS, Soto AM** 2007 Exposure to environmentally relevant doses of the xenoestrogen

bisphenol-A alters development of the fetal mouse mammary gland. Endocrinology 148:116-127

126. **Belli P, Bellaton C, Durand J, Balleydier S, Milhau N, Mure M, Mornex JF, Benahmed M, Le Jan C** 2010 Fetal and neonatal exposure to the mycotoxin zearalenone induces phenotypic alterations in adult rat mammary gland. Food Chem Toxicol 48:2818-2826

127. **Markey CM, Luque EH, Munoz De Toro M, Sonnenschein C, Soto AM** 2001 In utero exposure to bisphenol A alters the development and tissue organization of the mouse mammary gland. Biol Reprod 65:1215-1223

128. **Moon HJ, Han SY, Shin JH, Kang IH, Kim TS, Hong JH, Kim SH, Fenton SE** 2007 Gestational exposure to nonylphenol causes precocious mammary gland development in female rat offspring. J Reprod Dev 53:333-344

129. **Moral R, Wang R, Russo IH, Lamartiniere CA, Pereira J, Russo J** 2008 Effect of prenatal exposure to the endocrine disruptor bisphenol A on mammary gland morphology and gene expression signature. J Endocrinol 196:101-112

130. **Munoz-de-Toro M, Markey CM, Wadia PR, Luque EH, Rubin BS, Sonnenschein C, Soto AM** 2005 Perinatal exposure to bisphenol-A alters peripubertal mammary gland development in mice. Endocrinology 146:4138-4147

131. **Rayner JL, Enoch RR, Fenton SE** 2005 Adverse effects of prenatal exposure to atrazine during a critical period of mammary gland growth. Toxicol Sci 87:255-266

132. **Moral R, Santucci-Pereira J, Wang R, Russo IH, Lamartiniere CA, Russo J** 2011 In utero exposure to butyl benzyl phthalate induces modifications in the morphology and the gene expression profile of the mammary gland: an experimental study in rats. Environ Health 10:5

133. **Hilakivi-Clarke L, Clarke R, Onojafe I, Raygada M, Cho E, Lippman M** 1997 A maternal diet high in n - 6 polyunsaturated fats alters mammary gland development, puberty onset, and breast cancer risk among female rat offspring. Proc Natl Acad Sci U S A 94:9372-9377

134. **de Assis S, Warri A, Cruz MI, Laja O, Tian Y, Zhang B, Wang Y, Huang TH, Hilakivi-Clarke L** 2012 High-fat or ethinyl-oestradiol intake during pregnancy increases mammary cancer risk in several generations of offspring. Nat Commun 3:1053

135. **Palmer JR, Hatch EE, Rosenberg CL, Hartge P, Kaufman RH, Titus-Ernstoff L, Noller KL, Herbst AL, Rao RS, Troisi R, Colton T, Hoover RN** 2002 Risk of breast cancer in women exposed to diethylstilbestrol in utero: prelimiinary results (United States). Cancer Causes Control 13:753-758

136. **Braun MM, Ahlbom A, Floderus B, Brinton LA, Hoover RN** 1995 Effect of twinship on incidence of cancer of the testis, breast, and other sites (Sweden). Cancer Causes Control 6:519-524

137. **Zhang X, Ho SM** 2011 Epigenetics meets endocrinology. J Mol Endocrinol 46:R11-32

138. **Dalvai M, Bystricky K** 2010 The role of histone modifications and variants in regulating gene expression in breast cancer. J Mammary Gland Biol Neoplasia 15:19-33

139. **Tsai MC, Manor O, Wan Y, Mosammaparast N, Wang JK, Lan F, Shi Y, Segal E, Chang HY** 2010 Long noncoding RNA as modular scaffold of histone modification complexes. Science 329:689-693

140. **Alves CP, Fonseca AS, Muys BR, de Barros ELBR, Burger MC, de Souza JE, Valente V, Zago MA, Silva WA, Jr.** 2013 The lincRNA Hotair is required for epithelial-to-mesenchymal transition and stemness maintenance of cancer cell lines. Stem Cells 31:2827-2832

141. **Li S, Hursting SD, Davis BJ, McLachlan JA, Barrett JC** 2003 Environmental exposure, DNA methylation, and gene regulation: lessons from diethylstilbesterol-induced cancers. Ann N Y Acad Sci 983:161-169

142. **Feng S, Jacobsen SE, Reik W** 2010 Epigenetic reprogramming in plant and animal development. Science 330:622-627

143. **Cloos PA, Christensen J, Agger K, Helin K** 2008 Erasing the methyl mark: histone demethylases at the center of cellular differentiation and disease. Genes Dev 22:1115-1140

144. **Turndrup Pedersen M, Helin K** 2010 Histone demethylases in development and disease. Trends Cell Biol 20:662-671

145. **Rodriguez-Paredes M, Esteller M** 2011 Cancer epigenetics reaches mainstream oncology. Nat Med 17:330-339

146. **Dolinoy DC, Weidman JR, Jirtle RL** 2007 Epigenetic gene regulation: linking early developmental environment to adult disease. Reprod Toxicol 23:297-307

147. **Ciccone DN, Su H, Hevi S, Gay F, Lei H, Bajko J, Xu G, Li E, Chen T** 2009 KDM1B is a histone H3K4 demethylase required to establish maternal genomic imprints. Nature 461:415-418

148. **Ungerer M, Knezovich J, Ramsay M** 2013 In utero alcohol exposure, epigenetic changes, and their consequences. Alcohol Res 35:37-46

149. **Reik W, Dean W, Walter J** 2001 Epigenetic reprogramming in mammalian development. Science 293:1089-1093

150. **Kafri T, Ariel M, Brandeis M, Shemer R, Urven L, McCarrey J, Cedar H, Razin A** 1992 Developmental pattern of gene-specific DNA methylation in the mouse embryo and germ line. Genes Dev 6:705-714

151. **Santos F, Dean W** 2004 Epigenetic reprogramming during early development in mammals. Reproduction 127:643-651

152. **Verma M, Srivastava S** 2002 Epigenetics in cancer: implications for early detection and prevention. Lancet Oncol 3:755-763

153. **Garro AJ, McBeth DL, Lima V, Lieber CS** 1991 Ethanol consumption inhibits fetal DNA methylation in mice: implications for the fetal alcohol syndrome. Alcohol Clin Exp Res 15:395-398

154. **Kaminen-Ahola N, Ahola A, Maga M, Mallitt KA, Fahey P, Cox TC, Whitelaw E, Chong S** 2010 Maternal ethanol consumption alters the epigenotype and the phenotype of offspring in a mouse model. PLoS Genet 6:e1000811

155. **Downing C, Flink S, Florez-McClure ML, Johnson TE, Tabakoff B, Kechris KJ** 2012 Gene expression changes in C57BL/6J and DBA/2J mice following prenatal alcohol exposure. Alcohol Clin Exp Res 36:1519-1529

156. **Liu Y, Balaraman Y, Wang G, Nephew KP, Zhou FC** 2009 Alcohol exposure alters DNA methylation profiles in mouse embryos at early neurulation. Epigenetics 4:500-511

157. **Stouder C, Somm E, Paoloni-Giacobino A** 2011 Prenatal exposure to ethanol: a specific effect on the H19 gene in sperm. Reprod Toxicol 31:507-512

158. **Perkins A, Lehmann C, Lawrence RC, Kelly SJ** 2013 Alcohol exposure during development: Impact on the epigenome. Int J Dev Neurosci 31:391-397

159. **Veazey KJ, Carnahan MN, Muller D, Miranda RC, Golding MC** 2013 Alcohol-induced epigenetic alterations to developmentally crucial genes regulating neural stemness and differentiation. Alcohol Clin Exp Res 37:1111-1122

160. **Bekdash RA, Zhang C, Sarkar DK** 2013 Gestational choline supplementation normalized fetal alcohol-induced alterations in histone modifications, DNA methylation, and proopiomelanocortin (POMC) gene expression in beta-endorphin-producing POMC neurons of the hypothalamus. Alcohol Clin Exp Res 37:1133-1142

161. **Doherty LF, Bromer JG, Zhou Y, Aldad TS, Taylor HS** 2010 In utero exposure to diethylstilbestrol (DES) or bisphenol-A (BPA) increases EZH2

expression in the mammary gland: an epigenetic mechanism linking endocrine disruptors to breast cancer. Horm Cancer 1:146-155

162. **Bromer JG, Zhou Y, Taylor MB, Doherty L, Taylor HS** 2010 Bisphenol-A exposure in utero leads to epigenetic alterations in the developmental programming of uterine estrogen response. Faseb J 24:2273-2280

163. **Martinez-Arguelles DB, Papadopoulos V** 2010 Epigenetic regulation of the expression of genes involved in steroid hormone biosynthesis and action. Steroids 75:467-476

164. **Control CfD** 2004 Alcohol consumption among women who are pregnant or who might become pregnant - United States. Morbidity and Mortality Weekly Report 53:1178-1181

165. **Sampson PD, Streissguth AP, Bookstein FL, Little RE, Clarren SK, Dehaene P, Hanson JW, Graham JM, Jr.** 1997 Incidence of fetal alcohol syndrome and prevalence of alcohol-related neurodevelopmental disorder. Teratology 56:317-326

166. **Barker DJ** 1998 In utero programming of chronic disease. Clin Sci (Lond) 95:115-128

167. **Hilakivi-Clarke L** 2007 Nutritional modulation of terminal end buds: its relevance to breast cancer prevention. Curr Cancer Drug Targets 7:465-474

168. **Williams JM, Daniel CW** 1983 Mammary ductal elongation: differentiation of myoepithelium and basal lamina during branching morphogenesis. Dev Biol 97:274-290

169. **Ruan W, Monaco ME, Kleinberg DL** 2005 Progesterone stimulates mammary gland ductal morphogenesis by synergizing with and enhancing insulin-like growth factor-I action. Endocrinology 146:1170-1178

170. **Song RX, Fan P, Yue W, Chen Y, Santen RJ** 2006 Role of receptor complexes in the extranuclear actions of estrogen receptor alpha in breast cancer. Endocr Relat Cancer 13 Suppl 1:S3-13

171. **Mihalick SM, Crandall JE, Langlois JC, Krienke JD, Dube WV** 2001 Prenatal ethanol exposure, generalized learning impairment, and medial prefrontal cortical deficits in rats. Neurotoxicol Teratol 23:453-462

172. **Miller MW** 1992 Circadian rhythm of cell proliferation in the telencephalic ventricular zone: effect of in utero exposure to ethanol. Brain Res 595:17-24

173. **Leeman RF, Heilig M, Cunningham CL, Stephens DN, Duka T, O'Malley SS** 2010 Ethanol consumption: how should we measure it? Achieving consilience between human and animal phenotypes. Addict Biol 15:109-124

174. **Russo J, Russo IH** 1987 Biological and molecular bases of mammary carcinogenesis. Lab Invest 57:112-137

175. **Adamo ML, Ma X, Ackert-Bicknell CL, Donahue LR, Beamer WG, Rosen CJ** 2006 Genetic increase in serum insulin-like growth factor-I (IGF-I) in C3H/HeJ compared with C57BL/6J mice is associated with increased transcription from the IGF-I exon 2 promoter. Endocrinology 147:2944-2955

176. **Fleming JM, Leibowitz BJ, Kerr DE, Cohick WS** 2005 IGF-I differentially regulates IGF-binding protein expression in primary mammary fibroblasts and epithelial cells. J Endocrinol 186:165-178

177. **Sasano H, Nagura H, Harada N, Goukon Y, Kimura M** 1994 Immunolocalization of aromatase and other steroidogenic enzymes in human breast disorders. Hum Pathol 25:530-535

178. **Simpson ER** 2000 Biology of aromatase in the mammary gland. J Mammary Gland Biol Neoplasia 5:251-258

179. **Callinan PA, Feinberg AP** 2006 The emerging science of epigenomics. Hum Mol Genet 15 Spec No 1:R95-101

180. **Jirtle RL, Skinner MK** 2007 Environmental epigenomics and disease susceptibility. Nat Rev Genet 8:253-262

181. **Butt AJ, Dickson KA, McDougall F, Baxter RC** 2003 Insulin-like growth factor-binding protein-5 inhibits the growth of human breast cancer cells in vitro and in vivo. J Biol Chem 278:29676-29685

182. **Bjornstrom L, Sjoberg M** 2005 Mechanisms of estrogen receptor signaling: convergence of genomic and nongenomic actions on target genes. Mol Endocrinol 19:833-842

183. **Sirianni R, Chimento A, Malivindi R, Mazzitelli I, Ando S, Pezzi V** 2007 Insulin-like growth factor-I, regulating aromatase expression through steroidogenic factor 1, supports estrogen-dependent tumor Leydig cell proliferation. Cancer Res 67:8368-8377

184. **Zhang B, Shozu M, Okada M, Ishikawa H, Kasai T, Murakami K, Nomura K, Harada N, Inoue M** 2010 Insulin-like growth factor I enhances the expression of aromatase P450 by inhibiting autophagy. Endocrinology 151:4949-4958

185. **Huynh H, Yang XF, Pollak M** 1996 A role for insulin-like growth factor binding protein 5 in the antiproliferative action of the antiestrogen ICI 182780. Cell Growth Differ 7:1501-1506

186. **Parisot JP, Leeding KS, Hu XF, DeLuise M, Zalcberg JR, Bach LA** 1999 Induction of insulin-like growth factor binding protein expression by ICI 182,780

in a tamoxifen-resistant human breast cancer cell line. Breast Cancer Res Treat 55:231-242

187. **Breese CR, Sonntag WE** 1995 Effect of ethanol on plasma and hepatic insulin-like growth factor regulation in pregnant rats. Alcohol Clin Exp Res 19:867-873

188. **Singh SP, Srivenugopal KS, Ehmann S, Yuan XH, Snyder AK** 1994 Insulin-like growth factors (IGF-I and IGF-II), IGF-binding proteins, and IGF gene expression in the offspring of ethanol-fed rats. J Lab Clin Med 124:183-192

189. **Mauceri HJ, Unterman T, Dempsey S, Lee WH, Conway S** 1993 Effect of ethanol exposure on circulating levels of insulin-like growth factor I and II, and insulin-like growth factor binding proteins in fetal rats. Alcohol Clin Exp Res 17:1201-1206

190. **Fatayerji N, Engelmann GL, Myers T, Handa RJ** 1996 In utero exposure to ethanol alters mRNA for insulin-like growth factors and insulin-like growth factor-binding proteins in placenta and lung of fetal rats. Alcohol Clin Exp Res 20:94-100

191. **Breese CR, D'Costa A, Ingram RL, Lenham J, Sonntag WE** 1993 Long-term suppression of insulin-like growth factor-1 in rats after in utero ethanol exposure: relationship to somatic growth. J Pharmacol Exp Ther 264:448-456

192. **Aros S, Mills JL, Iniguez G, Avila A, Conley MR, Troendle J, Cox C, Cassorla F** 2011 Effects of prenatal ethanol exposure on postnatal growth and the insulin-like growth factor axis. Horm Res Paediatr 75:166-173

193. **Bocchinfuso WP, Lindzey JK, Hewitt SC, Clark JA, Myers PH, Cooper R, Korach KS** 2000 Induction of mammary gland development in estrogen receptor-alpha knockout mice. Endocrinology 141:2982-2994

194. **Russo J, Russo IH** 2008 Breast development, hormones and cancer. Adv Exp Med Biol 630:52-56

195. **Lan N, Yamashita F, Halpert AG, Sliwowska JH, Viau V, Weinberg J** 2009 Effects of prenatal ethanol exposure on hypothalamic-pituitary-adrenal function across the estrous cycle. Alcohol Clin Exp Res 33:1075-1088

196. **Lieber CS, DeCarli LM** 1989 Liquid diet technique of ethanol administration: 1989 update. Alcohol Alcohol 24:197-211

197. **Lochry EA, Shapiro NR, Riley EP** 1980 Growth deficits in rats exposed to alcohol in utero. J Stud Alcohol 41:1031-1039

198. **Driscoll CD, Streissguth AP, Riley EP** 1990 Prenatal alcohol exposure: comparability of effects in humans and animal models. Neurotoxicol Teratol 12:231-237

199. **Creighton-Taylor JA, Rudeen PK** 1991 Prenatal ethanol exposure and opiatergic influence on puberty in the female rat. Alcohol 8:187-191

200. **McGivern RF, Raum WJ, Handa RJ, Sokol RZ** 1992 Comparison of two weeks versus one week of prenatal ethanol exposure in the rat on gonadal organ weights, sperm count, and onset of puberty. Neurotoxicol Teratol 14:351-358

201. **McGivern RF, McGeary J, Robeck S, Cohen S, Handa RJ** 1995 Loss of reproductive competence at an earlier age in female rats exposed prenatally to ethanol. Alcohol Clin Exp Res 19:427-433

202. **Wilson ME, Handa RJ** 1997 Gonadotropin secretion in infantile rats exposed to ethanol in utero. Alcohol 14:497-501

203. **Murugan S, Zhang C, Mojtahedzadeh S, Sarkar DK** 2013 Alcohol exposure in utero increases susceptibility to prostate tumorigenesis in rat offspring. Alcohol Clin Exp Res 37:1901-1909

204. **Institute of Medicine** 2002 Dietary Reference Intakes for Energy, Carbohydrate, Fiber, Fat, Fatty Acids, Cholesterol, Protein, and Amino Acids. Washington D.C. The National Academies Press

205. **Bello NT, Walters AL, Verpeut JL, Cunha PP** 2013 High-fat diet-induced alterations in the feeding suppression of low-dose nisoxetine, a selective norepinephrine reuptake inhibitor. J Obes 2013:457047

206. **Buettner R, Parhofer KG, Woenckhaus M, Wrede CE, Kunz-Schughart LA, Scholmerich J, Bollheimer LC** 2006 Defining high-fat-diet rat models: metabolic and molecular effects of different fat types. J Mol Endocrinol 36:485-501

207. **Abel E** 1979 Effects of ethanol exposure during different gestation weeks of pregnancy on maternal weight gain and intrauterine growth retardation in the rat. Neurobehavioral Toxicology 1:145-151

208. **Hammond ME, Hayes DF, Dowsett M, Allred DC, Hagerty KL, Badve S, Fitzgibbons PL, Francis G, Goldstein NS, Hayes M, Hicks DG, Lester S, Love R, Mangu PB, McShane L, Miller K, Osborne CK, Paik S, Perlmutter J, Rhodes A, Sasano H, Schwartz JN, Sweep FC, Taube S, Torlakovic EE, Valenstein P, Viale G, Visscher D, Wheeler T, Williams RB, Wittliff JL, Wolff AC** 2010 American Society of Clinical Oncology/College Of American Pathologists guideline recommendations for immunohistochemical testing of estrogen and progesterone receptors in breast cancer. J Clin Oncol 28:2784-2795

209. **Haslam SZ, Shyamala G** 1979 Effect of oestradiol on progesterone receptors in normal mammary glands and its relationship with lactation. Biochem J 182:127-131

210. **Katzenellenbogen BS, Norman MJ** 1990 Multihormonal regulation of the progesterone receptor in MCF-7 human breast cancer cells: interrelationships among insulin/insulin-like growth factor-I, serum, and estrogen. Endocrinology 126:891-898

211. **Brisken C** 2013 Progesterone signalling in breast cancer: a neglected hormone coming into the limelight. Nat Rev Cancer 13:385-396

212. **Knutson TP, Lange CA** 2014 Tracking progesterone receptor-mediated actions in breast cancer. Pharmacol Ther 142:114-125

213. **Brisken C, Heineman A, Chavarria T, Elenbaas B, Tan J, Dey SK, McMahon JA, McMahon AP, Weinberg RA** 2000 Essential function of Wnt-4 in mammary gland development downstream of progesterone signaling. Genes Dev 14:650-654

214. **Faivre EJ, Lange CA** 2007 Progesterone receptors upregulate Wnt-1 to induce epidermal growth factor receptor transactivation and c-Src-dependent sustained activation of Erk1/2 mitogen-activated protein kinase in breast cancer cells. Mol Cell Biol 27:466-480

215. **Rajaram RD, Brisken C** 2012 Paracrine signaling by progesterone. Mol Cell Endocrinol 357:80-90

216. **Obr AE, Edwards DP** 2012 The biology of progesterone receptor in the normal mammary gland and in breast cancer. Mol Cell Endocrinol 357:4-17

217. **Hagan CR, Lange CA** 2014 Molecular determinants of context-dependent progesterone receptor action in breast cancer. BMC Med 12:32

218. **Yang J, Weinberg RA** 2008 Epithelial-mesenchymal transition: at the crossroads of development and tumor metastasis. Dev Cell 14:818-829

219. **Kim HJ, Litzenburger BC, Cui X, Delgado DA, Grabiner BC, Lin X, Lewis MT, Gottardis MM, Wong TW, Attar RM, Carboni JM, Lee AV** 2007 Constitutively active type I insulin-like growth factor receptor causes transformation and xenograft growth of immortalized mammary epithelial cells and is accompanied by an epithelial-to-mesenchymal transition mediated by NF-kappaB and snail. Mol Cell Biol 27:3165-3175

220. **Sorokin AV, Chen J** 2013 MEMO1, a new IRS1-interacting protein, induces epithelial-mesenchymal transition in mammary epithelial cells. Oncogene 32:3130-3138

221. **Yanagawa J, Walser TC, Zhu LX, Hong L, Fishbein MC, Mah V, Chia D, Goodglick L, Elashoff DA, Luo J, Magyar CE, Dohadwala M, Lee JM, St John MA, Strieter RM, Sharma S, Dubinett SM** 2009 Snail promotes CXCR2

ligand-dependent tumor progression in non-small cell lung carcinoma. Clin Cancer Res 15:6820-6829

222. **Come C, Magnino F, Bibeau F, De Santa Barbara P, Becker KF, Theillet C, Savagner P** 2006 Snail and slug play distinct roles during breast carcinoma progression. Clin Cancer Res 12:5395-5402

223. **de Herreros AG, Peiro S, Nassour M, Savagner P** 2010 Snail family regulation and epithelial mesenchymal transitions in breast cancer progression. J Mammary Gland Biol Neoplasia 15:135-147

224. **Mani SA, Guo W, Liao MJ, Eaton EN, Ayyanan A, Zhou AY, Brooks M, Reinhard F, Zhang CC, Shipitsin M, Campbell LL, Polyak K, Brisken C, Yang J, Weinberg RA** 2008 The epithelial-mesenchymal transition generates cells with properties of stem cells. Cell 133:704-715

225. **Masui T, Ota I, Yook JI, Mikami S, Yane K, Yamanaka T, Hosoi H** 2014 Snail-induced epithelial-mesenchymal transition promotes cancer stem cell-like phenotype in head and neck cancer cells. Int J Oncol 44:693-699

226. **Zhu LF, Hu Y, Yang CC, Xu XH, Ning TY, Wang ZL, Ye JH, Liu LK** 2012 Snail overexpression induces an epithelial to mesenchymal transition and cancer stem cell-like properties in SCC9 cells. Lab Invest 92:744-752

227. **Fan F, Samuel S, Evans KW, Lu J, Xia L, Zhou Y, Sceusi E, Tozzi F, Ye XC, Mani SA, Ellis LM** 2012 Overexpression of snail induces epithelial-mesenchymal transition and a cancer stem cell-like phenotype in human colorectal cancer cells. Cancer Med 1:5-16

228. **Zhou W, Lv R, Qi W, Wu D, Xu Y, Liu W, Mou Y, Wang L** 2014 Snail contributes to the maintenance of stem cell-like phenotype cells in human pancreatic cancer. PLoS One 9:e87409

229. **Yee D, Cullen KJ, Paik S, Perdue JF, Hampton B, Schwartz A, Lippman ME, Rosen N** 1988 Insulin-like growth factor II mRNA expression in human breast cancer. Cancer Res 48:6691-6696

230. **Osborne CK, Coronado EB, Kitten LJ, Arteaga CI, Fuqua SA, Ramasharma K, Marshall M, Li CH** 1989 Insulin-like growth factor-II (IGF-II): a potential autocrine/paracrine growth factor for human breast cancer acting via the IGF-I receptor. Mol Endocrinol 3:1701-1709

231. **Paik S** 1992 Expression of IGF-I and IGF-II mRNA in breast tissue. Breast Cancer Res Treat 22:31-38

232. **Cullen KJ, Smith HS, Hill S, Rosen N, Lippman ME** 1991 Growth factor messenger RNA expression by human breast fibroblasts from benign and malignant lesions. Cancer Res 51:4978-4985

233. **Singer C, Rasmussen A, Smith HS, Lippman ME, Lynch HT, Cullen KJ** 1995 Malignant breast epithelium selects for insulin-like growth factor II expression in breast stroma: evidence for paracrine function. Cancer Res 55:2448-2454

234. **Lee AV, Darbre P, King RJ** 1994 Processing of insulin-like growth factor-II (IGF-II) by human breast cancer cells. Mol Cell Endocrinol 99:211-220

235. **Mathieu M, Vignon F, Capony F, Rochefort H** 1991 Estradiol down-regulates the mannose-6-phosphate/insulin-like growth factor-II receptor gene and induces cathepsin-D in breast cancer cells: a receptor saturation mechanism to increase the secretion of lysosomal proenzymes. Mol Endocrinol 5:815-822

236. **Manni A, Badger B, Wei L, Zaenglein A, Grove R, Khin S, Heitjan D, Shimasaki S, Ling N** 1994 Hormonal regulation of insulin-like growth factor II and insulin-like growth factor binding protein expression by breast cancer cells in vivo: evidence for stromal epithelial interactions. Cancer Res 54:2934-2942

237. **McCampbell AS, Walker CL, Broaddus RR, Cook JD, Davies PJ** 2008 Developmental reprogramming of IGF signaling and susceptibility to endometrial hyperplasia in the rat. Lab Invest 88:615-626

238. **Holm TM, Jackson-Grusby L, Brambrink T, Yamada Y, Rideout WM, 3rd, Jaenisch R** 2005 Global loss of imprinting leads to widespread tumorigenesis in adult mice. Cancer Cell 8:275-285

239. **Ogawa O, Eccles MR, Szeto J, McNoe LA, Yun K, Maw MA, Smith PJ, Reeve AE** 1993 Relaxation of insulin-like growth factor II gene imprinting implicated in Wilms' tumour. Nature 362:749-751

240. **Rainier S, Johnson LA, Dobry CJ, Ping AJ, Grundy PE, Feinberg AP** 1993 Relaxation of imprinted genes in human cancer. Nature 362:747-749

241. **Roy RN, Gerulath AH, Cecutti A, Bhavnani BR** 2000 Loss of IGF-II imprinting in endometrial tumors: overexpression in carcinosarcoma. Cancer Lett 153:67-73

242. **Cui H, Cruz-Correa M, Giardiello FM, Hutcheon DF, Kafonek DR, Brandenburg S, Wu Y, He X, Powe NR, Feinberg AP** 2003 Loss of IGF2 imprinting: a potential marker of colorectal cancer risk. Science 299:1753-1755

243. **Okamoto K, Morison IM, Taniguchi T, Reeve AE** 1997 Epigenetic changes at the insulin-like growth factor II/H19 locus in developing kidney is an early event in Wilms tumorigenesis. Proc Natl Acad Sci U S A 94:5367-5371

244. **Ravenel JD, Broman KW, Perlman EJ, Niemitz EL, Jayawardena TM, Bell DW, Haber DA, Uejima H, Feinberg AP** 2001 Loss of imprinting of insulin-like growth factor-II (IGF2) gene in distinguishing specific biologic subtypes of Wilms tumor. J Natl Cancer Inst 93:1698-1703

245. **Giani C, Pinchera A, Rasmussen A, Fierabracci P, Bonacci R, Campini D, Bevilacqua G, Trock B, Lippman ME, Cullen KJ** 1998 Stromal IGF-II messenger RNA in breast cancer: relationship with progesterone receptor expressed by malignant epithelial cells. J Endocrinol Invest 21:160-165

246. **Perks CM, Bowen S, Gill ZP, Newcomb PV, Holly JM** 1999 Differential IGF-independent effects of insulin-like growth factor binding proteins (1-6) on apoptosis of breast epithelial cells. J Cell Biochem 75:652-664

247. **Akkiprik M, Feng Y, Wang H, Chen K, Hu L, Sahin A, Krishnamurthy S, Ozer A, Hao X, Zhang W** 2008 Multifunctional roles of insulin-like growth factor binding protein 5 in breast cancer. Breast Cancer Res 10:212

248. **McGuire WL, Jr., Jackson JG, Figueroa JA, Shimasaki S, Powell DR, Yee D** 1992 Regulation of insulin-like growth factor-binding protein (IGFBP) expression by breast cancer cells: use of IGFBP-1 as an inhibitor of insulin-like growth factor action. J Natl Cancer Inst 84:1336-1341

249. **Li X, Cao X, Li X, Zhang W, Feng Y** 2007 Expression level of insulin-like growth factor binding protein 5 mRNA is a prognostic factor for breast cancer. Cancer Sci 98:1592-1596

250. **Kass SU, Pruss D, Wolffe AP** 1997 How does DNA methylation repress transcription? Trends Genet 13:444-449

251. **Bird AP** 1986 CpG-rich islands and the function of DNA methylation. Nature 321:209-213

252. **Brenet F, Moh M, Funk P, Feierstein E, Viale AJ, Socci ND, Scandura JM** 2011 DNA methylation of the first exon is tightly linked to transcriptional silencing. PLoS One 6:e14524

253. **Reed K, Poulin ML, Yan L, Parissenti AM** 2010 Comparison of bisulfite sequencing PCR with pyrosequencing for measuring differences in DNA methylation. Anal Biochem 397:96-106

254. **Zhang Y, Rohde C, Tierling S, Stamerjohanns H, Reinhardt R, Walter J, Jeltsch A** 2009 DNA methylation analysis by bisulfite conversion, cloning, and sequencing of individual clones. Methods Mol Biol 507:177-187

255. **Ho SM, Tang WY** 2007 Techniques used in studies of epigenome dysregulation due to aberrant DNA methylation: an emphasis on fetal-based adult diseases. Reprod Toxicol 23:267-282

256. **Frommer M, McDonald LE, Millar DS, Collis CM, Watt F, Grigg GW, Molloy PL, Paul CL** 1992 A genomic sequencing protocol that yields a positive display of 5-methylcytosine residues in individual DNA strands. Proc Natl Acad Sci U S A 89:1827-1831

257. **Clark SJ, Harrison J, Paul CL, Frommer M** 1994 High sensitivity mapping of methylated cytosines. Nucleic Acids Res 22:2990-2997

258. **Herman JG, Graff JR, Myohanen S, Nelkin BD, Baylin SB** 1996 Methylation-specific PCR: a novel PCR assay for methylation status of CpG islands. Proc Natl Acad Sci U S A 93:9821-9826

259. **Licchesi JD, Herman JG** 2009 Methylation-specific PCR. Methods Mol Biol 507:305-323

260. **Tost J, Gut IG** 2007 DNA methylation analysis by pyrosequencing. Nat Protoc 2:2265-2275

261. **Li LC, Dahiya R** 2002 MethPrimer: designing primers for methylation PCRs. Bioinformatics 18:1427-1431

262. **Darst RP, Pardo CE, Ai L, Brown KD, Kladde MP** 2010 Bisulfite sequencing of DNA. Curr Protoc Mol Biol Chapter 7:Unit 7 9 1-17

263. **Ottaviano YL, Issa JP, Parl FF, Smith HS, Baylin SB, Davidson NE** 1994 Methylation of the estrogen receptor gene CpG island marks loss of estrogen receptor expression in human breast cancer cells. Cancer Res 54:2552-2555

264. **Ferguson AT, Lapidus RG, Baylin SB, Davidson NE** 1995 Demethylation of the estrogen receptor gene in estrogen receptor-negative breast cancer cells can reactivate estrogen receptor gene expression. Cancer Res 55:2279-2283

265. **Lapidus RG, Nass SJ, Butash KA, Parl FF, Weitzman SA, Graff JG, Herman JG, Davidson NE** 1998 Mapping of ER gene CpG island methylation-specific polymerase chain reaction. Cancer Res 58:2515-2519

266. **Lapidus RG, Ferguson AT, Ottaviano YL, Parl FF, Smith HS, Weitzman SA, Baylin SB, Issa JP, Davidson NE** 1996 Methylation of estrogen and progesterone receptor gene 5' CpG islands correlates with lack of estrogen and progesterone receptor gene expression in breast tumors. Clin Cancer Res 2:805-810

267. **Yenbutr P, Hilakivi-Clarke L, Passaniti A** 1998 Hypomethylation of an exon I estrogen receptor CpG island in spontaneous and carcinogen-induced mammary tumorigenesis in the rat. Mech Ageing Dev 106:93-102

268. **Kurian JR, Olesen KM, Auger AP** 2010 Sex differences in epigenetic regulation of the estrogen receptor-alpha promoter within the developing preoptic area. Endocrinology 151:2297-2305